UNIVERSITY OF CALIFRONIA, SAN DIEGO

The Mucosal/Epithelial Barrier Disruption and Transport of Pancreatic Digestive Enzymes in Early Stages of Intestinal Ischemia

A dissertation submitted in partial satisfaction of the requirements for

the degree Doctor of Philosophy

in

Bioengineering with Specialization in Multi-scale Biology

by

Marisol Chang

Committee in charge:

Professor Geert W Schmid-Schönbein, Chair
Professor Lars Bode
Professor Pedro Cabrales
Professor Mark Ellisman
Professor Marcos Intaglietta

2012

The Dissertation of Marisol Chang is approved, and it is acceptable in quality and form of publication on microfilm and electronically:

_____

_____

_____

_____

_____

Chair

University of California, San Diego

2012

DEDICATION

A mi mamá Isaura ay mi tía Maria quienes me enseñaron que con esfuerzo y dedicación todo es posible

EPIGRAPH

"**Permeability** is defined as a relative openness between ego and non-ego and expansiveness toward the world; **impermeability** is defined as a relative closedness between ego and non-ego and a degree of seclusiveness from the world."

GJ Rose. (1972). Ego Boundaries: By Bernard Landis.

TABLE OF CONTENTS

LIST OF ABBREVIATIONS

Body Weight (BW)

Normal saline (NS)

Splanchnic arterial occlusion (SAO)

Tranexamic acid (TA)

Acarbose (ACA)

Nafamostat Mesilate (ANGD)

No inhibitor (NI)

Intramuscular (IM)

Intravenous (IV)

Perfluorocarbon (PFC)

Dimethylthiolurea (DMTU)

Thiobarbituric Acid Reactive Substances (TBARS)

LIST OF FIGURES

ACKNOWLEDGEMENTS

First of all I would like to thank Professor Geert W. Schmid-Schönbein for sharing his devotion towards shock research and letting me work in a project that he is very devoted and passionate about. I want to thank him for letting me work in his lab for supporting and believing in me during difficult times. I want to thank my committee members Professors Lars Bode, Pedro Cabrales, Mark Ellisman and Marcos Intaglietta for their suggestions and comments.

I also want to thank all the members of the Microcirculation lab for all the moments shared throughout all this six years. I want to thank Erik Kistler M.D. for his collaboration and numerous advices among those the proper use of the semicolon. I thank Alexander Penn, Ph.D. for teaching me how to perform surgery in the rat, without this valuable skill this thesis would probably have a different title. I thank Edward Tran for his numerous advices and support during my early Ph.D. years. I thank Angela Chen Ph.D. for her continuous support and her kind words. I want to thank Rafi Mazor Ph.D. for offering his unconditional critical thinking and technical support. I thank Tom Alsaigh, Shakti Valdez, Noi Plongthongkum and Amy Chen for their friendship and continuous moral support making grad school very enjoyable. I thank Elizabeth Pocock M.D. for making lab life very fun and Angelina Altshuler for making lab life very interesting with her vivacious personality. I want to specially thank Jason Chow for the numerous lunch hours we share and for the unforgettable chats about grad life. I thank Frank for making sure everything run smoothly in the lab allowing me to do all my experiments without delay. I thank Alex Hu J.D. and Sharon Kwan-I Wu for providing a great support during the earlier years of grad school.

I thank my classmates in special Octavio Mondragon-Palomino for his unconditional friendship in both good and difficult times. Yessenia Lopez and Joanna So who made my first year of Ph.D. very unforgettable.

I want to thank friends I made during my first year and who became an import support throughout the course of my PhD. I want to thank the Takens and its extended family for all the fun moments that made grad school memorable: Mary Pacold , Didem Unat, Winnie Wen, Gjergji Zyba, Patrick Verkaik, Panos Voulgaris, Vipul Bhargava, Yuvraj Agarwal and Gunjan Gupta. Thank you guys for everything.

Last but not least I want to thank my all my family: I want to start by thanking my sisters Sandra Julieth and Monica for their support and encouragement. I want to dearly thank my sister Monica for opening all the doors and smoothing the path to college for me. Without her determination to get a college education in the US when all odds were against us I would not be writing this thesis. I thank my mom Isaura for giving up everything so her daughters could have it all. I thank my aunt Maria for dedicating her whole life to take care her nieces so we could grow up and become who we are now. I thank Jose Nieves Gonzales for his unconditional support and for being there every time I have needed a father figure. I thank my niece Maria Camila and nephew Miguel Alejandro for giving a motive to not give up so I can look after them. I thank my husband Nikolaos Trogkanis for his unconditional love and support every single day since we met. I thank him for the numerous instances he has helped me; from setting up differential equations, finding shorter and effective ways to capture and stitch pictures; to listening to my complains and concerns.

Chapters 2 and 3, in full, are submitted material to Shock Journal as it appears in "Disruption of the Intestinal Mucin Layer Allows Entry of Digestive Enzymes during Early Periods of Intestinal Ischemia" by Chang M., Kistler E. B., Schmid-Schönbein G.W. The dissertation author is the primary author of this manuscript.

Chapters 4 and 5, in full, are submitted material to Plos One as it appears in "Breakdown of Mucin as Barrier to Digestive Enzymes in the Ischemic Rat Small Intestine" by Chang M., Alsaigh T., Kistler E. B., Schmid-Schönbein G.W. The dissertation author is the primary author of this manuscript.

Chapter 6, in full, is currently being prepared for submission for publication of the material by Chang M., Cabrales P. and Schmid-Schönbein G.W. The dissertation author is the primary author of this manuscript.

VITA AND PUBLICATIONS

2006	Bachelor of Science, University of Texas at Arlington
2006	Master of Science, University of Texas at Arlington
2012	Doctor of Philosophy, University of California San Diego

MANUSCRIPTS:

- Chang M., Kistler E. B., Schmid-Schönbein G.W. Disruption of the Intestinal Mucin Layer Allows Entry of Digestive Enzymes during Early Periods of Intestinal Ischemia. Shock Journal 2012. 37(3): 297.

- Chang M., Alsaigh T., Kistler E. B., Schmid-Schönbein G.W. Breakdown of Mucin as Barrier to Digestive Enzymes in the Ischemic Rat Small Intestine. (Under revision, Plos One)

- Kistler E. B., Alsaigh T., Chang M., Schmid-Schönbein G.W. Impaired Small Bowel Barrier Integrity In The Presence Of Lumenal Pancreatic Digestive Enzymes Leads To Circulatory Shock. Shock journal 2012 (in press)

- Chang M., Cabrales P., Schmid-Schönbein G.W. Enteral Supplementation with Oxygen or ATP Protects Mucin in the Mucosal Barrier during Early Periods of Gut Ischemia. (in preparation)

ABSTRACTS:

- Chang M, Cabrales P, Schmid-Schönbein G.W. Enteral Supplementation with Oxygen or ATP Protects Mucin in the Mucosal Barrier during Early Periods of Gut Ischemia. 35th Annual Conference on Shock June 9-13, 2012; Miami, FL.

- Chang M, Alsaigh T, Kistler E. B, Schmid-Schönbein G.W. Mucin Protects against Trypsin-mediated Increases in Intestinal Epithelial Permeability. Experimental Biology, April 21-25, 2012; San Diego, CA.

- Chang M, Schmid-Schönbein G.W. Enzymatic degradation of intestinal mucin and transport of digestive enzymes during gut ischemia. 34th Annual Conference on Shock; June 11-14, 2011; Norfolk, VA.

- Chang M, Kistler E. B, Schmid-Schönbein G.W. Digestive Degradation of Intestinal Mucin during Splanchnic Ischemia. Experimental Biology, FASEB J, in press, 2011

- Chang M, Schmid-Schönbein, G.W. Pancreatic digestive enzymes activity and transport across the ischemic intestine in early stages of shock. 9TH World Congress for Microcirculation; September 26-28, 2010; Paris, France.

- Chang M, Schmid-Schönbein G.W. Serine Protease Inhibition during Early Intestinal Ischemia: A Treatment against Autodigestion in Shock. TATRC Grand Challenge Semifinalist in 11th Annual UC Systemwide Bioengineering Symposium; UC Davis; June 17-19, 2010; Davis, CA.

- Chang M, Schmid-Schönbein G.W. Transport of Pancreatic Digestive Enzymes across the Intestinal Barrier in Early Stages of Shock. 33rd Annual Conference on Shock; June 12-15, 2010; Portland, OR.

- Chang M, Schmid-Schönbein G.W. Disruption of the Intestinal Mucin Layer and Entry of Pancreatic Digestive Enzymes in Early Stages of Shock. Experimental Biology 2010; April 24-28; Anaheim, CA

- Chang M, Schmid-Schönbein G.W. Serine Protease Blockade Provides A Protection Against Intestinal Ischemic Injury. UCSD Jacobs School of Engineering 29th Annual Research Expo. UC San Diego; April 15, 2010, La Jolla, CA.

- Chang M, Schmid-Schönbein, G.W. Digestive Protease Transport and Mechanism for Disruption of the Epithelial Barrier in Early Stages of Shock. 3rd Annual Interfaces Research Symposium; UC San Diego; Dec 4, 2010; La Jolla, CA

- Chang M, Schmid-Schönbein G.W. Digestive Protease Transport and Mechanism for Disruption of the Epithelial Barrier in Early Stages of Shock. Frontiers in Microcirculation: Control Processes and Clinical Applications. The Microcirculatory Society, Inc; 2009 October 16-17; University of Missouri; Columbia, MI.

- Chang M, Schmid-Schönbein G.W. Digestive Protease Transport and Mechanism for Disruption of the Epithelial Barrier in Early Stages of Shock. 10th UC System wide Bioeng. Symposium, UC Merced; June 19-21, 2009; Merced, CA.

- Chang M, Schmid-Schönbein G.W. The Role of Digestive Enzymes in Intestinal Permeability after Ischemic Shock. UCSD Jacobs School of Engineering 28th Annual Research Expo; February 19, 2009; UC San Diego; La Jolla; CA.

- Chang M, Kwan-I Wu, Spatial Model of IP3 production and ETA Receptor Ligand Binding. 2nd Annual UCSD Interfaces Research Symposium; June 13, 2008; UC San Diego, CA,

- Chang M, Wilk-Blaszczak M. The role of a pH sensing receptor in mast cells migration and adhesion to ECM proteins. Experimental Biology 2005 (Physiology). San Diego, CA, April 2005

- Chang M, Wilk-Blaszczak M. The effect of acidic pH on mast cell adhesion to extracellular matrix proteins. Annual Celebration of Excellence by Students. Arlington, TX, April 2004

- Chang M, Wilk-Blaszczak M. The effect of acidic pH on mast cell adhesion to extracellular matrix proteins. Texas National McNair Research Conference. Denton, TX, February 2004

- Chang M, Wilk-Blaszczak M. The effect of acidic pH on mast cell adhesion to extracellular matrix proteins. Sigma Xi Student Research Conference. Los Angeles, CA, November 2003

ORAL PRESENTATIONS:

- Chang M, Alsaigh T, Kistler E. B, Schmid-Schönbein G.W. Mucin Protects against Trypsin-mediated Increases in Intestinal Epithelial Permeability. ASIP 2012 Annual Meeting at Experimental Biology, April 21-25, 2012; San Diego, CA.

- Chang M., Schmid-Schönbein G.W. Serine Protease Inhibition during Early Intestinal Ischemia: A Treatment against Autodigestion in Shock. TATRC Grand Challenge Semifinalist in 11th Annual UC System wide Bioengineering Symposium; University of California Davis; June 17-19, 2010; Davis, CA.

- Chang M., Schmid-Schönbein G.W. Digestive Protease Transport and Mechanism for Disruption of the Epithelial Barrier in Early Stages of Shock. 3rd Annual Interfaces Research Symposium; University of California San Diego; December 4, 2010; La Jolla, CA

- Chang M., Schmid-Schönbein G.W. Digestive Protease Transport and Mechanism for Disruption of the Epithelial Barrier in Early Stages of Shock. Frontiers in Microcirculation: Control Processes and Clinical Applications. The Microcirculatory Society, Inc; October 16-17, 2009; University of Missouri; Columbia, MI.

- Chang M., Wilk-Blaszczak M. The effect of acidic pH on mast cell adhesion to extracellular matrix proteins. Alpha Chi Bi-regional Convention. University of Texas at Arlington; April 2004; Arlington, TX.

- Chang M., Wilk-Blaszczak M. The effect of acidic pH on mast cell adhesion to extracellular matrix proteins. McNair Scholars Program Summer Research; University of Texas at Arlington August 2003; Arlington, TX.

ABSTRACT OF THE DISSERTATION

The Mucosal/Epithelial Barrier Disruption and Transport of Pancreatic Digestive Enzymes in Early Stages of Intestinal Ischemia

by

Marisol Chang

Doctor of Philosophy in Bioengineering with Specialization in Multi-scale Biology

University of California, San Diego, 2012

Professor Geert W Schmid-Schönbein, Chair

Following reduced blood flow or trauma (e.g. in a car accident, explosion, burn, major surgery) a cascade of reactions leads to Shock and subsequently multi-organ failure (MOF) even if the organs were not affected by the initial trauma. Identifying the root cause of shock is of extraordinary importance and one of the greatest challenges for Bioengineering analysis. Shock is associated with one of the highest levels of mortality and no effective medical treatment exists. We have obtained evidence that pancreatic digestive enzymes are key players and we hypothesize that the intestinal mucosal/epithelial layer provides a physical barrier that prevents the entry of digestive

enzymes, normally contained within the lumen of the intestine, and during ischemic states this layer becomes disrupted allowing access of these enzymes into the intestinal wall. The rationale for the proposed study is to provide an enhanced understanding of fundamental mechanisms in the degradation of the mucosal epithelial barrier and subsequent transport of digestive enzymes. In this study I propose to investigate during early stages of intestinal ischemia the transport and activity of digestive enzymes across the epithelial wall and determine changes in the mucosal epithelial barrier. I will investigate mechanisms leading to the disruption of the mucosal barrier using a rat model of splanchnic ischemia as well as non-ischemic models designed to understand whether events characteristic of ischemia, such hypoxia, ATP depletion or drop in pH, are responsible for the disruption of the mucosal/epithelial barrier. Furthermore, I will investigate alterations in intestinal permeability in order to understand the mechanism by which digestive enzymes or any other cytotoxic mediators are transported into the systemic circulation. The results of these studies will determine the role of the mucosal epithelial barrier in the transport of digestive enzymes into the intestinal wall and it will provide insight into the development of new treatments for shock.

Chapter 1

Introduction to Shock

1.1 Shock History and Definition

While Greek physicians such as Hippocrates and Galen where the first to recognize the post-traumatic syndrome(1), the term shock is credited to the French surgeon Henri Francois Le Dran, when in 1737 he used the term *choc* to indicate a severe impact or jolt (2). Later the word "shock" was translated to indicate the sudden deterioration of a patient's condition when major trauma has occurred (2). Subsequently the term 'shock' started to be widely used in the clinical setting becoming a new research field. Initially the term *shock* was used to indicate the immediate response to massive trauma; and its definition consisted in a description of its clinical signs (2). The arrival of technology later allowed proposing a new and more appropriate definition.

Today it is widely accepted that in humans shock is often the final pathway through which a variety of pathologic processes lead to cardiovascular failure and death (3). Thus a most appropriate definition of shock can be defined "the state in which profound and wide spread reduction of effective perfusion leads first to reversible, and then, if prolonged, to irreversible cellular injury" (4). As such, shock is perhaps the most common and important problem encountered by physicians (5). Shock together with

respiratory failure, accounts for most emergent admissions in the intensive care unit (ICU) (6). Shock is one of the most common causes of death in the US today (7), it is the primary cause of late-stage morbidity in the ICU (8, 9); it accounts for the majority of deaths on the modern battlefield and for approximately one million deaths around the globe (7, 10).

1.2 Shock Classification

The importance of shock as a medical problem can be recognized by the distinction of its different forms. All forms of shock increase the probability of other major co-morbidities, such as serious infections, adult respiratory distress syndrome (ARDS), multiple organ dysfunction syndrome (MODS). A classification of shock was first proposed in 1972 by Hinshaw and Cox based on cardiovascular characteristics (11). The classification includes: 1) hypovolemic, 2) cardiogenic, 3) obstructive, and 4) distributive.

1.2.1 Hypovolemic Shock :Remains a major contributor to early mortality from trauma, the most common cause of death in persons under the age of 45 (12). It is characterized by a loss in circulatory volume, which results in decreased venous return, decreased filling of the cardiac chambers, and hence a decreased cardiac output leading to increase in systemic vascular resistance (SVR) (2).

1.2.2 Cardiogenic Shock: It is the leading cause of in-hospital mortality in the United States (13). It is primarily dependent on poor cardiac pump function and failure; it is the major component of the mortality associated with cardiovascular disease (2).

1.2.3 Obstructive shock: It is the result of an obstruction to flow in the cardiovascular circuit. It is associated with a physical impairment to adequate forward circulatory flow involving mechanisms different than primary myocardial or valvular dysfunction (2).

1.2.4 Distributive or vasogenic shock: Septic shock is the most common form, and it is the most frequent cause of death in the intensive care unit (ICU) in the United States (14, 15). This type of shock is associated with not only poor vascular tone in the peripheral circulation but also non-uniform distribution of blood flow to organs within the body (2).

1.3 Pathophysiology of Shock

Shock involves common cellular metabolic processes that results in the inability of cells to obtain and/or utilize oxygen in sufficient quantity to optimally meet their metabolic requirements and typically end in cell injury, organ failure and death (1, 5). The pathogenesis of shock involves: cellular ischemia, circulating or local inflammatory mediators, and free radical injury. Baker et al. showed that roughly half of trauma deaths occur at the scene before transport of the patient mostly due to central nervous system (CNS) and major vascular trauma (16). He also showed that another 8% of deaths occur early, principally from hemorrhage and CNS injuries, and 40% of patients die later from brain injury or multiple-organ failure (MOF) (17). Baker also popularized the trimodal distribution of trauma deaths; in this distribution the majority of the immediate deaths occur within the first couple of hours after injury. Early deaths occur within 5 hours after injury and late deaths occur in the following weeks after injury (17).

1.3.1 Cellular Injury in shock: The cellular injury encountered in most forms of shock results from ineffective perfusion leading to cellular ischemia. Hypoperfusion decreases

the delivery of nutrients to the cells leading to diminished ATP production (18). There are many essential ATP-dependent intracellular metabolic processes that may be affected or impaired as intracellular levels of ATP fall, making the intestine, liver and kidney particularly sensitive to these changes (19).

1.3.2 Microvascular function in shock: Microvessels are essential for providing an adequate cardiac output and subsequently ensure appropriate perfusion to all tissue organs. Irreversible hemorrhagic and septic shock results in peripheral vascular failure. Other microvascular pathologic processes occurring in shock include disruption of integrity of endothelial cell barrier leading to loss of plasma proteins, decrease in plasma oncotic pressure, interstitial edema and fall in circulating volume (20). In addition there is microvascular clotting and microthrombi leading to further inadequate distribution of perfusion within tissue (21).

1.4 The Gut and Shock

The gut is relatively sensitive to circulatory failure; hypoperfusion, sympathetic stimulation, and inflammatory injury associated with shock results in typical clinical gut injury manifestation which include ileus, erosive gastritis, pancreatitis, acalculous cholecystitis and colonic submucosal hemorrhage (5, 22). Lillehei was among the first ones to show evidence indicating the importance of the gut in the early development of shock (23). He showed an association between development of severe or irreversible shock and the mucosal necrosis of the gut (23-25). Chiu also demonstrated that the degree of development of the mucosal injury following periods of hypotension and shock depends on the duration of the impairment blood flow in the intestine (26).

During mesenteric ischemia, the perfusion of the different layers of the intestine is redistributed disproportionately, favoring the more metabolically active areas (27). However because of increased metabolic demand at the villus tip, and the countercurrent shunting of oxygen at the villus base, the villus tip remains preferentially susceptible to ischemic injury (27). Grum was the first one to use a non-invasive technique to monitor oxygen changes in the gut (28); with this technique it was demonstrated that oxygenation remains adequate until oxygen delivery has been reduced below a certain point. In addition, a drop in gastric mucosa pH has been associated with morbidity and mortality in patients admitted to the ICU (29, 30). Recent studies suggest that enteric ischemia produced by circulatory shock and free radical injury with resuscitation may breach gut barrier integrity (22, 31).

Hemorrhagic lesions in the small intestinal mucosa have been reported in dogs (24-26, 32), cats (33-35) and similar mucosal lesions have also been reported in patients dying in shock (36-42). A characteristic feature is that these lesions appear first at the tip of the villi, and in cases where the entire villus is destroyed the deeper layers of the intestinal wall are still free from inflammatory changes (26, 33). Together these findings suggest that the reduction in oxygen delivery, which leads to tissue hypoxia despite compensatory mechanism, is likely to be the pathophysiological mechanism of intestinal ischemia observed in shock. Other authors, however, have demonstrated that in sepsis there are other mechanisms necessary for the formation of intestinal mucosal injury in addition to impaired intestinal blood flow and reduced oxygen consumption encountered in the gut (16, 43).

1.4.1 Digestive Enzymes: The mechanisms by which severe trauma, hemorrhage, ischemia and burns initiate a cascade of events leading to shock is still not completely elucidated. Digestive enzymes and their products located in the lumen of the intestine are potential major candidates to mediate the inflammation and necrosis in shock. It has been shown that ischemic intestines, contain cytotoxic mediators and that this cytotoxicity may be the result of digestive enzymes from the intestinal lumen acting on either the tissue of the intestine or on ingested food (44). Among the four general classes of digestive enzymes of the pancreas (proteases, amylases, lipases and nucleases) the major proinflammatory and cytotoxic factors have been found to be generated by means of serine proteases and lipases (45).

1.4.2 Digestive Enzyme Blockade: It was also demonstrated that the cytotoxicity found in the mediators can be prevented by the use of broad-spectrum pancreatic digestive enzyme inhibitor such as phenylmethylsulfonyl fluoride (PMSF) (44). In addition blockade of pancreatic digestive enzymes with nafamostat mesilate (ANGD) or gabexate mesilate (FOY) in the lumen of the ileum serves to reduce the level of inflammatory mediators in shock produced by occlusion of the superior mesentery artery (46, 47). It was further shown that the protection provided by protease inhibition is not enhanced by supplementation with oxygen free radical blockers such as Allopurinol, indicating that oxygen free radicals may not the major player in the shock cascade (46, 47). Furthermore, while intraluminal pancreatic protease inhibition improves mean arterial blood pressure and reduces the formation of neutrophil cell activators during shock (46); intravenos administration of a serine protease inhibitor during intestinal ischemia and

reperfusion has only a mild effect on mean arterial blood pressure and neutrophil cell activation (48).

1.5 Goals and Overview of this Dissertation

Shock due to trauma and subsequently multiple organ failure (MOF) is the primary cause of late-stage morbidity around the globe (8, 9). However, the mechanisms by which these events take place it is still not fully understood, no effective medical treatments exist and no bioengineering analysis about the sequence of events that leads to rapid organ failure. There is agreement that some of the early signs of inflammation in shock and MOF originate in the small intestine (41, 44, 49). During shock states, pancreatic digestive enzymes may escape from the lumen of the intestine and are capable of digesting tissue components as well as generating inflammatory and/or cytotoxic mediators that subsequently escape through the mucosal epithelial barrier (44, 45, 49-55). Inhibition of pancreatic proteases in the lumen of the intestine during shock has been shown to prevent intestinal cell dysfunction and leakage of cytotoxic mediators into the systemic circulation (47, 55). Understanding the mechanism by which intestinal ischemia, as a result of a trauma, results in shock and subsequently multiple organ failure is the key to find an effective treatment.

The **objective** of this thesis is to elucidate the mechanism by which digestive enzymes enter the wall of the intestine during gut ischemia.

My **hypothesis** is that during the early phase of an ischemic event digestive enzymes are transported from the lumen of the intestine into the intestinal wall due to disruption of the mucosal/epithelial barrier. The initial insult after ischemia in the gut

results in disruption to the mucosal/epithelial barrier allowing entry of the powerful digestive enzymes from the lumen of the intestine into the intestinal wall and subsequently to the systemic circulation where the autodigestion process is initiated.

To examine this hypothesis, I investigate the following Aims: 1) Determine whether digestive enzymes leak into the intestinal wall during early periods of ischemia. 2) Identify damage in the mucosal and epithelial barrier during gut ischemia. 3) Assess the role of mucin as a barrier to digestive enzymes. 4) Determine possible roles of digestive enzymes in the degradation of the intestinal barrier; and 5) Establish whether ischemic events such as oxygen and ATP depletion and pH change in the lumen of the intestine lead to the disruption of the mucosal layer and degradation of mucin during intestinal ischemia.

These Aims are described in Chapters 2-6; Chapter 7 presents the conclusions and future directions.

1.6 References

1. Sethi AK, Sharma P, Mohta M, & Tyagi A (2003) Shock- A Short Review. *Indian Journal of Anesthesia*:346.

2. Sethi A, Sharma P, Mohta M, & Tyagi A (2003) Shock–A short review. *Indian J Anesth* 47:245-359.

3. Frost P & Wise M (2006) Recognition and management of the patient with shock. *Acute medicine* 5(2):43.

4. Kumar A & Parrillo JE (2001) Shock: Classification, pathophysyology, and approach to management. *Critical Care Medicine. Principles of Diagnosis and Management in the Adults*, eds Parrillo JE & Dellinger RP (Mosby, London), pp 291-339.

5. Parrillo JE & Dellinger RP (2001) *Critical care medicine: principles of diagnosis and management in the adult* (Mosby Inc).

6. Rodriguez RM & Rosenthal MH (2002) Etiology and Pathophysiology of Shock. *Critical Care Medicine - Perioperative Management*, eds Murray MJ, Coursin DB, Pearl RG, & Prough DS (Lippincott William & Wilkins, London), 2nd Ed, pp 192-205.

7. Anonymous (2008) World Health Organization: World Health Statistics Annual. 2008.

8. Hoyt DB, Junger WG, & Ozkan AN (1993) Humoral mechanism. *Pathophysiology of Shock, Sepsis, and Organ Failure*, eds Schlag G & Red lH (Springer-Verlag, Berlin), pp 111-130.

9. Yao YM, Redl H, Bahrami S, & Schlag G (1998) The inflammatory basis of trauma/shock-associated multiple organ failure. (Translated from eng) *Inflamm Res* 47(5):201-210 (in eng).

10. Holcomb J, *et al.* (2007) Causes of death in US Special Operations Forces in the global war on terrorism: 2001-2004. (Translated from eng) *US Army Med Dep J*:24-37 (in eng).

11. Hinsaw LB & Cox BG (1972) *The fundamental mechanisms of shock* (Plenum Press, New York).

12. Heron M, *et al.* (2009) Deaths: Final data for 2006. National Vital Statistics Reports.

13. Research NRCCoT, Research CoT, & Medicine Io (1985) *Injury in America: a continuing public health problem* (Natl Academy Pr).

14. Martin GS, Mannino DM, Eaton S, & Moss M (2003) The epidemiology of sepsis in the United States from 1979 through 2000. *N engl j med* 348(16):1546-1554.

15. Hall MJ, Williams SN, DeFrances CJ, & Golosinskiy A (2011) Inpatient Care for Septicemia or Sepsis: A Challenge for Patients and Hospitals. *NCHS Data Brief* 62(June):1-7.

16. Fink MP, Kaups KL, Wang HL, & Rothschild HR (1991) Maintenance of superior mesenteric arterial perfusion prevents increased intestinal mucosal permeability in endotoxic pigs. (Translated from eng) *Surgery* 110(2):154-160; discussion 160-151 (in eng).

17. Baker CC, Oppenheimer L, Stephens B, Lewis FR, & Trunkey DD (1980) Epidemiology of trauma deaths. (Translated from eng) *Am J Surg* 140(1):144-150 (in eng).

18. Mela L, Bacalzo Jr LV, & Miller L (1971) Defective oxidative metabolism of rat liver mitochondria in hemorrhagic and endotoxin shock. *American Journal of Physiology--Legacy Content* 220(2):571-577.

19. Chaudry I, Sayeed M, & Baue A (1976) Alterations in high-energy phosphates in hemorrhagic shock as related to tissue and organ function. *Surgery* 79(6):666.

20. Carden DL & Granger DN (2000) Pathophysiology of ischaemia–reperfusion injury. *The Journal of pathology* 190(3):255-266.

21. Shah D, Dutton R, Newell J, & Powers Jr S (1977) Vascular autoregulatory failure following trauma and shock. p 11.

22. Bhagwat A & Hawk W (1966) Terminal hemorrhagic necrotizing enteropathy (THNE). A retrospective clinicopathologic study with a review of literature. *The American journal of gastroenterology* 45(3):163.

23. Lillehei RC (1957) The Intestinal Factor in Irreversible Hemorrhagic Shock. (Translated from English) *Surgery* 42(6):1043-1054 (in English).

24. Lillehei RC, Dietzman RH, & Movsas S (1967) The visceral circulation in shock. (Translated from eng) *Gastroenterology* 52(2):468-471 (in eng).

25. Lillehei RC, Longerbeam JK, Bloch JH, & Manax WG (1964) The Nature of Irreversible Shock: Experimental and Clinical Observations. (Translated from eng) *Ann Surg* 160:682-710 (in eng).

26. Chiu CJ, McArdle AH, Brown R, Scott HJ, & Gurd FN (1970) Intestinal mucosal lesion in low-flow states. I. A morphological, hemodynamic, and metabolic reappraisal. (Translated from eng) *Arch Surg* 101(4):478-483 (in eng).

27. Ceppa EP, Fuh KC, & Bulkley GB (2003) Mesenteric hemodynamic response to circulatory shock. (Translated from eng) *Curr Opin Crit Care* 9(2):127-132 (in eng).

28. Grum CM, *et al.* (1984) Adequacy of tissue oxygenation in intact dog intestine. (Translated from eng) *J Appl Physiol* 56(4):1065-1069 (in eng).

29. Doglio GR, *et al.* (1991) Gastric mucosal pH as a prognostic index of mortality in critically ill patients. (Translated from eng) *Critical care medicine* 19(8):1037-1040 (in eng).

30. Gutierrez G, *et al.* (1992) Gastric intramucosal pH as a therapeutic index of tissue oxygenation in critically ill patients. (Translated from eng) *Lancet* 339(8787):195-199 (in eng).

31. Astiz M, Rackow E, & Weil M (1993) Pathophysiology and treatment of circulatory shock. *Critical care clinics* 9(2):183.

32. Wiggers CJ (1950) *Physiology of shock* (Commonwealth Fund).

33. Ahren C & Haglund U (1973) Mucosal lesions in the small intestine of the cat during low flow. (Translated from eng) *Acta Physiol Scand* 88(4):541-550 (in eng).

34. Haglund U, Abe T, Ahren C, Braide I, & Lundgren O (1976) The intestinal mucosal lesions in shock. I. Studies on the pathogenesis. (Translated from eng) *Eur Surg Res* 8(5):435-447 (in eng).

35. Falk A, Redfors S, Myrvold H, & Haglund U (1985) Small intestinal mucosal lesions in feline septic shock: a study on the pathogenesis. (Translated from eng) *Circ Shock* 17(4):327-337 (in eng).

36. Penner A & Bernheim AI (1939) Acute postoperative esophageal, gastric and duodenal ulcerations. *Arch. Path* 28.

37. Penner A & Bernheim AI (1939) Acute postoperative enterocolitis. A study on the pathologic nature of shock. *Arch. Path* 27.

38. Marston A (1962) The bowel in shock. The role of mesenteric arterial disease as a cause of death in the elderly. (Translated from eng) *Lancet* 2(7252):365-370 (in eng).

39. Bounous G (1969) "Tryptic enteritis": its role in the pathogenesis of stress ulcer and shock. (Translated from eng) *Can J Surg* 12(4):397-409 (in eng).

40. Carey JS, Okada F, Monson DO, Yao ST, & Shoemaker WC (1967) Intestinal infarction in shock with survival after resection. Relation of the intestinal lesion to shock with high cardiac output. (Translated from eng) *Jama* 199(6):422-425 (in eng).

41. Hugon JS & Bounous G (1971) Intestinal lesions in low flow states: electron microscopic study. *Vascular Disorders of the Intestine*, ed Boley SJ (Appleton and Century Crofts, New York), pp 123-144.

42. Haglund U, Hulten L, Ahren C, & Lundgren O (1975) Mucosal lesions in the human small intestine in shock. (Translated from eng) *Gut* 16(12):979-984 (in eng).

43. Fink MP, Antonsson JB, Wang HL, & Rothschild HR (1991) Increased intestinal permeability in endotoxic pigs. Mesenteric hypoperfusion as an etiologic factor. (Translated from eng) *Arch Surg* 126(2):211-218 (in eng).

44. Penn AH, Hugli TE, & Schmid-Schönbein GW (2007) Pancreatic enzymes generate cytotoxic mediators in the intestine. (Translated from eng) *Shock* 27(3):296-304 (in eng).

45. Waldo SW, Rosario HS, Penn AH, & Schmid-Schönbein GW (2003) Pancreatic digestive enzymes are potent generators of mediators for leukocyte activation and mortality. (Translated from eng) *Shock* 20(2):138-143 (in eng).

46. Fitzal F, DeLano F, Young C, Rosario H, & Schmid-Schönbein G (2000) Pancreatic protease inhibition during shock attenuates cell activation and peripheral inflammation. *Journal of vascular research* 39(4):320-329.

47. Mitsuoka H & Schmid-Schönbein GW (2000) Mechanisms for blockade of in vivo activator production in the ischemic intestine and multi-organ failure. (Translated from eng) *Shock* 14(5):522-527 (in eng).

48. Kistler E, Lefer A, Hugli T, & Schmid-Schönbein G (2000) Plasma activation during splanchnic arterial occlusion shock. *Shock* 14(1):30.

49. Penn AH, Kistler EB, & Schmid-Schönbein GW (2008) Bioengineering of inflammation and cell activation: Autodigestion in shock. *Bioengineering in Cell and Tissue Research*, eds Artman G & Chien S (Springer Verlag, Berlin), pp 511-527.

50. Tamion F, *et al.* (1997) Gut ischemia and mesenteric synthesis of inflammatory cytokines after hemorrhagic or endotoxic shock. (Translated from English) *Am J Physiol-Gastr L* 36(2):G314-G321 (in English).

51. Roumen RM, Hendriks T, Wevers RA, & Goris JA (1993) Intestinal permeability after severe trauma and hemorrhagic shock is increased without relation to septic complications. (Translated from eng) *Arch Surg* 128(4):453-457 (in eng).

52. Roumen RM, *et al.* (1993) Cytokine patterns in patients after major vascular surgery, hemorrhagic shock, and severe blunt trauma. Relation with subsequent adult respiratory distress syndrome and multiple organ failure. (Translated from eng) *Ann Surg* 218(6):769-776 (in eng).

53. Rupani B, *et al.* (2007) Relationship between disruption of the unstirred mucus layer and intestinal restitution in loss of gut barrier function after trauma hemorrhagic shock. (Translated from eng) *Surgery* 141(4):481-489 (in eng).

54. Sutherland NG, Bounous G, & Gurd FN (1968) Role of intestinal mucosal enzymes in the pathogenesis of shock. (Translated from eng) *J Trauma* 8(3):350-380 (in eng).

55. Mitsuoka H, Kistler EB, & Schmid-Schönbein GW (2000) Generation of in vivo activating factors in the ischemic intestine by pancreatic enzymes. (Translated from eng) *Proc Natl Acad Sci U S A* 97(4):1772-1777 (in eng).

Chapter 2

Transport of Pancreatic Digestive Enzymes during Intestinal Ischemia Across de Intestinal Wall

2.1 Introduction

Ischemic injury of the small intestine as a result of insufficient blood flow in the splanchnic circulation manifests in different conditions, such as small bowel obstruction (1, 2), arterial and venous thrombosis (3), or vasoconstriction after cardiac surgery (4-6). Patients with splanchnic ischemic injury are at risk of developing shock and multiple organ failure (7-12) with consequent high morbidity and mortality (13-17). However, the mechanism by which these events take place is still not fully understood, increasing evidence suggests that pancreatic digestive enzymes play an important role in different models of shock (18-23). Digestive enzymes and their products located in the lumen of the intestine are potential major candidates to mediate the inflammation and necrosis in shock. It has been shown that ischemic intestines, contain cytotoxic mediators and that this cytotoxicity may be the result of digestive enzymes from the intestinal lumen acting on either the tissue of the intestine or on ingested food (18). Among the four general

classes of digestive enzymes of the pancreas (proteases, amylases, lipases and nucleases) the major proinflammatory and cytotoxic factors have been found to be generated by means of serine proteases and lipases (19).

2.2 Use of Protease Inhibitors as Treatment Shock

Blockade of digestive enzymes in the lumen of the intestine prior to intestinal ischemia has been reported to prevent intestinal cell dysfunction, generation of inflammatory and/or cytotoxic mediators and their leakage into the systemic circulation (18, 23-27). It was demonstrated that the cytotoxicity found in mediators of shock can be prevented by the use of broad-spectrum pancreatic digestive enzyme inhibitor such as phenylmethylsulfonyl fluoride (PMSF) (18) and aprotinin (24). In addition blockade of pancreatic digestive enzymes with nafamostat mesilate (ANGD) or gabexate mesilate (FOY) in the lumen of the ileum serves to reduce the level of inflammatory mediators in shock produced by occlusion of the superior mesentery artery (23, 27). Furthermore, while intraluminal pancreatic protease inhibition improves mean arterial blood pressure and reduces the formation of neutrophil cell activators during shock (27); intravenous administration of a serine protease inhibitor during intestinal ischemia and reperfusion has only a mild effect on mean arterial blood pressure and neutrophil cell activation (28). It was further shown that the protection provided by protease inhibition is not enhanced by supplementation with oxygen free radical blockers such as Allopurinol, indicating that oxygen free radicals may not the major player in the shock cascade (23, 27). In addition to serine protease inhibitors, lipase inhibitor such as orlistat has also been shown to reduce cytotoxicity resulting from free fatty acids (24).

2.3 Tranexamic Acid as a potential new treatment for shock

Tranexamic acid (TA) is a synthetic derivative of the amino acid lysine that exerts its antifibrinolytic effect though the reversible blockade of the lysine binding site on plasminogen molecules (29, 30). TA also inhibits thrombin (30) and enterokinase mediated conversion of trypsinogen to trypsin (31). TA is usually intravenously administered at 10 mg/kg body weight followed by infusion of 1mg/kg every hour. At this dose TA reduces postoperative blood losses in patients undergoing cardiac surgery with cardiopulmonary bypass (32). TA has similar efficacy to aprotinin and it is 5-10 times more potent in binding to plasminogen/plasmin molecules as compared to ε-aminocaproic acid (EACA). Maximum plasma concentration of TA are attained within 3 hours of an oral dose (32) and over 95% is eliminated unchanged in the urine after 24 hours (32). Since TA is already used in the clinic as an antifibrinolytic agent and due to its potential to inhibit trypsin by different pathways, TA offers an opportunity to be used as an enteral treatment during intestinal ischemia.

2.4 Aims of this Chapter

The hypothesis of the study presented in this chapter is that under normal conditions luminal pancreatic serine proteases are contained in the intestinal lumen, however during intestinal ischemia these enzymes enter the intestinal wall and thereby exacerbate intestinal injury. Thus, the aim is to examine the levels of enzyme activity in the intestinal wall during early periods of intestinal ischemia. The extent to which tranexamic acid injection into the lumen of the intestine prior to ischemia affects the levels of enzyme activity in the intestinal wall was determined. Furthermore, I

investigated whether digestive enzymes find access into the systemic circulation after entering the intestinal wall and whether this is prevented by TA treatment in the lumen of the intestine.

2.5 Materials and Methods

2.5.1 Animal Groups: All animal protocols were reviewed and approved by the University of California San Diego Animal Subjects Committee. Male Wistar rats (300-350g, Harlan Sprague Dawley Inc, Indianapolis, IN) were randomly assigned to one of five groups: a sham group (SHAM), two ischemic groups with splanchnic arterial occlusion (SAO) for 15 and 30 min (SAO15, SAO30) and two ischemic SAO groups with enteral tranexamic acid (TA) treatment (SAO15+TA, SAO30+TA); n=4 per group.

2.5.2 Shock model: Rats were kept on solid food restriction with water ad libitum for 12 hours prior to surgery, tranquilized with Xylazine (20 mg/ml, 0.2 μL/g BW) and anesthetized with Nembutal (50 mg/ml, 1 μL/g BW), followed by cannulation of the left femoral vein and artery. In the SHAM and SAO groups 0.9% normal saline (NS), 3ml/100g BW, was injected into the lumen of the intestine while in the treatment group (SAO+TA) tranexamic acid (Sigma Scientific, St. Louis, MO), 1 mg/g BW, in NS was used. After 30 min the superior mesenteric and celiac arteries were isolated and ligated (SAO and SAO+TA groups) or isolated without ligation (SHAM). Animals were euthanized after 30 min (SHAM) and after 15 or 30 min (SAO and SAO+TA).

2.5.3 Tissue processing: Jejunal segments (~1 cm in length) without removal of luminal contents were suspended in Tissue-Tek O.C.T. Compound (Sakura Finetek, Torrance,

CA), snap frozen in isopentane/liquid nitrogen, and stored in -80^{o}C for further analysis. Cryosections (5 µm thickness) along the longitudinal axis of the villi were used throughout all experiments.

2.5.4 Intestine homogenates: In separate experiments, 1cm equally spaced segments of the intestine were excised. For western blot assays luminal contents were washed with NS, followed by homogenization with CelLytic™ (Sigma) in the presence of protease inhibitors (5mM EDTA, 5mM N-Ethylmaleimide, 25mM iodoacetamide, 5mM benzamidine, 300mM acarbose, 5mM 6-aminocaproic acid, 1mM protease inhibitor cocktail, (Sigma Scientific)) to inhibit further degradation. For enzyme activity assays intestinal luminal contents were retained to measure enzyme activity in the whole intestine and homogenization with CelLytic™ was done without addition of protease inhibitors. Homogenates were centrifuged (16,000g for 15 min at 4°C), the supernatant was collected and protein concentration was assessed with the bicinchoninic acid protein assay (Thermo Scientific, Rockford, IL).

2.5.5 Enzyme Activity: The enzyme activity of specific enzymes were carried out at 37^{o}C with substrates specific for chymotrypsin (glutaryl-L-phenylalanine 7-amido-4-methylcoumarin, 49737, Sigma Scientific) (33), trypsin and papain (Nα-benzoyl-L-arginine-7-amido-methylcoumarin hydrochloride B7260, Sigma Scientific) (34), and human leukocyte and porcine pancreatic elastase (N-methoxysuccinyl-Ala-Ala-Pro-val-7-amido-4-methylcoumarin, M9771, Sigma Scientific) (35). The substrates were diluted in the buffers as previously described (34-36). The initial rates of hydrolysis were measured by the fluorescent intensity of 7-amido-4-methylcoumarin cleaved from the substrates by

the enzymes: trypsin from porcine pancreas (T0303, Sigma Scientific), chymotrypsin from bovine pancreas (C4129, Sigma Scientific), and elastase from porcine pancreas (E1250, Sigma Scientific). Fluorescence was measured with a microplate reader (SpectraMax Gemini XS model; Molecular Devices) at 380nm emission and 460nm excitation wavelengths.

Inhibitory properties of TA was determined by incubation of 50μg/ml of the corresponding enzyme with or without TA (300mM, 160mM and 50mM) for 1 hour followed by incubation with varying concentrations of the specific substrates. Enzyme activity of intestine homogenates was determined by homogenization of jejunal sections without enzyme inhibitors, as previously described. 100μg of protein was loaded in each well containing the specific fluorescent substrates for trypsin, chymotrypsin or elastase (50μM). The initial velocity of the reaction was calculated as the rate of fluorescent units per μg of protein per minute.

2.5.6 Western blot: Jejunal sections were homogenized and centrifuged (16,000g for 15 min at 4°C) with CelLytic™ M buffer (Sigma Scientific), without protease inhibitors. Protein concentration was assessed with the bicinchoninic acid protein assay (23225, Thermo Scientific, Rockford, IL). Samples were prepared in SDS loading buffer (Biorad, Richmond, CA), reduced with β-mercaptoethanol and boiled for 4 min at 100^{o}C; 20 μg of protein/lane were loaded for each group and run in an SDS polyacrylamide gel and then transferred onto nitrocellulose membranes. Afterwards membranes were blocked in 5% non-fat milk for 1 hour and incubated in primary antibodies overnight against trypsin (sc-137077, Santa Cruz Biotechnology, 1:1000 dilution) and chymotrypsin (ab35694,

Abcam, Cambridge, MA, 1:300 dilution). Membranes were incubated with appropriate secondary antibodies (Santa Cruz Biotechnology) and developed using the chemiluminescent substrate (Super Signal West Pico, Thermo Scientific). The exposed x-ray films were scanned and analyzed using the gel analysis tool of the NIH ImageJ software.

2.5.7 Histology: Cryosections were fixed in cold acetone followed by staining with hematoxylin (Vector Lab, Burlingame, CA) and eosin (Sigma Scientific) mounted with VectaMount Permanent Mounting Medium (Vector Lab) and observed under an inverted microscope (Olympus IX70, 20X objective, 0.5 numerical aperture).

2.5.8 In-situ Zymography: Enzyme activity of serine protease was assessed by visualization of fluorescence resulting from the proteolytic cleavage of intramolecularly quenched substrates (37-39) specific for chymotrypsin (2mM), trypsin (1mM) and elastase (1mM), as described in the Section on Enzyme Activity. Each substrate was diluted to its final concentration in 1% low melting point agarose (Sigma Scientific) and kept at 37^{o}C. 10μl substrate was added on sections thawed at 37^{o}C followed by gelation for 5 min at 4^{o}C. The tissue/substrate was incubated for 1 hour at 37^{o}C and immediately observed with an inverted microscope (20X objective) using appropriate fluorescent filters.

2.5.9 Gelatin zymography: Plasma from the femoral artery was aliquoted and stored in -80^{o}C until use. Plasma samples (0.6 μl), with only a single freeze/thaw cycle, were mixed in loading buffer (Biorad) without reducing agent or boiling and loaded (10 μl/well) into 12% SDS acrylamide gels cross-linked with gelatin (1 mg/ml). After electrophoresis the

gels were incubated in renaturing buffer (Titron-X100 2.5% v/v) with gentle agitation for 60 min at room temperature. Subsequently, the gels were incubated in developing buffer (50 mM Tris base, 150 mM NaCl, 5 μM ZnCl2, 5 mM CaCl2.3H2O, 3 mM sodium azide) overnight for 16 hrs at 37^{o}C. In addition, other gels were renatured and developed in the presence of 300mM TA. Afterwards the gels were stained with 0.5% coomassie blue in 40% methanol and 10% acetic acid for 4 hrs and destained with destaining buffer (40% ethanol, 10% acetic acid) twice for 30 min.

2.5.10 Image analysis: Images were digitized (8 bit, 0 to 255 light intensities), corrected for random noise and background illumination followed by digital measurements of the intensity of the fluorescent or light signal in digital units (D.U., NIH ImageJ software). Mean fluorescent/light intensity is defined as the sum of all pixel intensities divided by the sum of all pixels in the selected area (D.U./pixel) (Figure 1); total fluorescent/light intensity is defined as the sum of all the pixel intensities in the selected area (D.U.) (Figure 1). The intestinal villi length was measured as the height from the tip to the base of the villi. The crypt length was measured from the base of the villi to the submucosa. Villi thickness was measured as the width at the base of the villi. Mucosal muscle thickness was measured as the length from the submucosa to the serosa.

Forty measurements per animal (n=4) per group were made. The enzyme activity on the intestinal tissue was measured as the mean fluorescent intensity on micrographs of four cryosections per animal (n=4) per group. A rectangular area covering 2-3 villi from the villi tip to the muscle was selected for each micrograph; the intestine was outlined and the mean fluorescent intensity was calculated on the outlined area. The enzyme

penetration from the tip to the intestinal wall was determined as the mean fluorescent intensity on an area covering a single villi; each intestinal crossection was further divided into five regions from the villi tip to the serosa: villi tip, mid villi, crypt and muscularis mucosa, submucosa, and muscularis externa. Sixteen villi were measured over four sections per animal (n=4) per group.

2.5.11 Statistical Analysis: Results are presented as mean±SEM. Unpaired comparisons of mean values between groups were carried out by one-way ANOVA or two-way ANOVA followed by Bonferroni post-hoc. $P<0.05$ was considered significant.

2.6 Results

2.6.1 Intestinal morphology after SAO: The SHAM group had normal villi with intact epithelial cells. Lesions were seen already 15 min after SAO with the development of subepithelial spaces and denudation of the epithelial cells near the tip of the villi; a pronounced injury was observed after 30 min SAO with complete degradation of the villus tip. Intraluminal treatment with TA prevented villi injury (Figure 2.2). The villi length decreased by 10% after 15 min SAO and significantly decreased by 49% after 30 min SAO (Figure 2.3). Blockade of digestive enzymes with TA did not prevent reduction in villi length (Figure 2.3); and the average crypt length remained constant among groups. The villi thickness significantly increased by 31% after 30 min SAO as compared to SHAM; and there was a similar trend towards an increase of villi thickness in the presence of TA (Figure 2.3). The thickness of the muscularis exterior remained constant among groups.

2.6.2 Inhibitory profile of Tranexic Acid in vitro: Tranexamic acid (TA) was incubated with serine proteases 50μg/ml (trypsin, chymotrypsin and elastase) to test its ability to inhibit them. TA at 300mM inhibited trypsin activity by 86%, 160mM TA inhibited trypsin by 75% and 50mM TA inhibited it by 47% (Figure 2.4A). TA did not inhibit chymotrypsin and slightly inhibited elastase (Figure 2.5A and 2.6A). The kinetic parameters of TA with the different enzymes are presented in (Figures 2.4B, 2.5B and 2.6B).

2.6.3 Enzyme activity of whole intestine homogenates: Protein levels of these enzymes the luminal contents for 4 animals are shown via western blot (Figure 2.7A,B).The activity levels of these digestive enzymes in the luminal contents (50μg of protein) of SHAM animals were high with trypsin having the highest activity (Figure 2.7C). The ability of TA (~200mM) to inhibit these digestive enzymes was tested in-vivo (Figure 2.8); both trypsin and chymotrypsin activity in whole intestine homogenates was significantly increased after 30 min of ischemia compared to sham animals. Whole intestinal homogenates in the TA treatment groups displayed a trend of decreased trypsin and chymotrypsin activity; elastase activity did not differ among groups. Protein levels of these enzymes remained constant among all groups for all three enzymes (Figure 2.9).

2.6.4 Enzyme activities in the intestinal wall after SAO: Next the ability of digestive enzymes to enter the wall of the intestine during intestinal ischemia was determined. After incubation with the specific substrates little enzyme activity was observed in the mucosa of the SHAM group, the enzyme activity were significantly elevated in the ischemic groups but not in the TA treatment groups (Figure 2.10, 2.12, 2.14). Trypsin

activity in the intestinal tissue increased 1.6X after 15 min SAO and significantly increased 3.4X after 30 min SAO as compared to SHAM. The presence of TA served to decrease trypsin activity on average by 28% after 15 min SAO and 47% ($p<0.05$) after 30 min SAO compared to SAO without treatment (Figure 2.11).

Chymotrypsin activity exhibited the same trend (Figure 2.13); the activity increased 1.2X after 15 min SAO and significantly increased 2.8X after 30 min SAO as compared to SHAM. In the presence of TA, the chymotrypsin activity significantly decreased by 43% after 30 min SAO as compared to SAO without treatment. Elastase activity also showed a similar trend (Figure 2.15); the enzyme activity significantly increased 2X after 15 min SAO and significantly increased 2.6X after 30 min SAO. In the presence of TA, elastase activity decreased on average by 34% after 15 min SAO and significantly decreased 33% after 30 min SAO as compared to SAO without treatment. The three different proteases already started to penetrate the epithelium of the villus tip at 15 min; elastase had the most activity and penetration at this time point (Figure 2.11.B, 2.13.B, and 2.15.B).

After 30 min ischemia, the villi were completely filled with digestive enzymes from the tip to the crypts. An increased enzymatic activity that was not inhibited by TA treatment was also observed in the submucosa area during ischemia.

Western blot analysis of intestine homogenates after removal of luminal contents confirmed increased levels of trypsin, chymotrypsin and elastase in the wall of the intestine (Figure 2.16A, B). The relative density of trypsin protein levels with respect to SHAM and β-actin increased 2X after 15 min SAO and significantly increased 5.2X after

30 min SAO, the relative density after luminal treatment with TA followed by 30 min SAO decreased by 34% as compared to 30 min SAO without treatment. Similarly, relative density of chymotrypsin protease values with respect to SHAM and β-actin increased 1.3X after 15 min SAO and significantly increased 2.3X after 30 min SAO, with TA treatment the relative density after 30 min SAO decreased by 56% as compared to 30 min SAO without treatment. Relative density of elastase with respect to SHAM and β-actin increased 1.1X after 15 min SAO and significantly increased 2.1X after 30 min SAO, with TA treatment the relative density after 30 min SAO decreased by 10% as compared to 30 min SAO without treatment.

2.6.5 Enzyme activities in rat plasma after SAO: To determine whether digestive enzymes from the lumen of the intestine are transported into the systemic circulation during ischemia gelatin zymography was carried out in rat plasma samples after the end of each surgery. A band at about 20 kDa was observed at the same location as porcine trypsin (Figure 2.17A). When the gel was renatured and developed in the presence of 300 mM TA the bands disappeared (Figure 2.17A). The relative density of the trypsin band with respect to the SHAM group increased by 20% after 15 min and significantly increased by 80% after 30 min SAO. With TA treatment, the relative density after 30 min SAO significantly decreased 28% as compared to 30 min SAO without treatment (Figure 2.17B).

Western blot shows increased levels of trypsin in plasma after SAO (Figure 2.18A). The relative density of plasma trypsin levels compared to SHAM increased 2.3X after 15 min and significantly increased 2.8X after 30 min SAO (Figure 2.18B).

Treatment with TA in the lumen of the intestine served to reduce the relative density by 27% after 15 min and by 25% after 30 min SAO as compared to the group without treatment (Figure 2.18B). Plasma chymotrypsin density levels were also increased in the SAO group and reduced after luminal inhibition with tranexamic acid (Figure 2.18B). Density levels of elastase did not significantly increased after ischemia but where significantly lower compared to the 30 min ischemic group (2.18B)

2.7 Discussion

The current results in the rat model of SAO show morphological damage to the intestine after 15 min and major damage after 30 min of intestinal ischemia. The damage to the mucosal barrier is accompanied by enhanced enzymatic activity of digestive serine proteases (trypsin, chymotrypsin, and elastase) in the wall of the intestine and is followed by appearance of a low molecular weight protease enzymatic activity in plasma. Tranexamic acid (TA) treatment in the lumen of the intestine prior to intestinal ischemia reduced villi damage, decreased enzyme activity in the intestinal wall.

Previous studies have shown that blockade of digestive enzymes with broad spectrum serine protease inhibitors such as aprotinin, gabexate mesylate, and nafamostat mesylate protect against villi destruction, inflammation in the intestine and the central circulation, and attenuate multi-organ failure in different models of shock (21, 23, 25-27). In this study we show that TA treatment in the lumen of the intestine appears to significantly prevent intestinal injury. TA, a plasminogen inhibitor used clinically as an anti-fibrinolytic agent (29, 30), also inhibits thrombin (30) and enterokinase mediated conversion of trypsinogen to trypsin (31). In our in-vitro experiment we see inhibition of

86% of trypsin activity with 300 mM TA and 75% with 160 mM; in the in-vivo experiments we used a dose of 1 mg/g body weight dissolved in 3ml/100g body weight, corresponding to approximately 200 mM. In the clinical setting TA is recommended at a dose of 10 mg/kg/day; even though the dose used in the current study is higher, it is within the inhibitory range for trypsin and below the $LD50_{oral}$ in the rat, (3 mg/g body weight) (31).

We have found, using equimolar concentrations of specific substrates with the same fluorescent hydrolysis product, that trypsin levels in whole intestine homogenates of the rat are higher during ischemia as compared to chymotrypsin and elastase; and that luminal TA treatment prior to ischemia resulted in inhibition of trypsin and to some extent inhibition of the other two enzymes in whole intestine homogenates. In addition, we show by in-situ zymography that the activity of all three enzymes is increased in the intestinal wall and that TA injection into the lumen of the intestine prior to intestinal ischemia not only results in decreased activity of trypsin in the wall of the intestine but also decreased chymotrypsin and elastase activity. However, our in vitro studies confirm that TA inhibits purified trypsin but did not effectively inhibit chymotrypsin or elastase. One possible explanation for this apparent discrepancy may be the fact that trypsin exhibits the highest proteolytic activity in the lumen of the intestine; it has also been shown in an ischemia/reperfusion model of shock that trypsin is capable of inducing accumulation of neutrophils and neutrophil derived MMP9 in the intestinal wall (26). Thus, it is possible that inhibition of trypsin by TA prevents the initial destruction of

some structures of the mucosal and epithelial barrier during ischemia and thereby attenuates entry and activation of other proteases into the intestinal wall.

In the current study we also found by use of gelatin zymography of plasma samples that during intestinal ischemia an increasing enzymatic activity of a low molecular weight enzyme that runs alongside purified trypsin. We also showed by Western blot higher levels of trypsin protein in plasma samples during ischemia as compared to sham; this evidence suggests that the enhanced proteolytic activity of the low molecular weight enzyme may be in part due to trypsin. Further studies to confirm the identity the enzyme responsible for the enzyme activity seen in the gelatin zymography needs to be carried out. The presence of enhanced enzyme activity in plasma during ischemia puts forward the idea that this activity may be due to pancreatic enzymes such as trypsin derived from the ischemic and injured intestine.

The evidence presented in this study indicates that trypsin among the digestive enzymes may be an important player in the development of ischemic injury. Once trypsin makes its way across the mucosal/epithelial barrier; it may activate other enzymes (38) and open a route of entry for other digestive enzymes to enter the intestinal wall and the systemic circulation.

Chapter 2 in full is submitted material to Shock journal as it appears in "Disruption of the Intestinal Mucin Layer Allows Entry of Digestive Enzymes during Early Periods of Intestinal Ischemia" by Chang M., Kistler E. B., Schmid-Schönbein G.W. The dissertation author is the primary author of this manuscript.

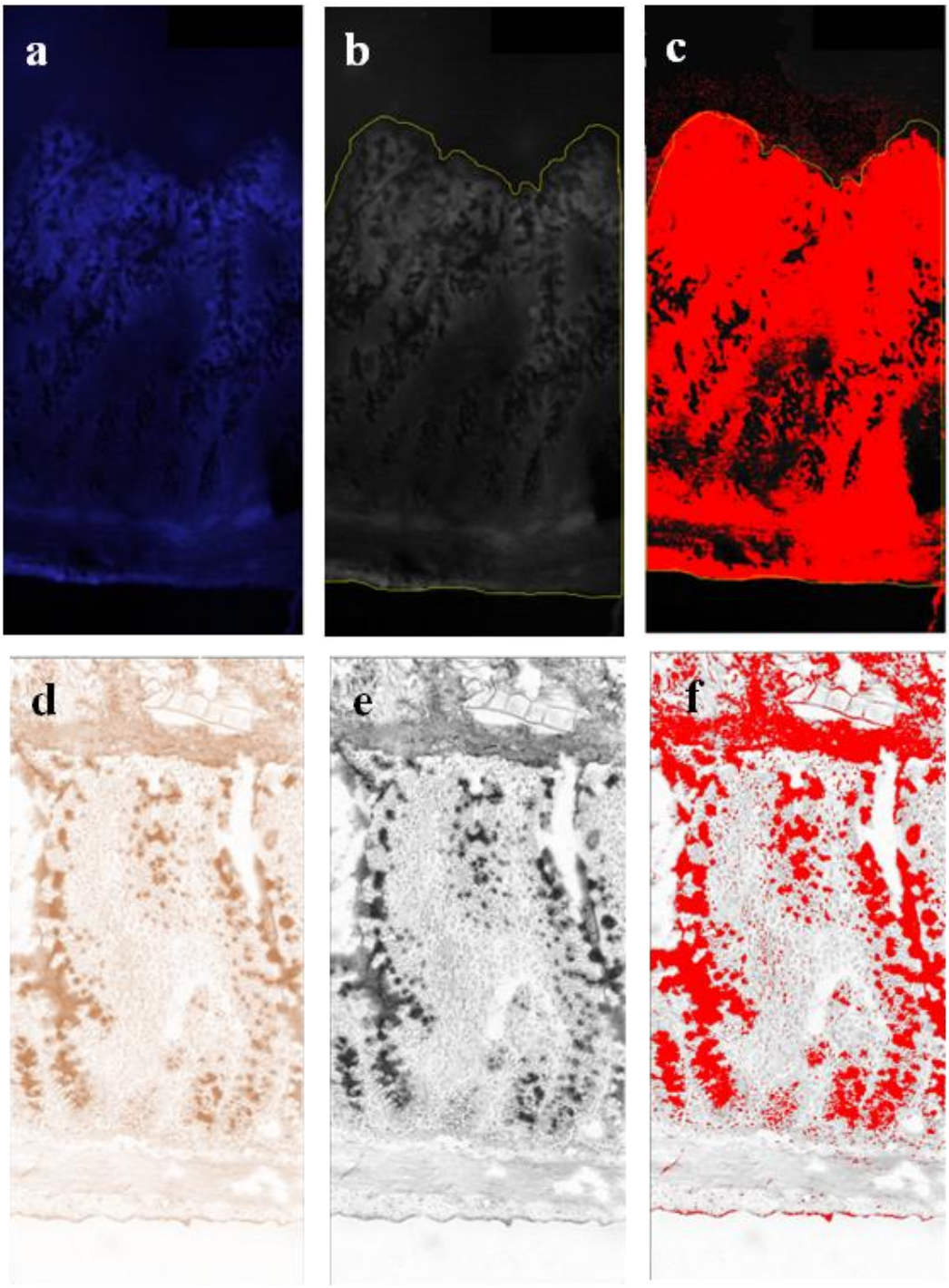

Figure 2.1 Image analyses. Images were corrected for random noise and background illumination and digitized to 8 bit a) Digital measurements of intensity of fluorescent b) area was selected and c) the sum of all pixels intensity divided by the sum of all pixels in selected area was measured (D.U/pixels^2) d) light signal was measured as f) the sum of all pixel intensities in the selected area (D.U).

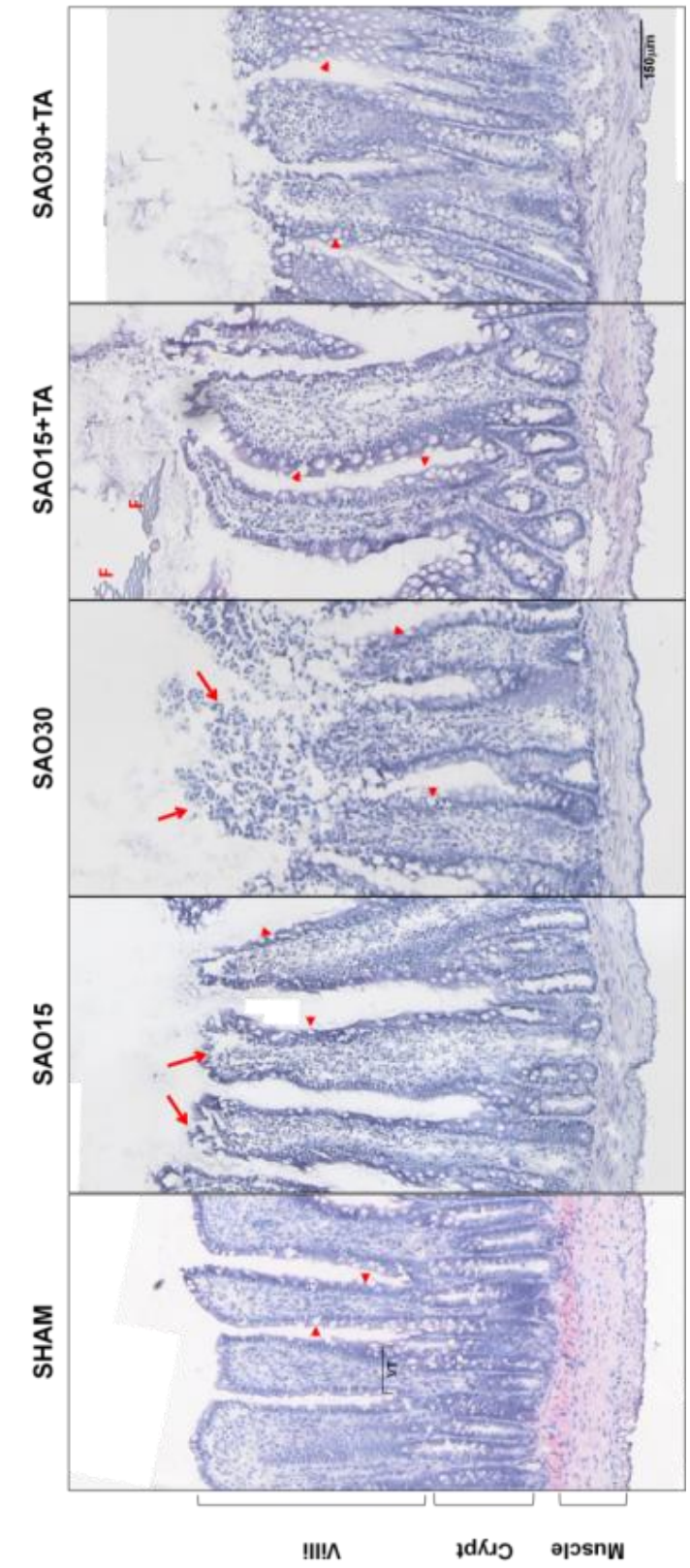

Figure 2.2 Intestinal morphology after SAO. Micrographs of jejunal frozen sections stained with hematoxylin and eosin. The sections were derived from frozen segments without removal of luminal food (F) or other luminal contents. Arrowheads show goblet cells and arrows show degeneration of villi.

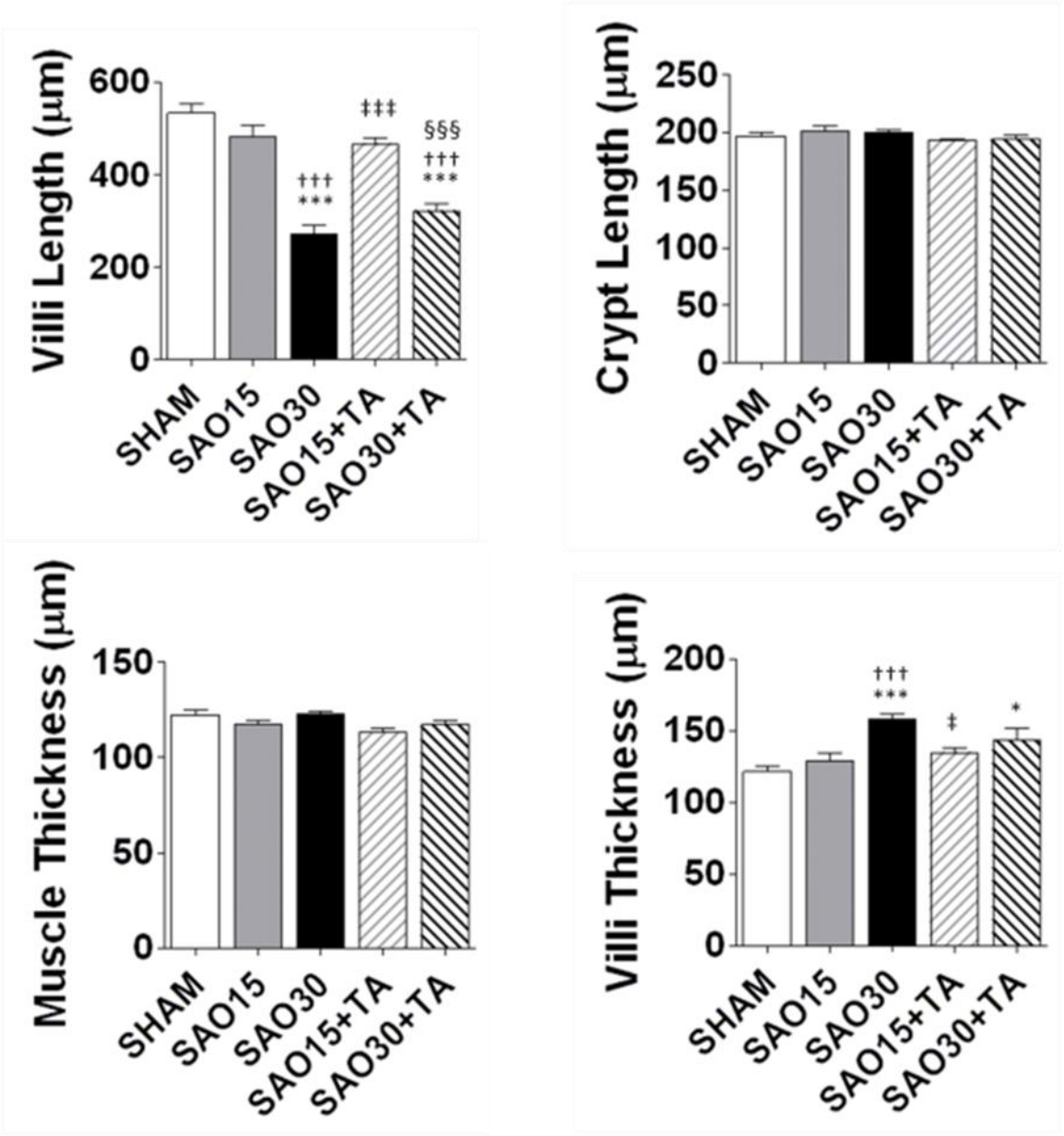

Figure 2.3 Measurements of villi parameters. Data shows mean length of villi and crypts as well as mean muscle layer and villi thickness (VT). Values are mean±SEM (n=4). *P <0.05, ***P<0.0001 compared to sham. †††P<0.0001 compared to 15 min SAO. ‡‡‡P<0.0001 compared to 30 min SAO, §§§P<0.0001 compared to 15 min SAO with Tranexamic Acid.

A

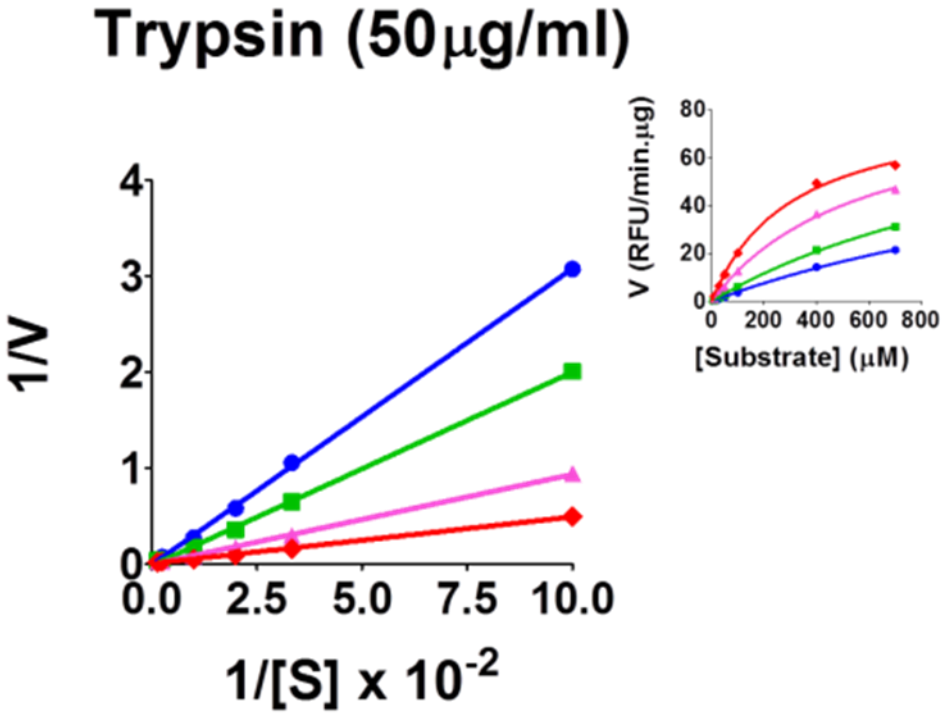

B

[TA]	Trypsin		
	V_{max}	K_m	R^2
300mM	81± 9	1915± 267	0.998
160mM	97± 8	1451± 163	0.998
50mM	87± 3	579± 41	0.998
0mM	84± 3	306± 22	0.996

Figure 2.4 Trypsin inhibitory profile with tranexamic acid. (**A**) Lineweaver-Burk Plot with inset Michaelis-Menten plot for trypsin inhibition with tranexamic acid with specific fluorescent substrate. **(B)** Values are mean±SEM of triplicate measurements, symbols used: TA 300mM (circle), TA 160mM (square), TA 50mM (triangle), TA 0mM (diamond). Enzyme kinetic parameters, V_{max} (RFU/min.µg), K_m (µM) for the enzymes with different concentrations of TA calculated after non-linear regression.

A

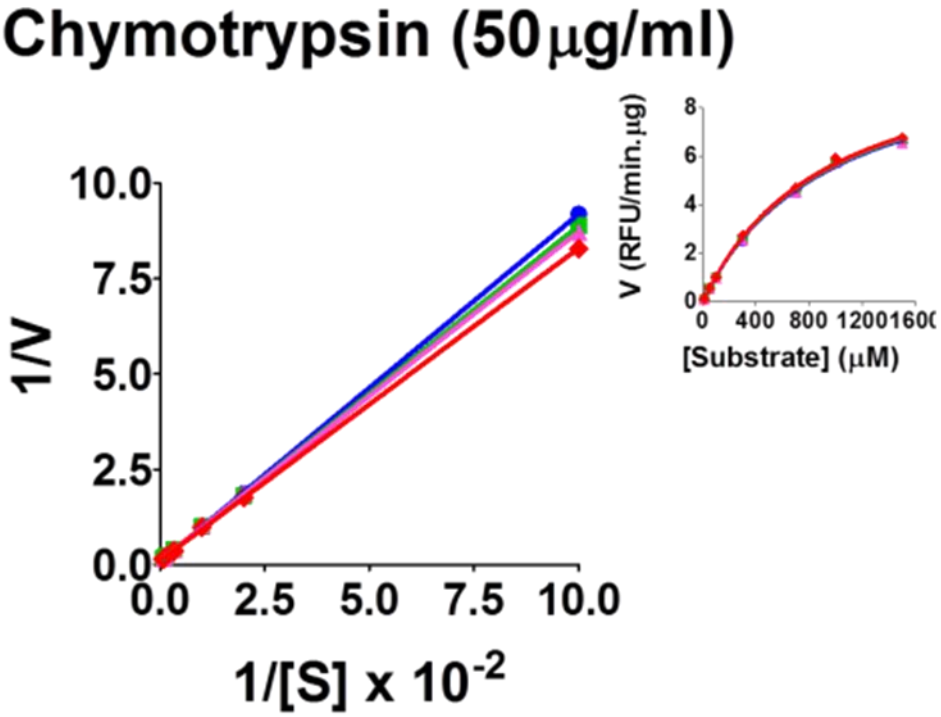

B

[TA]	Chymotrypsin		
	V_{max}	K_m	R^2
300mM	11± 0.4	972± 61	0.998
160mM	11± 0.3	999± 44	0.999
50mM	11± 0.4	985± 73	0.997
0mM	11± 0.3	911± 51	0.998

Figure 2.5 Chymotrypsin inhibitory profile with tranexamic acid. (**A**) Lineweaver-Burk Plot with inset Michaelis-Menten plot for chymotrypsin inhibition with tranexamic acid with cspecific fluorescent substrate. **(B)** Values are mean±SEM of triplicate measurements, symbols used: TA 300mM (circle), TA 160mM (square), TA 50mM (triangle), TA 0mM (diamond). Enzyme kinetic parameters, V_{max} (RFU/min.µg), K_m (µM) for the enzymes with different concentrations of TA calculated after non-linear regression.

A

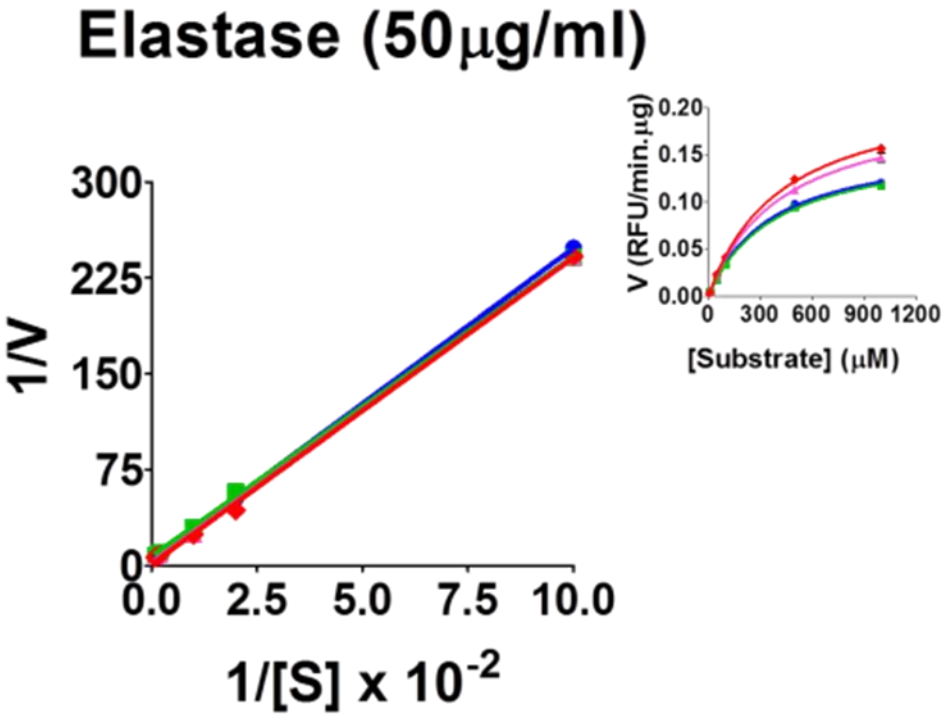

B

[TA]	Elastase		
	V_{max}	K_m	R^2
300mM	0.17± 0.004	364± 21	0.998
160mM	0.16± 0.004	389± 26	0.997
50mM	0.21± 0.007	425± 37	0.996
0mM	0.23± 0.006	424± 26	0.998

Figure 2.6 Elastase inhibitory profile with tranexamic acid. (**A**) Lineweaver-Burk Plot with inset Michaelis-Menten plot for elastase inhibition with tranexamic acid with specific fluorescent substrate. **(B)** Values are mean±SEM of triplicate measurements, symbols used: TA 300mM (circle), TA 160mM (square), TA 50mM (triangle), TA 0mM (diamond). Enzyme kinetic parameters, V_{max} (RFU/min.µg), K_m (µM) for the enzymes with different concentrations of TA calculated after non-linear regression.

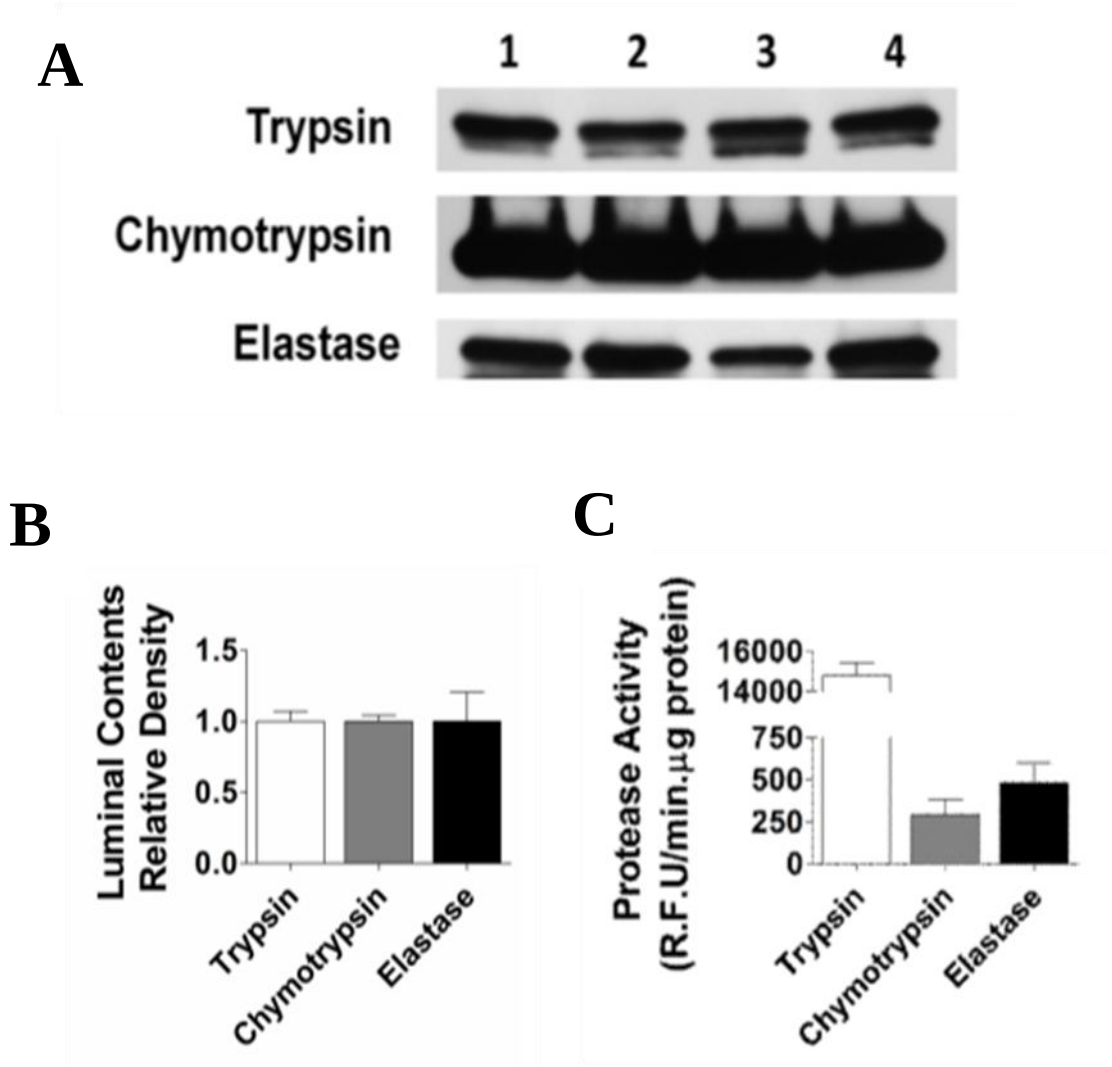

Figure 2.7 Protein levels of digestive enzymes in luminal contents. **(A)** Western blot of intestinal luminal contents for the enzymes; **(B)** Relative density of western blots, values are mean±SEM (n=4) **(C)** Activity of trypsin, chymotrypsin and elastase in intestinal luminal contents of sham animals using substrates specific for these enzymes.

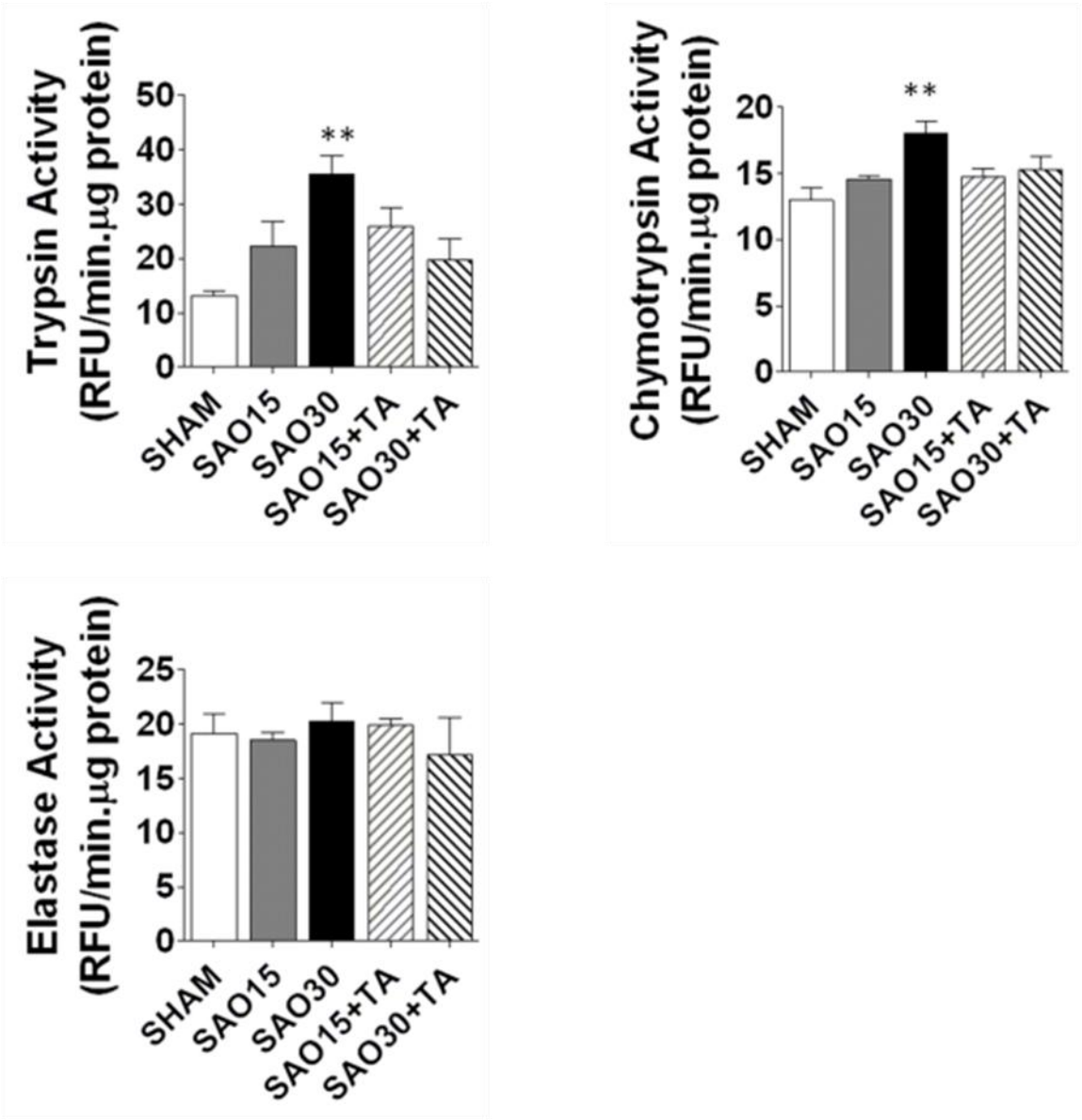

Figure 2.8 Enzymatic activity of whole intestine homogenates. In-vivo enzymatic activity of trypsin, chymotrypsin and elastase in whole intestine homogenates without removal of luminal contents, ** P<0.001 compared to sham.

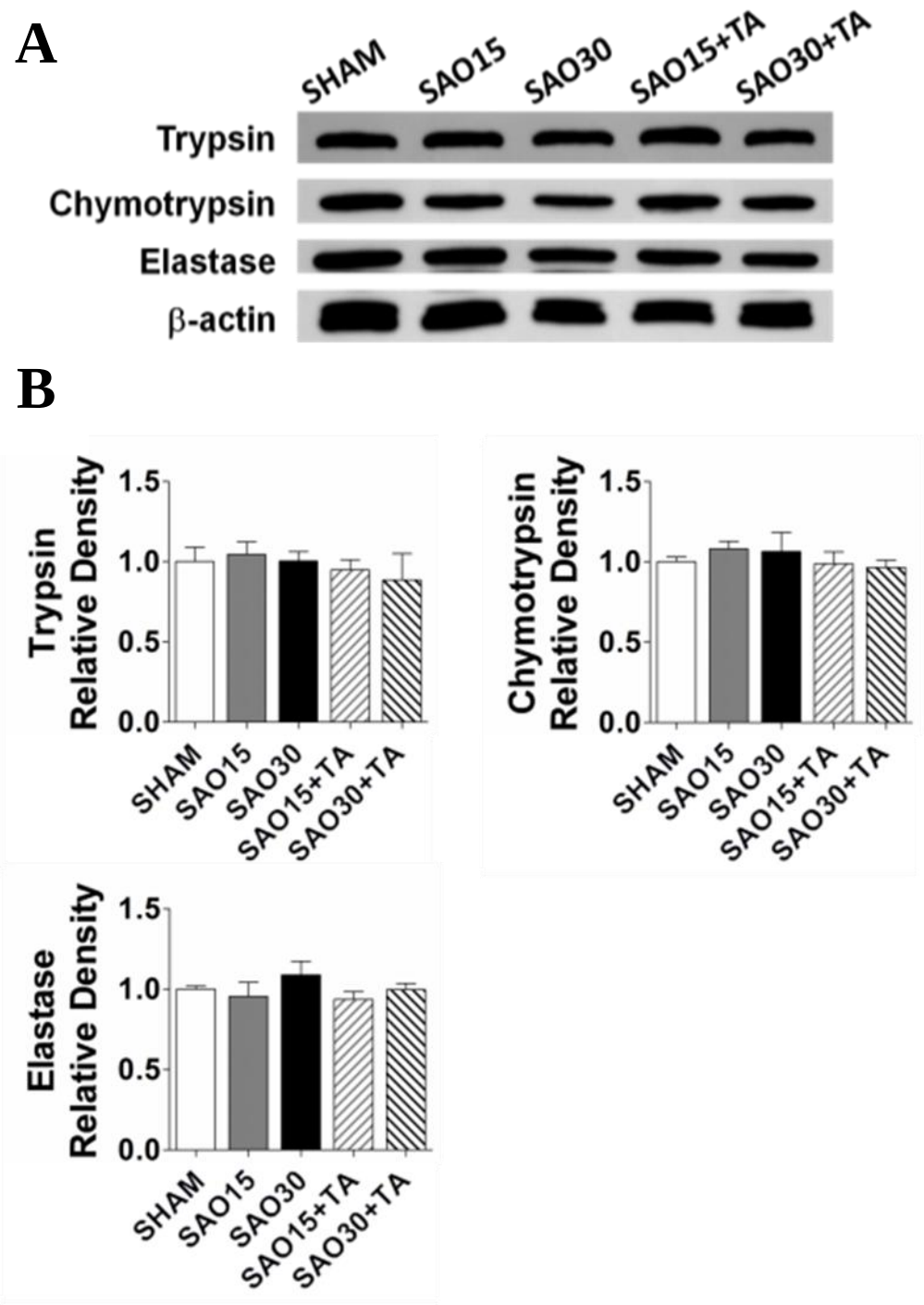

Figure 2.9 Protein levels of digestive enzymes in whole intestine homogenates. **(A)** Western blot of whole intestine homogenates for the three enzymes. **(B)** Relative density of westernblots, values are mean±SEM (n=4)/group.

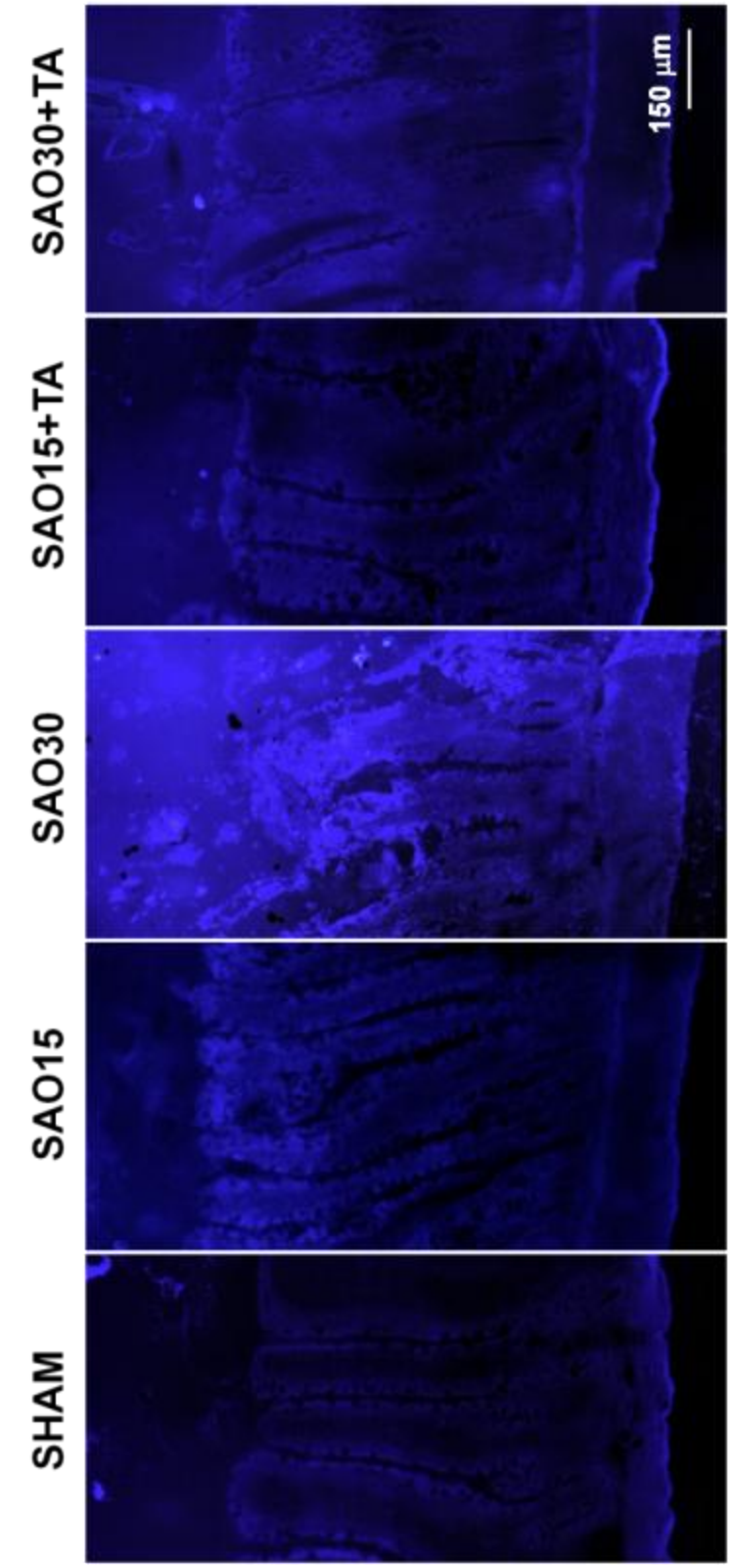

Figure 2.10 Trypsin in-situ zymography. Enzymatic activity of trypsin as assessed by *in-situ* zymography of specific substrates on jejunal sections .

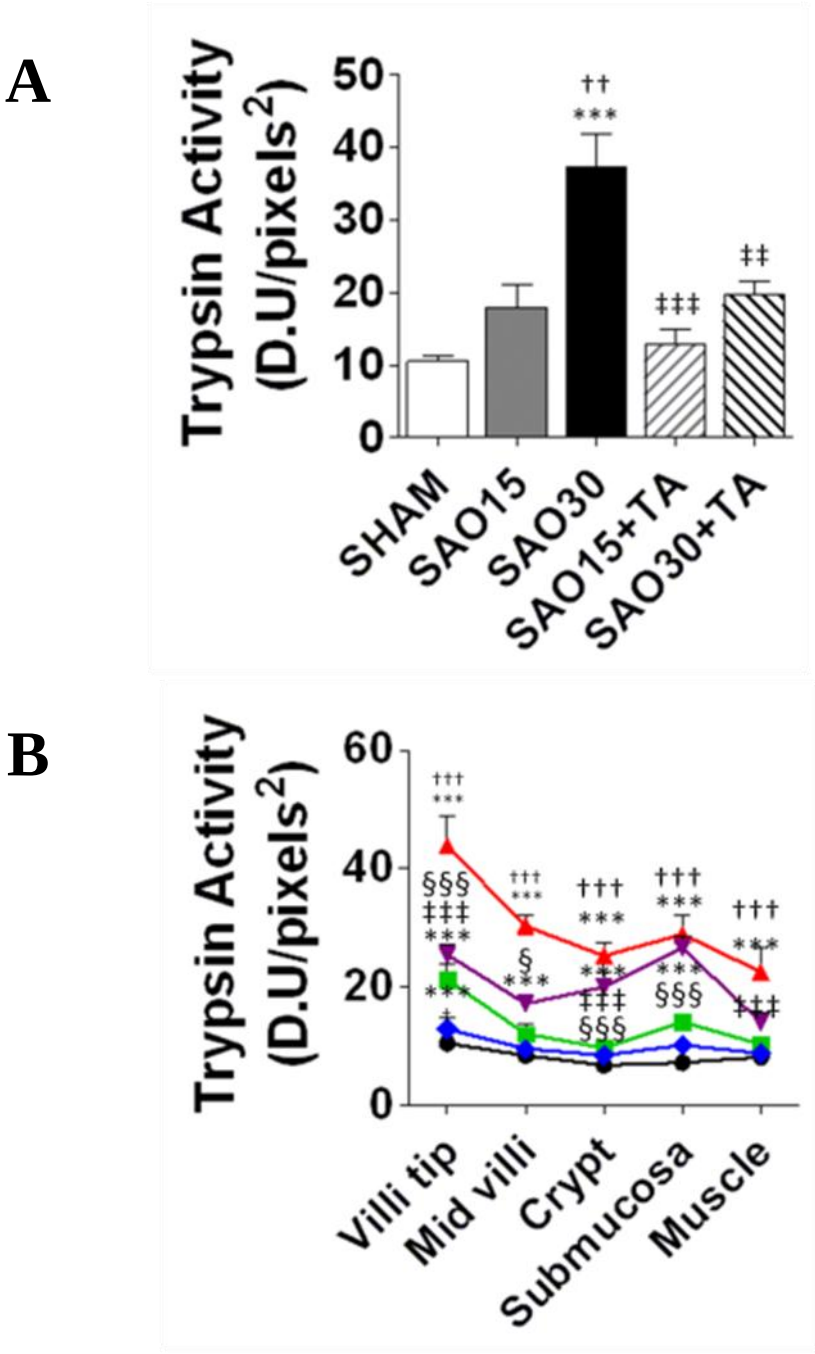

Figure 2.11 Trypsin activity measurements. (**A**) Trypsin enzymatic activity measured as mean fluorescent intensity of the fluorescent substrates. (**B**) Enzyme penetration from the villi tip to the intestinal muscle measured as mean fluorescent intensity of the fluorescent substrates. *P <0.05, **P<0.001, ***P<0.0001 compared to sham. †P <0.05, ††P<0.001, †††P<0.0001 compared to 15 min SAO. ‡P <0.05, ‡‡P<0.001, ‡‡‡P<0.0001 compared to 30 min SAO.

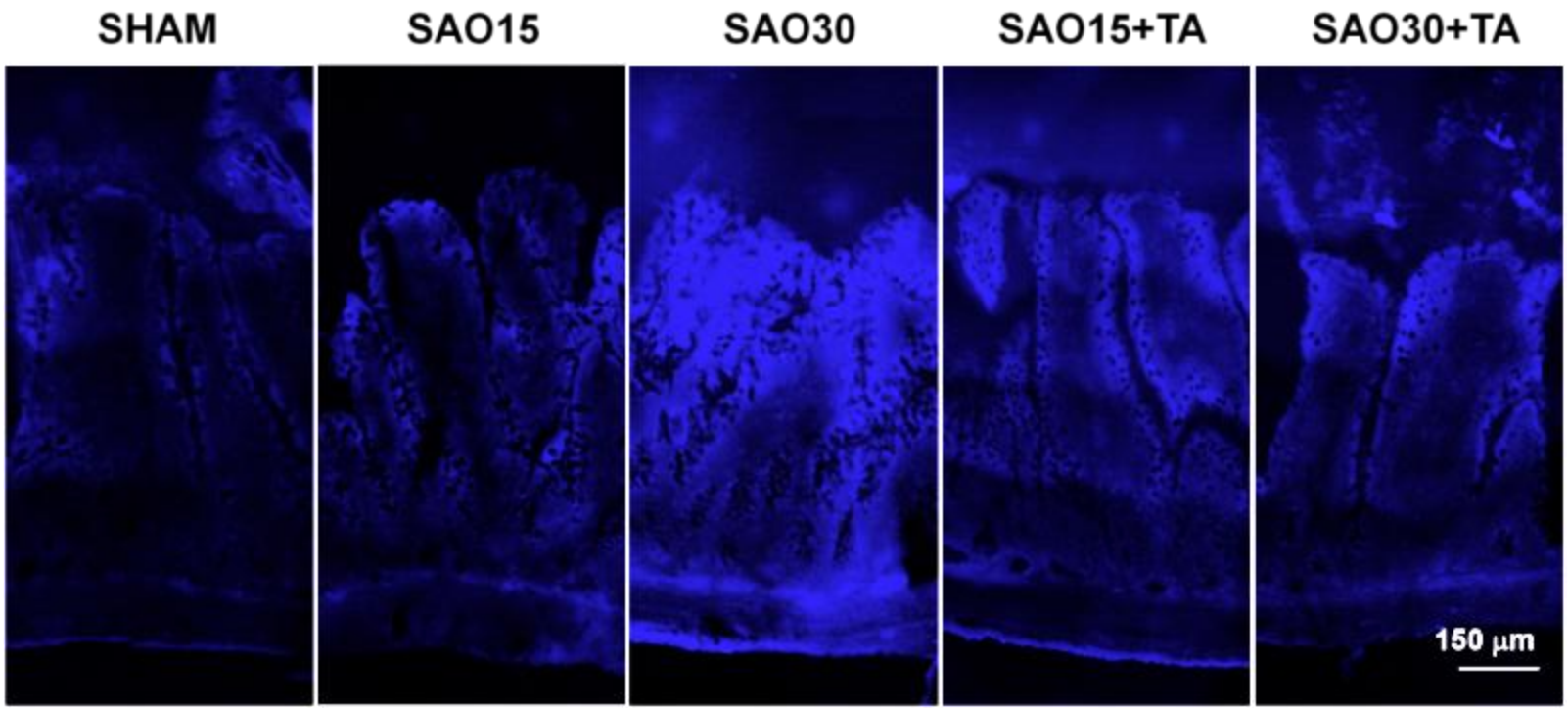

Figure 2.12 12Chymotrypsin in-situ zymography. Enzymatic activity of chymotrypsin as assessed by *in-situ* zymography of specific substrates on jejunal sections.

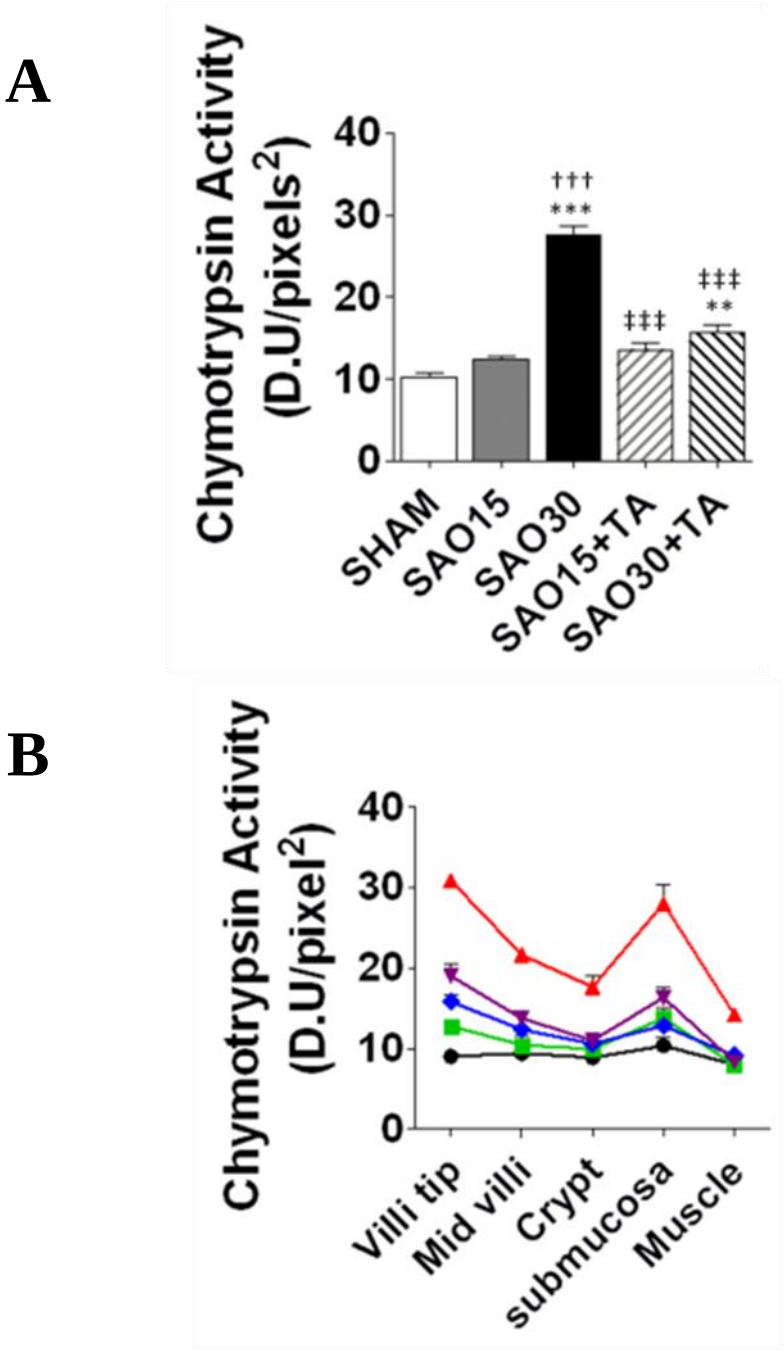

Figure 2.13 Chymotrypsin activity measurements. (**A**) Chymotrypsin enzymatic activity measured as mean fluorescent intensity of the fluorescent substrates. (**B**) Enzyme penetration from the villi tip to the intestinal muscle measured as mean fluorescent intensity of the fluorescent substrates. *P <0.05, **P<0.001, ***P<0.0001 compared to sham. †P <0.05, ††P<0.001, †††P<0.0001 compared to 15 min SAO. ‡P <0.05, ‡‡P<0.001, ‡‡‡P<0.0001 compared to 30 min SAO.

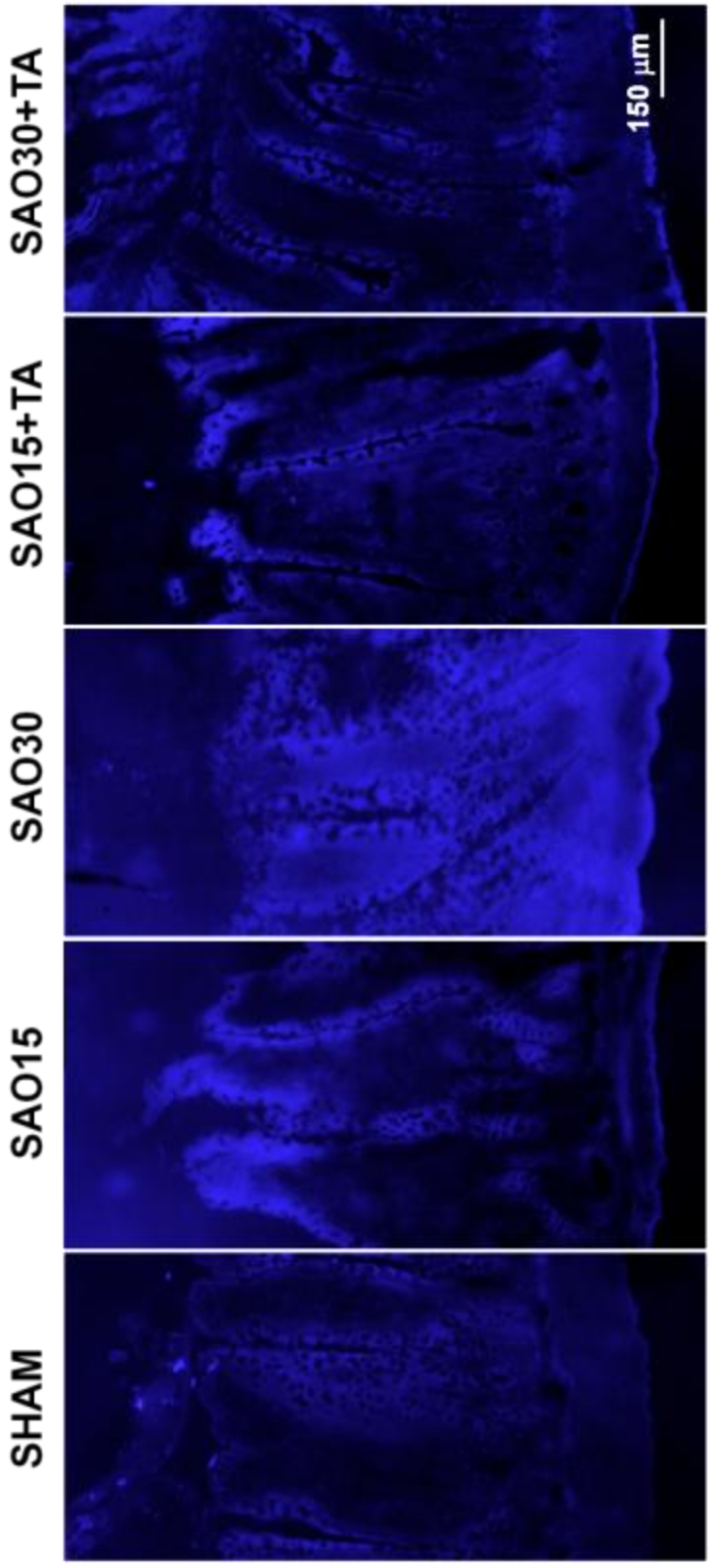

Figure 2.14 Elastase in-situ zymography. Enzymatic activity of elastase as assessed by *in-situ* zymography of specific substrates on jejunal sections.

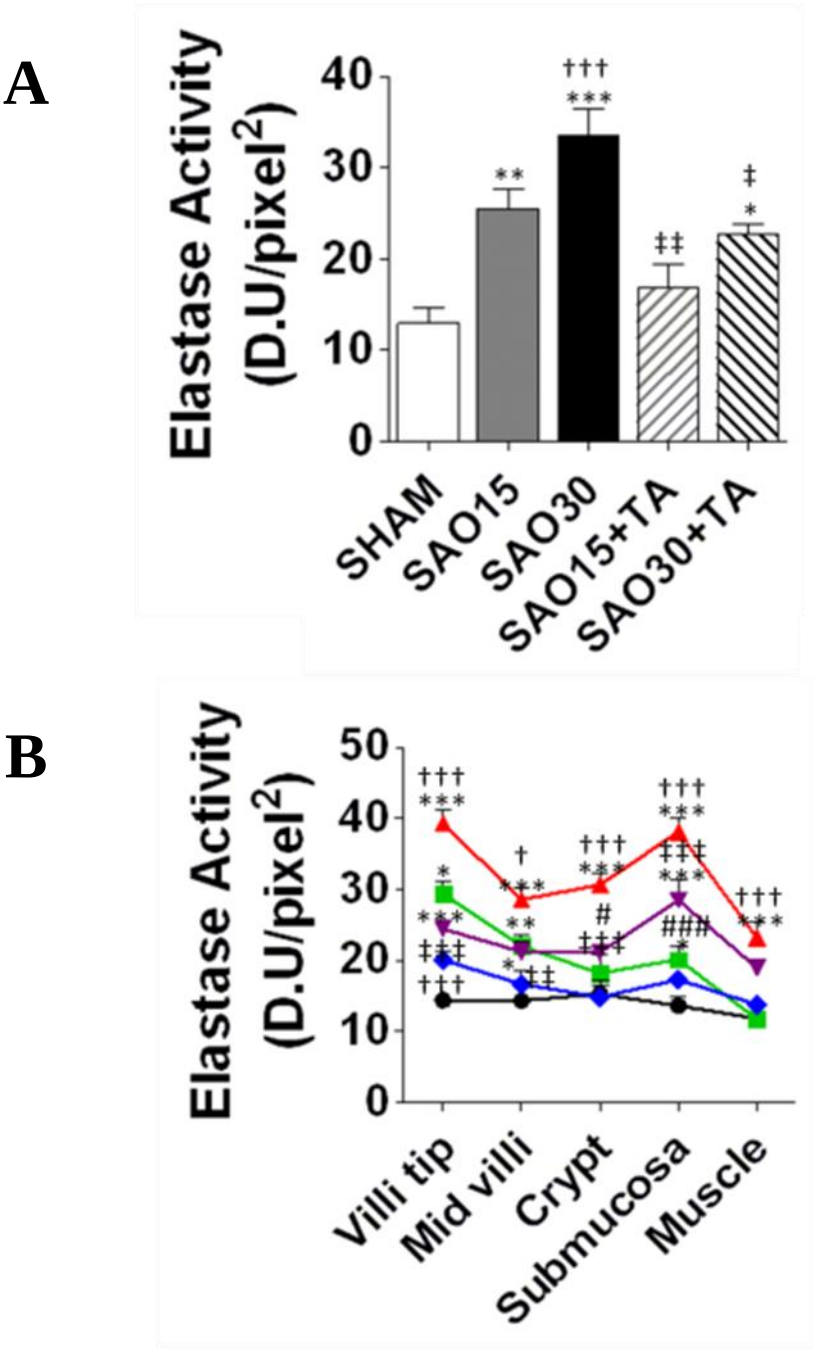

Figure 2.15 Elastase activity measurements. (**A**) Elastase enzymatic activity measured as mean fluorescent intensity of the fluorescent substrates. (**B**) Enzyme penetration from the villi tip to the intestinal muscle measured as mean fluorescent intensity of the fluorescent substrates. *P <0.05, **P<0.001, ***P<0.0001 compared to sham. †P <0.05, ††P<0.001, †††P<0.0001 compared to 15 min SAO. ‡P <0.05, ‡‡P<0.001, ‡‡‡P<0.0001 compared to 30 min SAO.

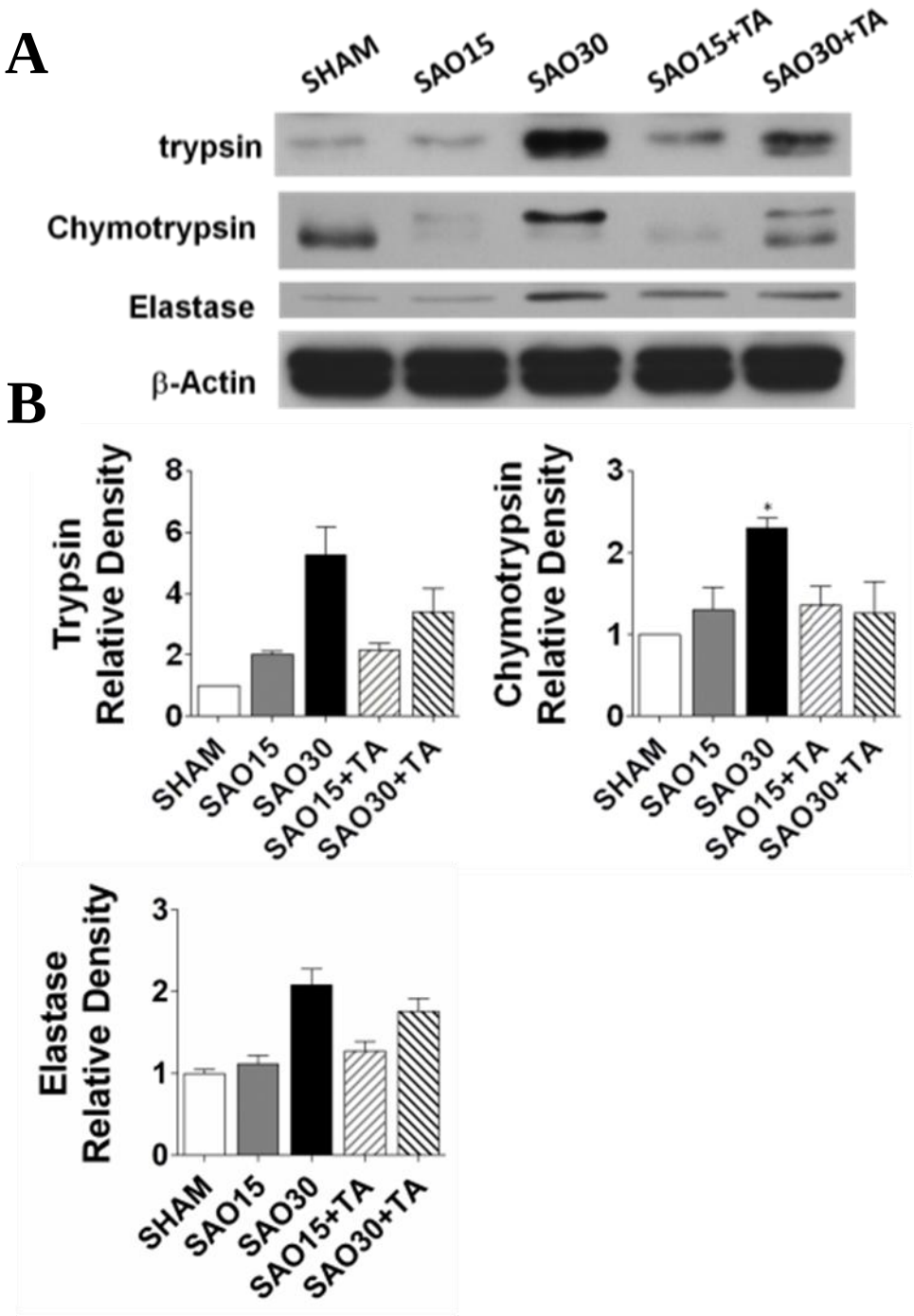

Figure 2.16 Protein levels of digestive enzymes in intestinal wall. Relative density of trypsin, chymotrypsin and elastase with respect of β-actin. Values are mean±SEM (n=4) (**E**). *P <0.05 compared to sham.

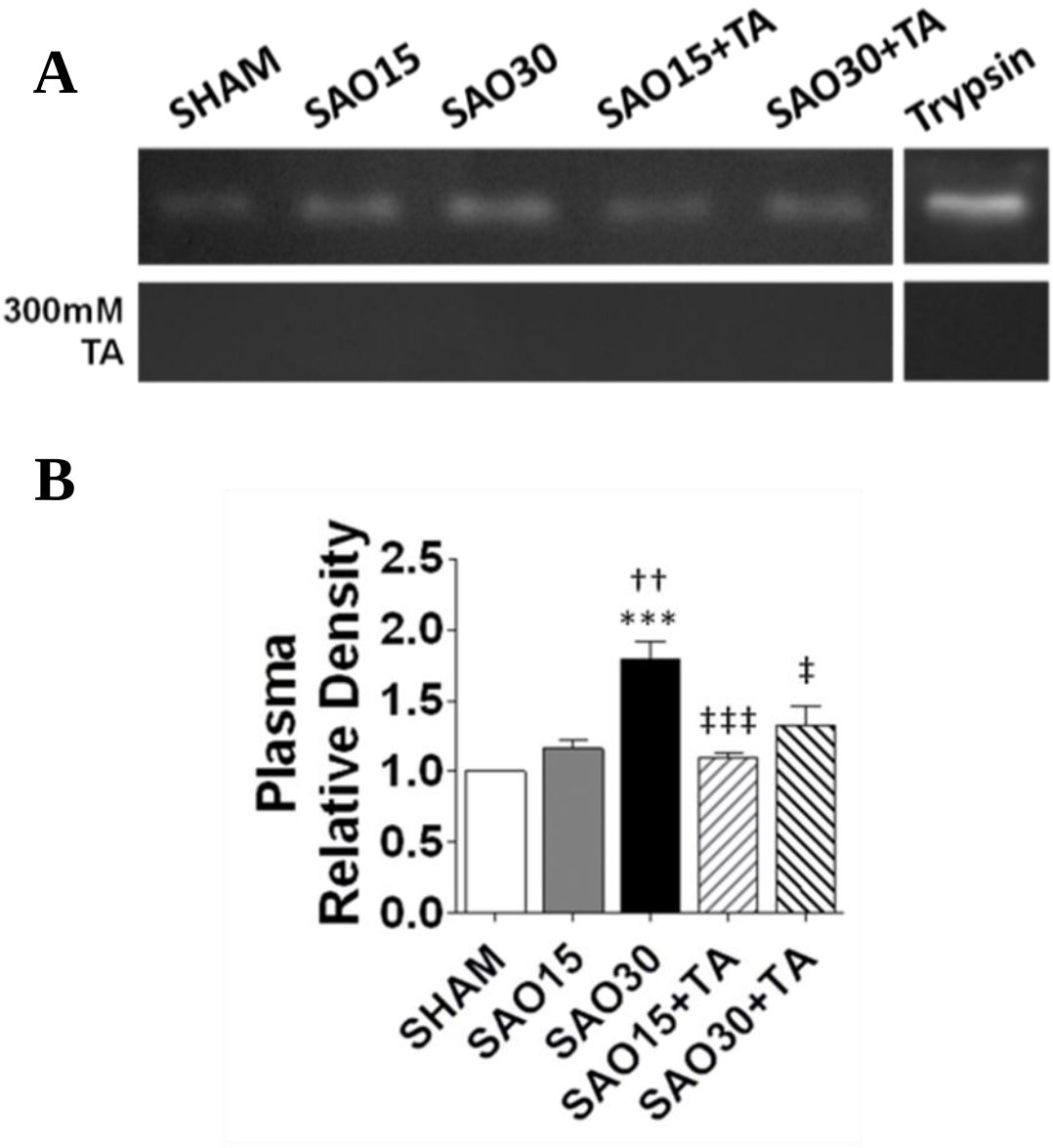

Figure 2.17 Protease activity in rat plasma. (**A**) Gelatin zymography of plasma without and with Tranexamic acid inhibition during renaturing and developing steps. Bands correspond to about 20kDa molecular weight. (**B**) Relative density of proteolytic enzyme activity. *P <0.05, ***P<0.0001 compared to sham. ††P<0.001, †††P<0.0001 compared to 15 min SAO. ‡‡P<0.001, ‡‡‡P<0.0001 compared to 30 min SAO, §§§P<0.0001 compared to 15 min SAO with TA.

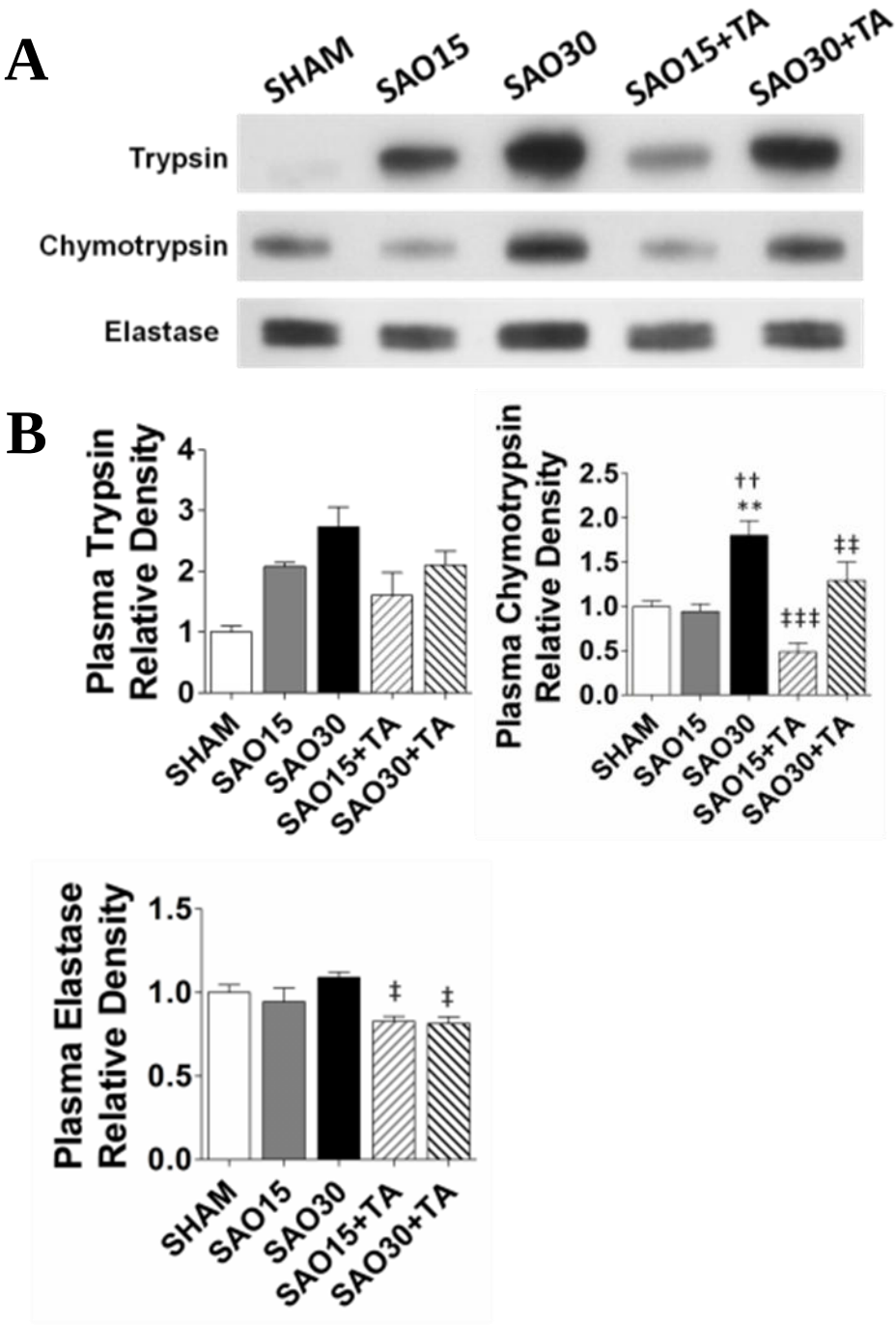

Figure 2.18 Protein levels of digestive enzymes in rat plasma. (**C**) Western blot of trypsin, chymotrypsin, and elastase in plasma. (**B**) Relative density of the three enzymes in plasma; values are mean±SEM (n=4/group). *P <0.05, ***P<0.0001 compared to sham. ††P<0.001, †††P<0.0001 compared to 15 min SAO. ‡‡P<0.001, ‡‡‡P<0.0001 compared to 30 min SAO, §§§P<0.0001 compared to 15 min SAO with TA.

2.8 References

1. Ellis H (1980) Internal overhealing: the problem of intraperitoneal adhesions. (Translated from eng) *World J Surg* 4(3):303-306 (in eng).

2. Perry JF, Smith GA, & Yonehiro EG (1955) Intestinal obstruction caused by adhesions; a review of 388 cases. (Translated from eng) *Annals of surgery* 142(5):810-816 (in eng).

3. Oldenburg WA, Lau LL, Rodenberg TJ, Edmonds HJ, & Burger CD (2004) Acute mesenteric ischemia: a clinical review. (Translated from eng) *Arch Intern Med* 164(10):1054-1062 (in eng).

4. Garofalo M, *et al.* (2002) Early diagnosis of acute mesenteric ischemia after cardiopulmonary bypass. (Translated from English) *J Cardiovasc Surg* 43(4):455-459 (in English).

5. Gennaro M, *et al.* (1993) Acute Mesenteric Ischemia after Cardiopulmonary Bypass. (Translated from English) *American Journal of Surgery* 166(2):231-236 (in English).

6. Allen KB, Salam AA, & Lumsden AB (1992) Acute Mesenteric Ischemia after Cardiopulmonary Bypass. (Translated from English) *Journal of Vascular Surgery* 16(3):391-396 (in English).

7. Barnett WO, Petro AB, & Williamson JW (1976) A current appraisal of problems with gangrenous bowel. (Translated from eng) *Annals of surgery* 183(6):653-659 (in eng).

8. Cheadle WG, Garr EE, & Richardson JD (1988) The importance of early diagnosis of small bowel obstruction. (Translated from eng) *Am Surg* 54(9):565-569 (in eng).

9. Anonymous (2008) World Health Organization: World Health Statistics Annual. 2008.

10. Jones H & Trueman E (1996) National Safety Council: Accident Facts. *Journal of Experimental Biology* 52(1):201-216.

11. Holcomb J, *et al.* (2007) Causes of death in US Special Operations Forces in the global war on terrorism: 2001-2004. (Translated from eng) *US Army Med Dep J*:24-37 (in eng).

12. Cowley RA (1976) The resuscitation and stabilization of major multiple trauma patients in a trauma center environment. *Clinical Medicine* 83:16-22.

13. Deitch EA, Xu DZ, Franko L, Ayala A, & Chaudry IH (1994) Evidence Favoring the Role of the Gut as a Cytokine-Generating Organ in Rats Subjected to Hemorrhagic-Shock. (Translated from English) *Shock* 1(2):141-146 (in English).

14. Hugon JS & Bounous G (1971) Intestinal lesions in low flow states: electron microscopic study. *Vascular Disorders of the Intestine*, ed Boley SJ (Appleton and Century Crofts, New York), pp 123-144.

15. Tamion F, *et al.* (1997) Gut ischemia and mesenteric synthesis of inflammatory cytokines after hemorrhagic or endotoxic shock. (Translated from English) *Am J Physiol-Gastr L* 36(2):G314-G321 (in English).

16. Maxwell RA, Fabian TC, Croce MA, & Davis KA (1999) Secondary abdominal compartment syndrome: an underappreciated manifestation of severe hemorrhagic shock. (Translated from eng) *The Journal of trauma* 47(6):995-999 (in eng).

17. Wattanasirichaigoon S, Menconi M, Delude R, & Fink M (1999) Effect of mesenteric ischemia and reperfusion or hemorrhagic shock on intestinal mucosal permeability and ATP content in rats. *Shock* 12(2):127.

18. Penn AH, Hugli TE, & Schmid-Schönbein GW (2007) Pancreatic enzymes generate cytotoxic mediators in the intestine. (Translated from eng) *Shock* 27(3):296-304 (in eng).

19. Waldo SW, Rosario HS, Penn AH, & Schmid-Schönbein GW (2003) Pancreatic digestive enzymes are potent generators of mediators for leukocyte activation and mortality. (Translated from eng) *Shock* 20(2):138-143 (in eng).

20. Rupani B, *et al.* (2007) Relationship between disruption of the unstirred mucus layer and intestinal restitution in loss of gut barrier function after trauma hemorrhagic shock. (Translated from eng) *Surgery* 141(4):481-489 (in eng).

21. Sutherland NG, Bounous G, & Gurd FN (1968) Role of intestinal mucosal enzymes in the pathogenesis of shock. (Translated from eng) *J Trauma* 8(3):350-380 (in eng).

22. Mitsuoka H, Kistler EB, & Schmid-Schönbein GW (2000) Generation of in vivo activating factors in the ischemic intestine by pancreatic enzymes. (Translated from eng) *Proc Natl Acad Sci U S A* 97(4):1772-1777 (in eng).

23. Mitsuoka H & Schmid-Schönbein GW (2000) Mechanisms for blockade of in vivo activator production in the ischemic intestine and multi-organ failure. (Translated from eng) *Shock* 14(5):522-527 (in eng).

24. Penn A & Schmid-Schönbein G (2008) The intestine as source of cytotoxic mediators in shock: free fatty acids and degradation of lipid-binding proteins.

American Journal of Physiology- Heart and Circulatory Physiology 294(4):H1779.

25. Deitch E, Shi H, Lu Q, Feketeova E, & Xu D (2003) Serine proteases are involved in the pathogenesis of trauma-hemorrhagic shock-induced gut and lung injury. *Shock* 19(5):452.

26. Fitzal F, *et al.* (2003) Pancreatic enzymes sustain systemic inflammation after an initial endotoxin challenge. *Surgery* 134(3):446-456.

27. Fitzal F, DeLano F, Young C, Rosario H, & Schmid-Schönbein G (2000) Pancreatic protease inhibition during shock attenuates cell activation and peripheral inflammation. *Journal of vascular research* 39(4):320-329.

28. Kistler E, Lefer A, Hugli T, & Schmid-Schönbein G (2000) Plasma activation during splanchnic arterial occlusion shock. *Shock* 14(1):30.

29. Nilsson IM (1980) Clinical pharmacology of aminocaproic and tranexamic acids. *Journal of Clinical Pathology* 33(Suppl 14):41.

30. Andersson L, *et al.* (1965) Experimental and Clinical Studies on AMCA, the Antifibrinolytically Active Isomer of p Aminomethyl Cyclohexane Carboxylic Acid. *Scandinavian Journal of Haematology* 2(3):230-247.

31. Dubber AHC, McNicol G, & Douglas A (1965) Amino methyl cyclohexane carboxylic acid (AMCHA), a new synthetic fibrinolytic inhibitor. *British Journal of Haematology* 11(2):237-245.

32. Dunn CJ & Goa KL (1999) Tranexamic acid: a review of its use in surgery and other indications. *Drugs* 57(6):1005-1032.

33. Zimmerman M, Ashe B, Yurewicz EC, & Patel G (1977) Sensitive assays for trypsin, elastase, and chymotrypsin using new fluorogenic substrates. (Translated from eng) *Anal Biochem* 78(1):47-51 (in eng).

34. Kanaoka Y, Takahashi T, & Nakayama H (1977) A new fluorogenic substrate for aminopeptidase. (Translated from eng) *Chem Pharm Bull (Tokyo)* 25(2):362-363 (in eng).

35. Castillo MJ, Nakajima K, Zimmerman M, & Powers JC (1979) Sensitive substrates for human leukocyte and porcine pancreatic elastase: a study of the merits of various chromophoric and fluorogenic leaving groups in assays for serine proteases. (Translated from eng) *Anal Biochem* 99(1):53-64 (in eng).

36. Zimmerman M, Yurewicz E, & Patel G (1976) A new fluorogenic substrate for chymotrypsin. (Translated from eng) *Anal Biochem* 70(1):258-262 (in eng).

37. Mook OR, Van Overbeek C, Ackema EG, Van Maldegem F, & Frederiks WM (2003) In situ localization of gelatinolytic activity in the extracellular matrix of metastases of colon cancer in rat liver using quenched fluorogenic DQ-gelatin. (Translated from eng) *J Histochem Cytochem* 51(6):821-829 (in eng).

38. Rosario HS, Waldo SW, Becker SA, & Schmid-Schönbein GW (2004) Pancreatic trypsin increases matrix metalloproteinase-9 accumulation and activation during acute intestinal ischemia-reperfusion in the rat. (Translated from eng) *Am J Pathol* 164(5):1707-1716 (in eng).

39. Yi CF, Gosiewska A, Burtis D, & Geesin J (2001) Incorporation of fluorescent enzyme substrates in agarose gel for in situ zymography. (Translated from eng) *Anal Biochem* 291(1):27-33 (in eng).

Chapter 3

Disruption of the Intestinal Barrier during Splanchnic Ischemia

3.1 Introduction

The lumen of the small contains bacteria and bacterial products, digested food products as well as luminal digestive enzymes, especially the pancreatic proteases. Should digestive enzymes come into direct contact with the enterocytes lining the intestinal villi, these cells could be digested in the same fashion as foodstuff in the lumen of the intestine. The intestinal barrier function is a critical host defense mechanism; failure in this barrier can have direct pathophysiologic consequences.

3.2 Mucosal Barrier and Shock

The concept of the mucus layer being an important protective barrier is well established in the stomach, where stress or ischemia-induced loss of the gastric mucus layer contributes to gastric mucosal injury by intraluminal acid. However, only few studies have addressed the importance of the small intestinal mucus layer as a barrier in shock states. Bounous was among the first authors to notice that products of intestinal origin often seen in the terminal stage of shock could appear in the blood stream as a

result of a defective intestinal barrier (1). Bounous also was the first one to suggest that deterioration of the intestinal mucosal may allow mucosal cells to be acted upon by intraluminal proteolytic enzymes such as trypsin and chymotrypsin (1). Thereafter others have reported a relationship between changes in the mucus layer and intestinal barrier (2-4).

3.2.1 Intestinal mucin is a glycoprotein (100-250 kDa) with about 20% peptide core and 80% carbohydrate (5); it makes up a large part of the mucus covering the mucosal barrier. Bounous suggested that the increase intestinal permeability that he observed in experiments with ischemic intestine could be directly related to the mucin in the mucosal layer. He concluded that a reduction in cellular respiration as a result of ischemia will rapidly decrease the production of mucin thus exposing epithelial cells to noxius materials (1). Others have suggested that the hydrophobic properties of the mucus gel are critical for the intestinal barrier function. Qin and Deitch showed that the superior mesenteric artery occlusion (SMAO) model with gut ischemic injury causes a dose-dependent decrease in mucosal hydrophobicity and an increase in gut permeability (6).

Mucins can be subdivided into secretory and membrane-associated forms.

3.2.2 Secreted mucin: Mucin 2 (MUC2) is the major gel-forming mucin secreted by goblet cells of the small and large intestines and is the main structural component of the mucus gel. MUC2 is assembled into large polymers by disulfide bonds between mucin subunits with a mass of ~ 2.5 MDa. The protective role of MUC2 in the intestine is maintained despite the abundant pancreatic digestive proteases. This protection is possible because its two large mucin domains are highly O-glycosylated and thus

resistant to proteolytic cleavage because the glycans prevent access of the proteases to the protein core (7). In contrast, N- and C-terminal cysteine-rich are less glycosylated, and the protein core is probably more exposed.

3.2.3 Membrane bound mucin: Cell surface mucins are transmembrane glycoproteins expressed at the apical surface of all mucosal epithelial cells. Ten cell surface mucin genes have been identified, and multiple genes are expressed in tissues at greatest risk of infection (8). The extracellular domain of these mucins forms an extremely large thread-like structure covered by a dense array of complex O-linked oligosaccharides and can be shed from the cell surface. They have a transmembrane domain and the cytoplasmic domains of cell surface mucins are highly conserved across species, undergo both serine and tyrosine phosphorylation, and interact with kinases and adaptor molecules (9-11), consistent with a role in signal transduction. However, the primary function of these mucins is not understood.

3.3 Epithelial Barrier and Shock

The normal functioning of the intestine depends on the maintenance of compositionally distinct, fluid-containing compartments lined by sheets of epithelial cells. In the gut, the lumen is separated from the lamina propria by the intestinal epithelium. An essential element in this process is the formation of adherent and tight junction between adjacent cells making up the epithelial sheet. Proper functioning of these junctions is essential to maintain normal physiologic processes; therefore alteration in intestinal epithelial function as a consequence of shock results in epithelial dysfunction in critical illness. It has been reported that in hemorrhagic shock the blood flow is

reduced (12) and consequently the villi are damaged (13, 14). In addition there is increased permeability to macromolecules in animals subjected to hemorrhage (15-18).

3.4 Aims of this Chapter

The hypothesis presented in this chapter is that that during intestinal ischemia there is a loss of function of the mucosal/epithelial barrier, permitting leakage of digestive enzymes. Previous studies have shown that the mucosal barrier is disrupted in shock (1, 19); mucin is the main component of this barrier and the mechanism leading to loss of function is yet to be determined. Thus, this study examines the disruption of two mucin isoforms (mucin2 and mucin13) and E-cadherin in epithelial cells during early periods of intestinal ischemia (15 and 30 min) and their relationship to digestive enzyme entry into the intestinal wall. In this chapter it is also examined the protective role of the use of tranexamic acid, a trypsin inhibitor, in the preservation of these two barriers.

3.5 Materials and Methods

3.5.1 Animal groups: All animal protocols were reviewed and approved by the University of California San Diego Animal Subjects Committee. Male Wistar rats (300-350g, Harlan Sprague Dawley Inc, Indianapolis, IN) were randomly assigned to one of five groups: a sham group (SHAM), two ischemic groups with splanchnic arterial occlusion (SAO) for 15 and 30 min (SAO15, SAO30) and two ischemic SAO groups with enteral tranexamic acid (TA) treatment (SAO15+TA, SAO30+TA); n=4 per group.

3.5.2 Shock model: Rats were kept on solid food restriction with water ad libitum for 12 hours prior to surgery, tranquilized with Xylazine (20 mg/ml, 0.2 μL/g BW) and

anesthetized with Nembutal (50 mg/ml, 1 μL/g BW), followed by cannulation of the left femoral vein and artery. In the SHAM and SAO groups 0.9% normal saline (NS), 3ml/100g BW, was injected into the lumen of the intestine while in the treatment group (SAO+TA) tranexamic acid (Sigma Scientific, St. Louis, MO), 1 mg/g BW, in NS was used. After 30 min the superior mesenteric and celiac arteries were isolated and ligated (SAO and SAO+TA groups) or isolated without ligation (SHAM). Animals were euthanized after 30 min (SHAM) and after 15 or 30 min (SAO and SAO+TA).

3.5.3 Tissue processing: Jejunal segments (~1 cm in length) without removal of luminal contents were suspended in Tissue-Tek O.C.T. Compound (Sakura Finetek, Torrance, CA), snap frozen in isopentane/liquid nitrogen, and stored in -80^{o}C for further analysis. Cryosections (5 μm thickness) along the longitudinal axis of the villi were used throughout all experiments.

3.5.4 Intestine homogenates: In separate experiments, 1cm equally spaced segments of the intestine were excised. For western blot assays luminal contents were washed with NS; followed by homogenization with CelLytic™ (Sigma) in the presence of protease inhibitors (5mM EDTA, 5mM N-Ethylmaleimide, 25mM iodoacetamide, 5mM benzamidine, 300mM acarbose, 5mM 6-aminocaproic acid, 1mM protease inhibitor cocktail, (Sigma Scientific)) to inhibit further degradation. To measure enzyme activity in the intestinal luminal, contents were retained to measure enzyme activity in the whole intestine; they were homogenized (CelLytic™) without addition of protease inhibitors. Homogenates were centrifuged (16,000g for 15 min at 4°C), the supernatant was

collected and protein concentration was assessed with the bicinchoninic acid protein assay (Thermo Scientific, Rockford, IL).

3.5.5 Western blot: Samples were prepared in SDS loading buffer (Biorad, Richmond, CA), reduced with β-mercaptoethanol and boiled for 4 min at 100^{o}C; 20 μg of protein/lane were loaded for each group and run in an SDS polyacrylamide gel and then transferred onto nitrocellulose membranes. Afterwards membranes were blocked in 5% non-fat milk for 1 hour and incubated in primary antibodies overnight. Mucin2 (H-300) and mucin13 (R-245) (sc-15334, sc-66973 Santa Cruz Biotechnology, Santa Cruz, CA, 1:1000 dilution) and for the intra- and extra-cellular domains of E-cadherin 1:300 (Abcam). Membranes were incubated with appropriate secondary antibodies (Santa Cruz Biotechnology) and developed using the chemiluminescent substrate (Super Signal West Pico, Thermo Scientific). The exposed x-ray films were scanned and analyzed using the gel analysis tool of the NIH ImageJ software.

3.5.6 Immunohistochemistry: Cryosections were fixed for 10 minutes in cold acetone and incubated overnight with primary antibody. Mucin2 (H-300) or mucin13 (R-245) were labeled using rabbit polyclonal antibody (sc-15334, sc-66973 Santa Cruz Biotechnology, 1:200 dilution) intracellular domain of E-cadherin 1:300 (Abcam); extracellular domain of E-cadherin 1:250 (Abcam) and then incubated with secondary antibody (ImmPRESS kit, Vector Lab). The slides were developed with 3,3´-diaminodbenzidine substrate (DAB, Vector Lab) counterstained with hematoxylin (Vector Lab), dehydrated, mounted using VectaMount Permanent Mounting Medium (Vector Lab) and observed under an inverted microscope (20X and 60X objective).

3.5.7 Alcian blue staining: Cryosections were fixed in Carnoy's fixative for 10 min, stained in 1% alcian blue solution in 3% acetic acid, pH 2.5 for 30 min, counterstained with hemotoxylin, dehydrated, and mounted using VectaMount Permanent Mounting Medium (Vector Lab) and observed under an inverted microscope (20X objective).

3.5.8 In-situ zymography/immunohistochemistry: The simultaneous visualization of enzyme activity and mucin was carried out using a modified protocol (20). Briefly, cryosections were fixed in 95% cold ethanol and protease activity was detected via proteolytic cleavage of fluorescent BODIPY TR-X casein 10 μg/ml (EnzChek®, Invitrogen, Carlsbad, CA) on tissue sections after 1-hour incubation at 37^{o}C. Subsequently, sections were fixed with 4% paraformaldehyde for 15 min, incubated overnight with mucin2 1:200 primary antibody and FITC secondary antibody 1:10000 (Santa Cruz Biotechnology) and observed on an inverted microscope (20X objective) using the appropriate fluorescent filters.

3.5.9 Image analysis: Images were digitized (8 bit, 0 to 255 light intensities), corrected for random noise and background illumination and then followed by digital measurements of the fluorescent or light signal intensity in digital units (D.U., NIH ImageJ software).

Mean fluorescent/light intensity is defined as the sum of all pixel intensities divided by the sum of all pixels in the selected area (D.U./pixel); total fluorescent/light intensity is defined as the sum of all the pixel intensities in the selected area (D.U).

A rectangular area covering 2-3 villi was selected for all groups. The images were adjusted to a threshold so only mucin staining was visible; mucin density was measured as the mean light intensity; the amount of mucin was measured as the total light intensity. Five tissue sections per animal (n=4) per group were analyzed. Mucin13 density was determined by placing a one-pixel wide line perpendicular to the epithelium; a profile plot of the light intensity values along the line was generated for 25 lines measured over four intestinal sections per animal (n=4). The plot profiles were aligned with respect to the maximum light intensity and then averaged. The average of these maximum intensity values were selected as measure for mucin13 density.

Mucin2 and protease activity colocalization was determined on simultaneously captured protease activity (red channel) and mucin density (green channel) micrographs. An area covering one villus was consistently selected for each group; each area was further divided into four regions: villi tip, mid villi, crypt, submucosal, and muscle layer. The mean fluorescent intensity over each region was measured for each channel. Twenty villi over four tissue sections per animal (n=4) per group were selected.

3.5.10 Statistical analysis: Results are presented as mean±SEM. Unpaired comparisons of mean values between groups were carried out by one-way ANOVA followed by Bonferroni post-hoc. $P<0.05$ was considered significant.

3.6 Results

3.6.1 Mucin carbohydrates in the rat small intestine after SAO: Mucin carbohydrates labeled with alcian blue were located inside the goblet cells within the villi, along the epithelium and in the lumen of the intestine (Figure 3.1). Mucin carbohydrate density

exhibited a trend towards a progressive decrease within the villi during the ischemic period. This trend was reduced in the presence of TA (Figure 3.2A). In the lumen, mucin carbohydrate density significantly decreased by 40% after 15 min SAO and further by 30% after 30 min SAO compared to SHAM. In the presence of TA, mucin density returned to levels observed in the SHAM group (Figure 3.2A). In general the total mucin density (villi+lumen) decreased in SAO and was restored with TA (Figure 3.2B).

This evidence suggests that in the normal state mucin carbohydrates are contained in compact form close to the villi and the lumen and during ischemic states mucin carbohydrates are dispersed in a less compact form more towards the lumen. The restoration of mucin carbohydrates in the presence of a protease inhibitor suggest that mucin carbohydrates disruption is mediated at least in part by a proteolytic mechanism.

3.6.2 Mucin2 in the rat small intestine after SAO: Mucin2 was present in the goblet cells within the villi and in the lumen of the intestine (Figure 3.3). The density of mucin2 in the villi was constant among the different groups but it decreased in the lumen after SAO even in the presence of TA (Figure 3.4A). In the lumen of the intestine mucin2 density decreased by 8% after 15 min SAO and significantly decreased by 11% after 30 min SAO as compared to SHAM. In the presence of TA, mucin2 density also significantly decreased as compared to SAO groups without treatment (Figure 3.4A). The amount of mucin2 in the villi significantly decreased after 30 min SAO and increased in the lumen, but the total amount of mucin2 (villi+lumen) remained constant among the groups (Figure 3.4B). The total mucin2 density (villi+lumen) decreased both

in ischemic states and with TA treatment suggesting that mucin2 is disrupted, but less likely via a proteolytic mechanism.

3.6.3 Mucin13 in the rat small intestine after SAO: Membrane bound mucin (mucin13) was observed on the intestinal epithelium along the brush border (Figure 3.5). The density of mucin13 decreased after 15 min and 30 min SAO. Serine protease inhibition with TA served to maintain mucin13 density after 15 min and 30 min SAO at the levels observed in SHAM (Figure 3.6). Mucin13 density significantly decreased by 34% after 15 min SAO and by 33% after 30 min SAO compared to SHAM. In the presence of TA, mucin13 density remained at levels found in the SHAM group.

3.6.4 Protein levels of mucin isoforms in intestine homogenates: Western blot analysis of Mucin2 shows that there is a decrease of mucin2 as ischemia progresses and this decrease is not prevented by TA treatment (Figure 3.7A). The relative density of mucin2 with respect to SHAM and β-actin after 15 min SAO significantly decreased by 30% and by 56% after 30 min SAO (Figure 3.7B). With TA treatment the relative density of mucin2 with respect to SHAM and β-actin after 15 min SAO significantly decreased by 50% and 56% after 30 min SAO (Figure 3.7B). Western blot of mucin13 also shows that mucin13 decreases with the progression of ischemia (Figure 3.7C). The relative density of mucin13 with respect to SHAM and β-actin after 15 min SAO decreased by 16% by 23% after 30 min SAO. With TA treatment the relative density of mucin13 after 15 min and 30 min SAO remained at SHAM levels (Figure 3.7C).

3.6.5 Serine protease entry across the intestinal mucin layer after SAO: Superposition of the protease activity label with casein substrate and mucin2

immunofluorescent staining on the same sections reveals that there is no detectable colocalization of protease activity and mucin (Figure 3.8). In addition as mucin2 levels decreased during SAO in various regions of the intestinal wall, the protease activity increased (Figure 3.9). During SAO, mucin2 was disrupted starting from the villi tips progressively towards the crypts and simultaneously proteases started to penetrate the villi (Figure 3.9). Luminal inhibition of the proteases with TA reduced enzyme activity levels to those observed in SHAM but did not restore mucin2 density. An increased enzymatic activity was also observed in the submucosa after ischemia; after 30 min SAO there was an enhanced protease activity at the level of the crypts co-localized with the Paneth cells (Figure 3.8).

3.6.6 Proteolytic cleavage of E-cadherin in rat intestine: Ischemia and reperfusion injury is characterized by disruption of intercellular junctions in epithelium (21). We labeled the intracellular and extracellular domains of E-cadherin to determine whether the epithelial junctions are proteolytically disrupted during ischemia and whether this process can be prevented by enteral TA protease inhibition in our model. In the sham control group both domains of E-cadherin are visible along the entire epithelium of each villus (Figure 3.10). In contrast, in ischemia visible morphological damage was accompanied by disruption of both domains of E-cadherin (Figure 3.10). TA treatment preserved intra- and extracellular domains of E-cadherin (Figure 3.11 A, B), an observation that was confirmed by Western blot analysis (Figure 3.12).

3.7 Discussion

The current results in the rat model of SAO show morphological damage to the intestine after 15 min and major damage after 30 min of intestinal ischemia accompanied by disruption of both mucosal and epithelial barriers. The damage to the mucosal barrier is accompanied by enhanced enzymatic activity of digestive serine proteases (trypsin, chymotrypsin, and elastase) in the wall of the intestine. Tranexamic acid (TA) treatment in the lumen of the intestine prior to intestinal ischemia reduced villi damage, decreased enzyme activity in the intestinal wall, and protected to some degree the mucus barrier.

Our results show that mucin2 (goblet cell-derived mucin) is disrupted during ischemia by a mechanism that appears to be independent of trypsin, since trypsin inhibition with TA during ischemia did not prevent it. In contrast, luminal treatment with TA prevented disruption of mucin13 (membrane bound mucin) and degradation of the carbohydrate portion of mucin during ischemia. This result indicates that disturbance of the mucin layer during ischemia is accompanied by entry of digestive enzymes into the wall of the intestine as seen by increased enzymatic activity as well as increased protein levels of trypsin and chymotrypsin by Western blot.

Double labeling of mucin2 and protease activity indicates that proteases and mucin exhibit a low degree of mixing on sections. This situation is observed in the non-ischemic state, with intact mucin located in both goblet cells and the mucin layer above the epithelium and low or no enzymatic activity in the intestinal wall. In contrast, enzymatic activity is observed at the tip of the villi as early as 15 min of ischemia accompanied by a decrease of the mucin density in the intestinal lumen. After 30 min

ischemia an enhanced enzymatic activity across the intestinal wall is observed with near absent mucin labeling in the lumen. There seems to be little or no colocalization of enzyme activity and mucin, which may suggest that digestive enzymes are not present in areas with intact mucin layer. This evidence suggests that the enhanced enzymatic activity observed in the lumen of the intestine may be due to entry of the digestive enzymes across the mucus layer.

Homotypic interactions of the extracellular domains of E-cadherin are responsible for preserving epithelial cell-cell integrity and may be important in preventing intestinal permeability present in shock (35). In this study we observed loss of both the intra- and extracellular domains of E-cadherin during ischemia, which was prevented by TA treatment. Disruption of E-cadherin in intestinal ischemia may increase intestinal permeability, thus providing an additional route of entry for digestive enzymes through the intestinal wall.

Evidence presented in this chapter indicates that the development of tissue injury observed during early periods of intestinal ischemia is the result of two interconnected processes involving disruption of the mucosal barrier and trypsin activation. Disruption of the mucin layer during ischemia allows activated trypsin to make its way across the epithelium where it may activate other enzymes and by proteolytic destruction of epithelial junction proteins open a route of entry for other digestive enzymes to enter the intestinal wall and the systemic circulation resulting in autodigestion.

Chapter 3 in full is submitted material to Shock journal as it appears in "Disruption of the Intestinal Mucin Layer Allows Entry of Digestive Enzymes during

Early Periods of Intestinal Ischemia" by Chang M., Kistler E. B., Schmid-Schönbein G.W. The dissertation author is the primary author of this manuscript.

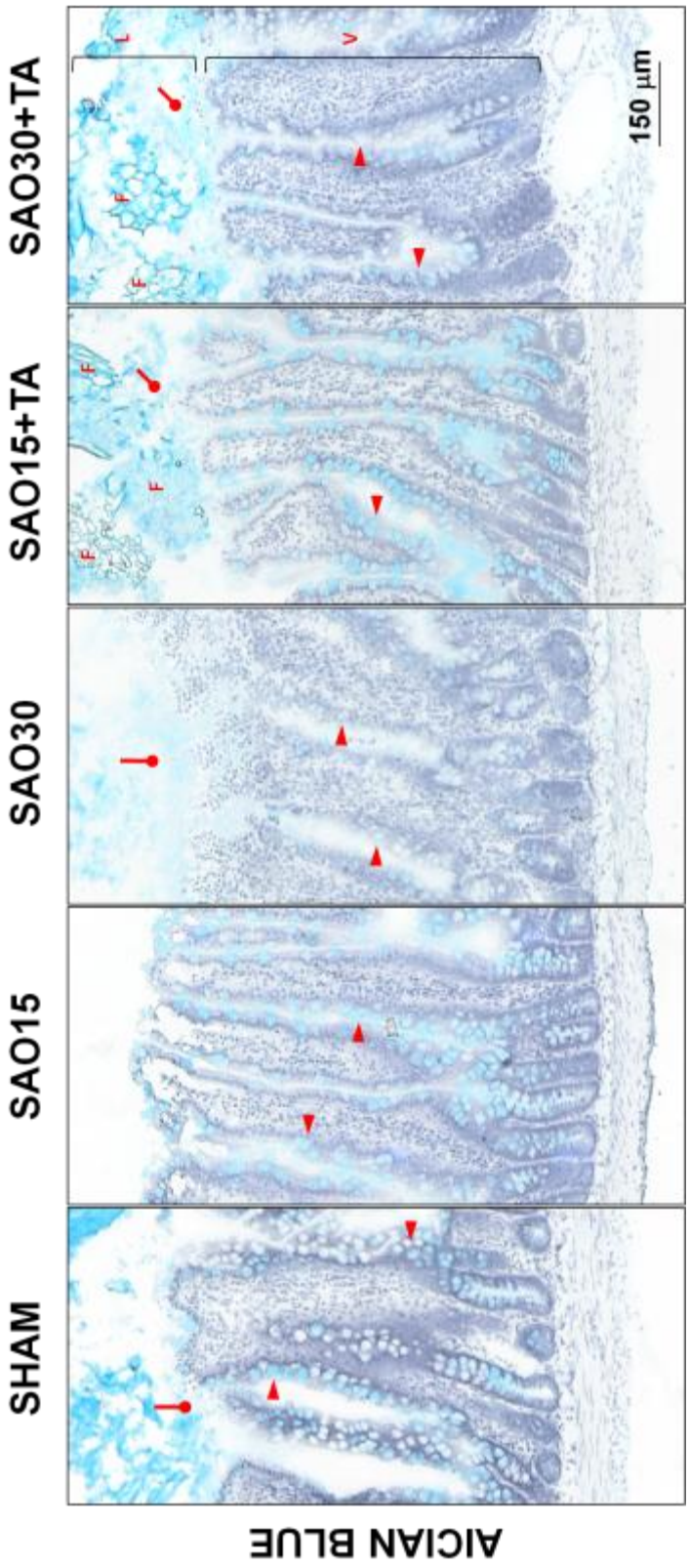

Figure 3.1 Alcian blue staining. Micrographs of jejunal frozen sections stained with alcian blue specific for the carbohydrate domain of mucin. The intestinal lumen (L), villi (V) and luminal food (F) residues are visible; arrowheads show mucin in goblet cells.

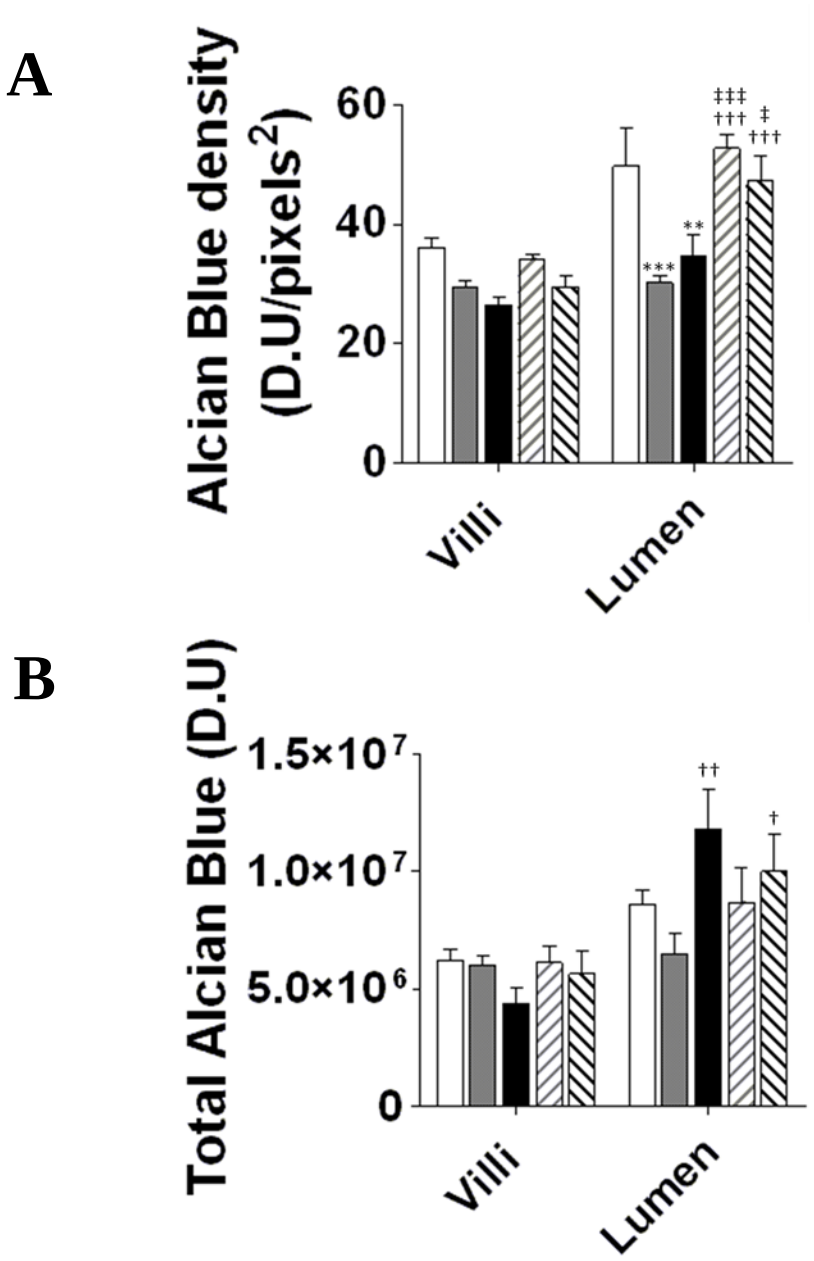

Figure 3.2 Alcian blue density measurements. Mucin density measured as the mean light intensity **(A)** and total mucin measured by the total light intensity **(B).** Values are mean±SEM (n=4). *P <0.05, ** P<0.001, ***P<0.0001 compared to sham. †P<0.05, ††P<0.001, †††P<0.0001 compared to 15 min SAO. ‡P<0.05, ‡‡P<0.001, ‡‡‡P<0.0001 compared to 30 min SAO (alcian blue and mucin2 staining).

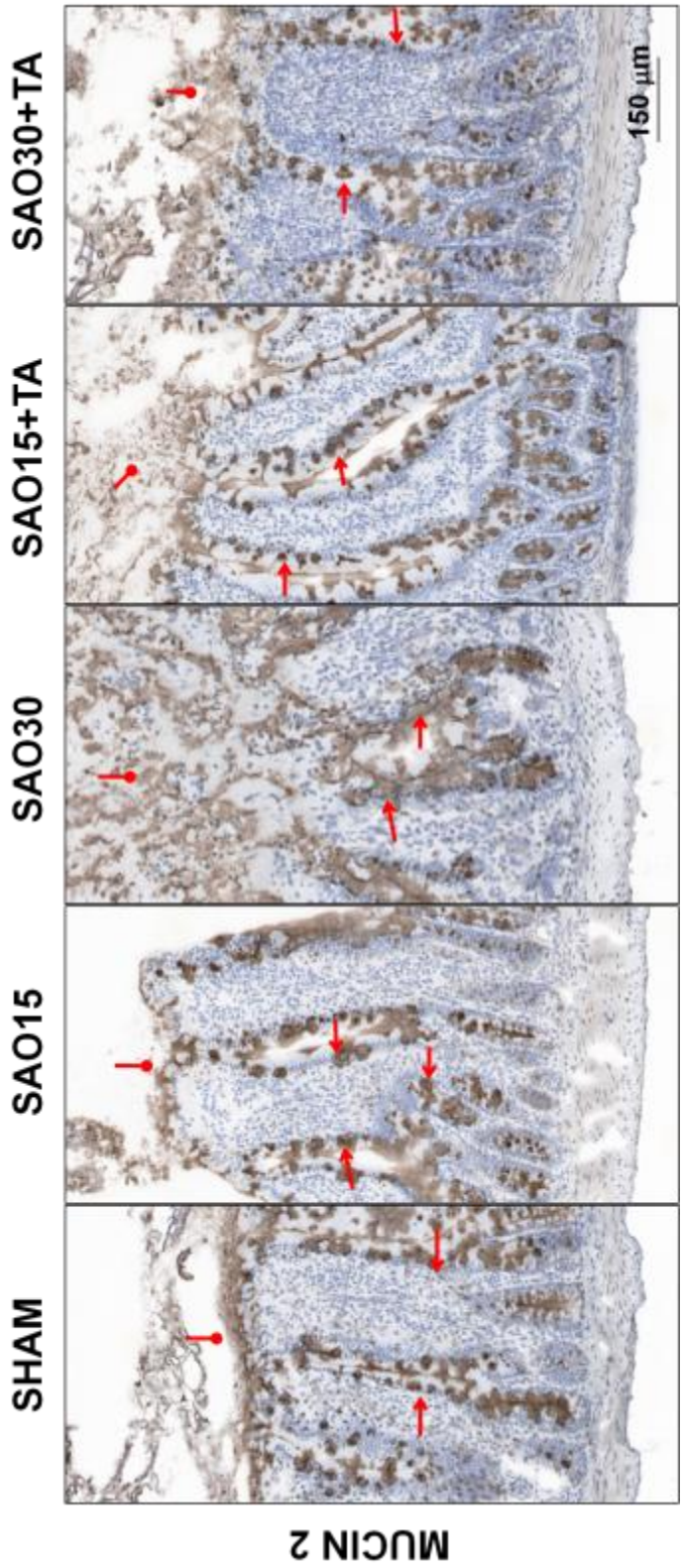

Figure 3.3 Mucin2 immunohistochemistry. Micrographs of jejunal frozen sections stained with immunoperoxidase staining against goblet cell-derived mucin2. Arrowheads show mucin in goblet cells, diamond arrows demonstrate luminal mucin

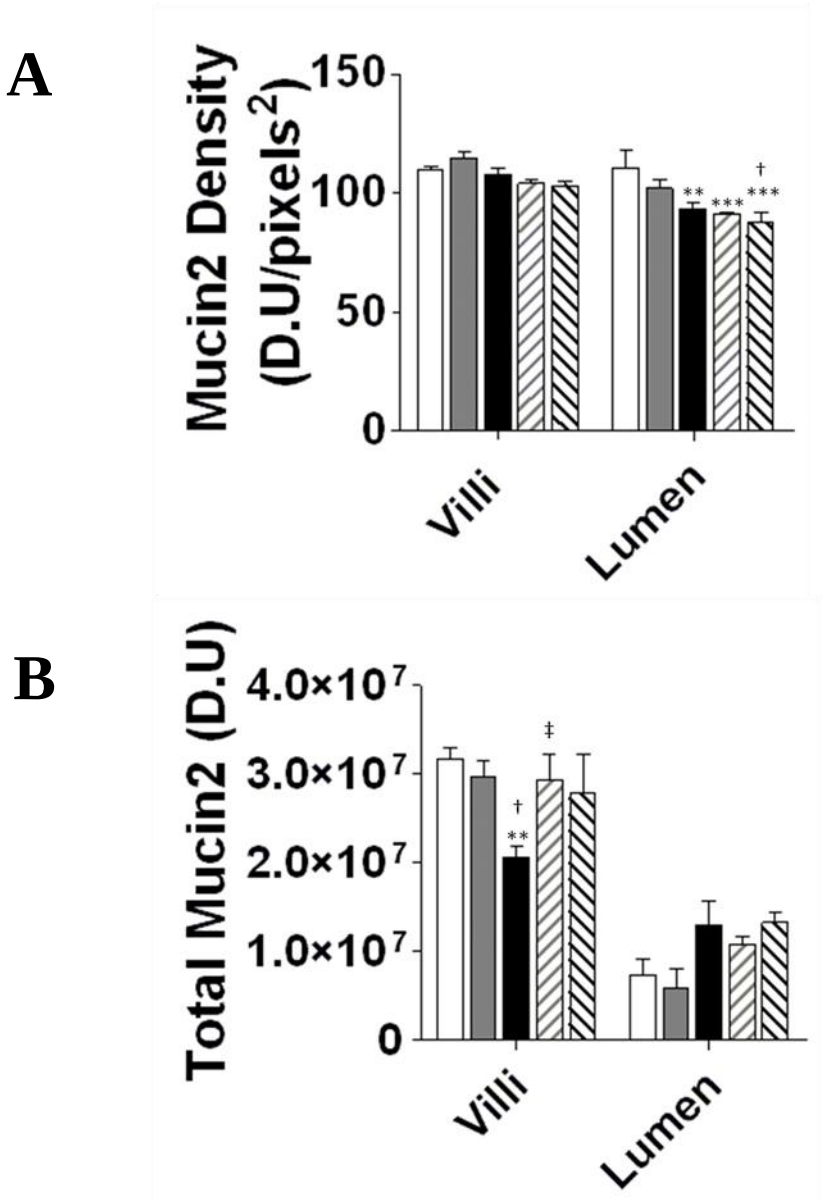

Figure 3.4 Mucin2 density measurements. Mucin2 density measured as the mean light intensity **(A)** and total mucin measured by the total light intensity **(B).** Values are mean±SEM (n=4). *P <0.05, ** P<0.001, ***P<0.0001 compared to sham. †P<0.05, ††P<0.001, †††P<0.0001 compared to 15 min SAO. ‡P<0.05, ‡‡P<0.001, ‡‡‡P<0.0001 compared to 30 min SAO (alcian blue and mucin2 staining).

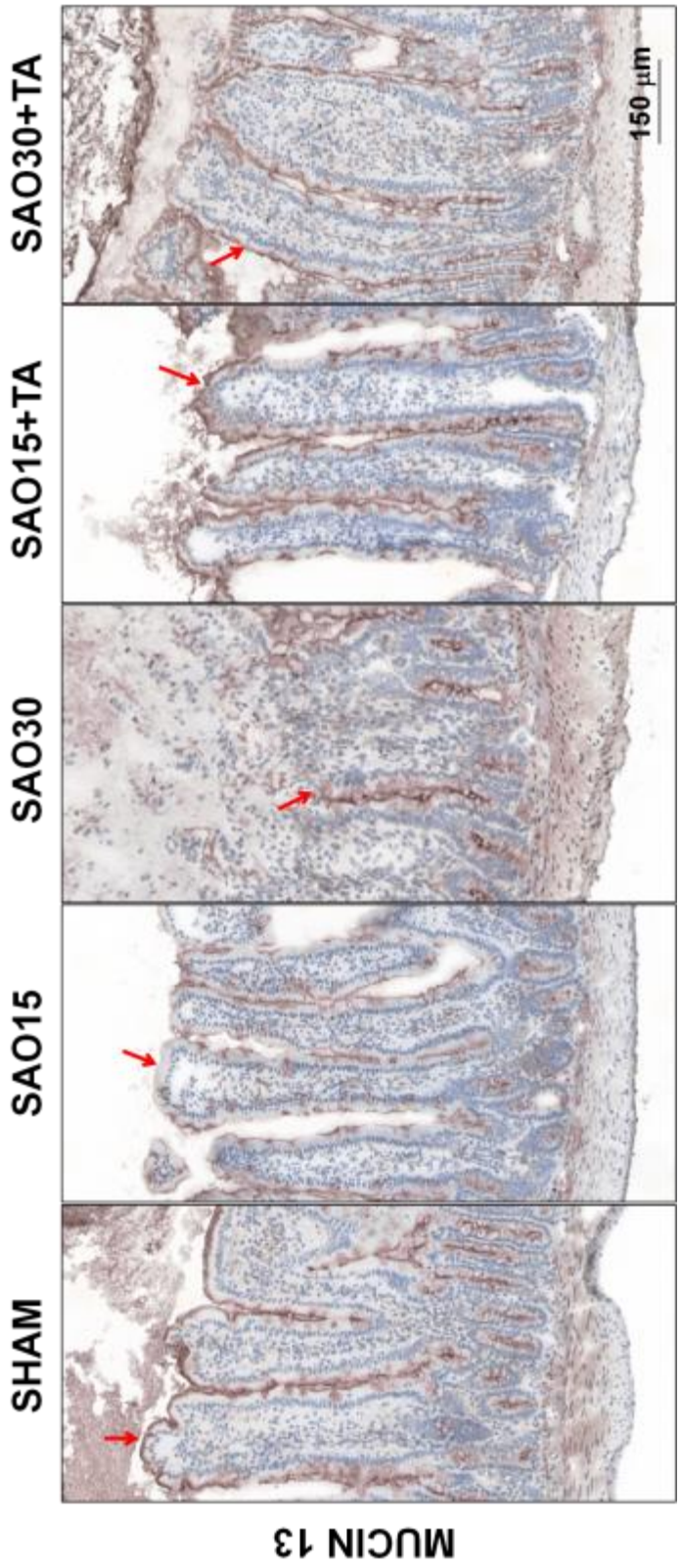

Figure 3.5 Mucin13 immunohistochemistry. Micrographs of jejunal frozen sections stained with immunoperoxidase staining against goblet cell-derived mucin13. Diamond arrows demonstrate luminal mucin and arrows show membrane-bound mucin.

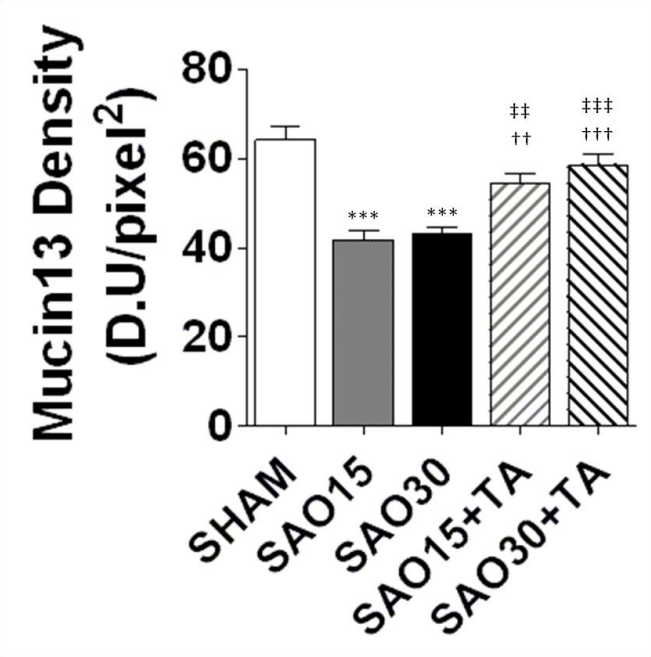

Figure 3.6 Mucin13 density Measurements. Mucin2 density measured as the mean light intensity (A) Values are mean±SEM (n=4). *P <0.05, ** P<0.001, ***P<0.0001 compared to sham. †P<0.05, ††P<0.001, †††P<0.0001 compared to 15 min SAO. ‡P<0.05, ‡‡P<0.001, ‡‡‡P<0.0001 compared to 30 min SAO (alcian blue and mucin2 staining).

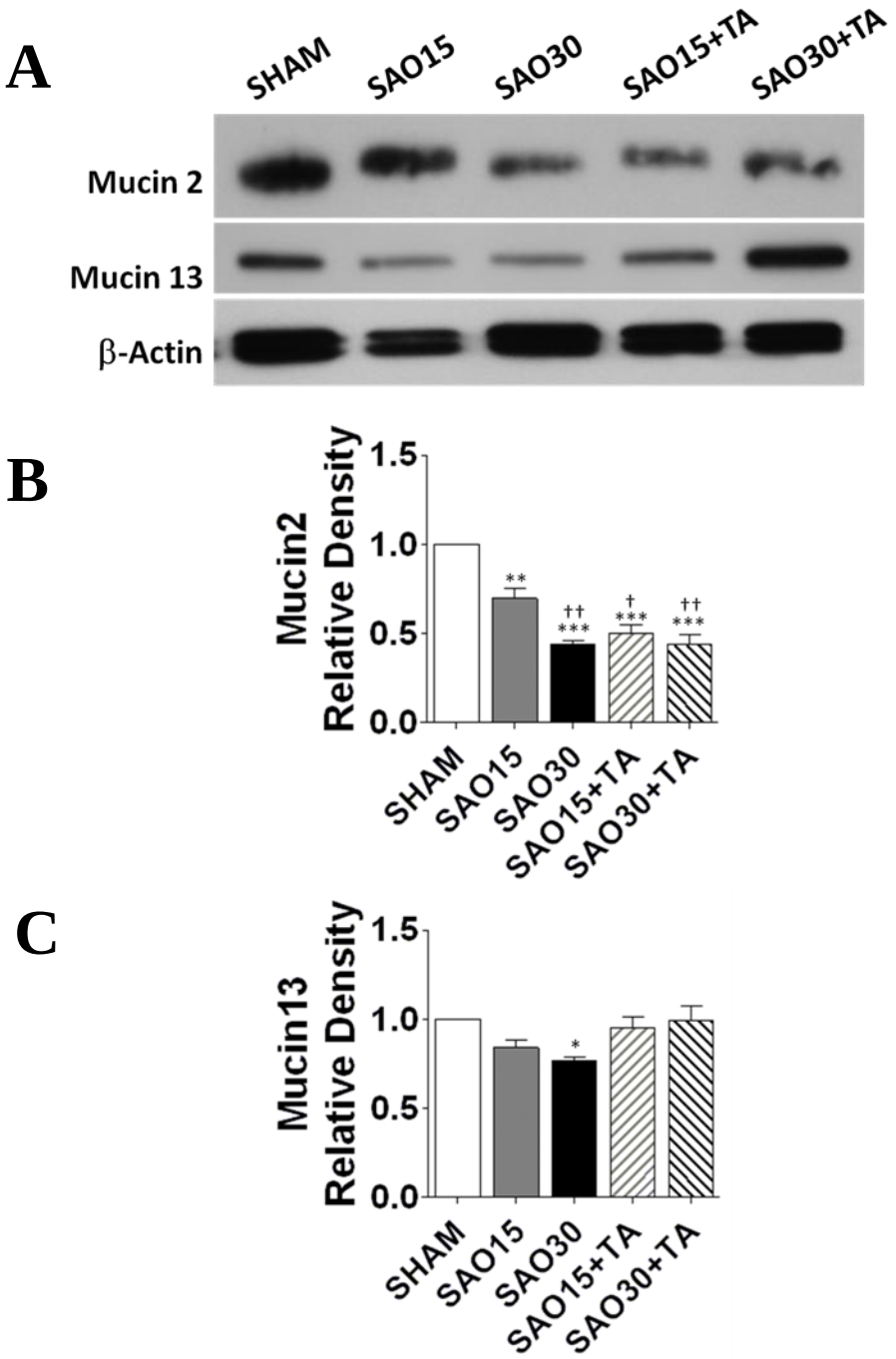

Figure 3.7 Western blot of mucin2, mucin13 and β-actin in intestine homogenates with removal of luminal contents (**A**). Relative density of mucin2 (**B**) and mucin13 with respect of β-actin (**C**). Values are mean±SEM (n=4). *P <0.05, ** P<0.001, ***P<0.0001 compared to sham. †P<0.05, ††P<0.001, †††P<0.0001 compared to 15 min SAO. ‡P<0.05, ‡‡P<0.001, ‡‡‡P<0.0001 compared to 30 min SAO (alcian blue and mucin2 staining).

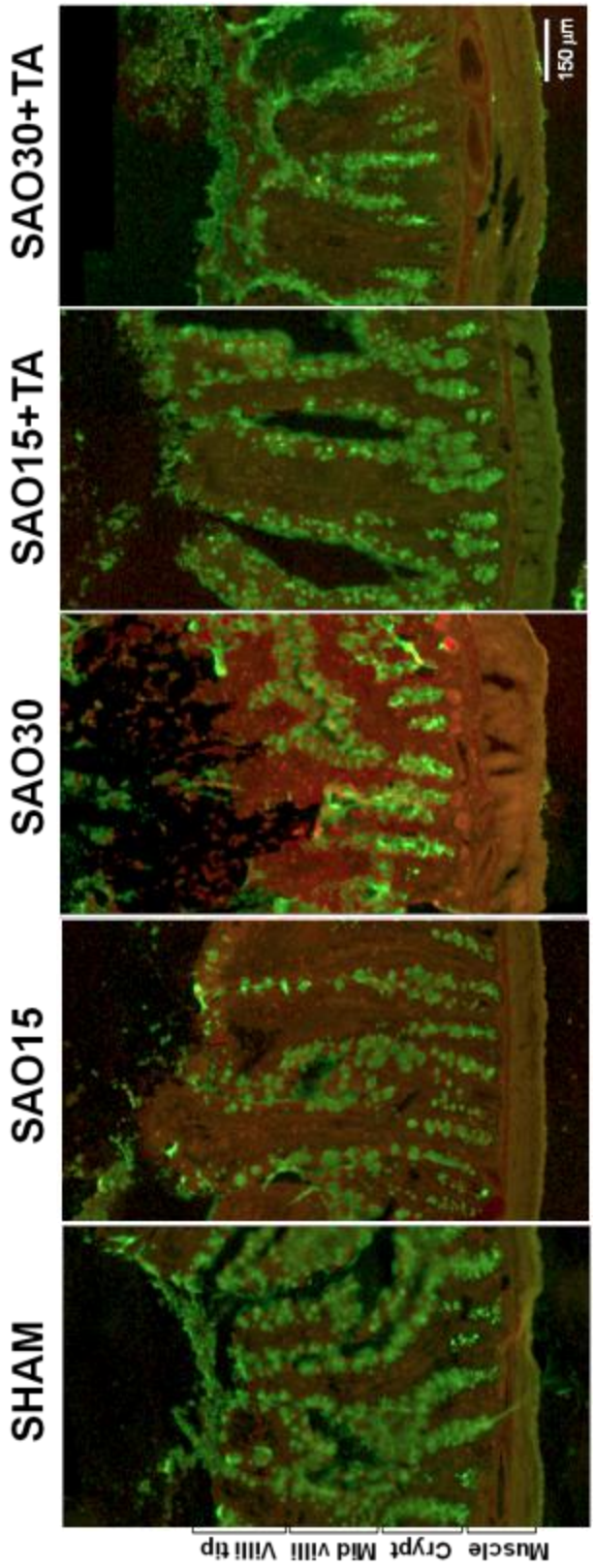

Figure 3.8 Serine protease activity and mucin2 co-localization. Micrographs of jejunal frozen sections with *in-situ* zymography of casein substrate specific for serine proteases (red) and immunofluorescent labeling against mucin2 (green).

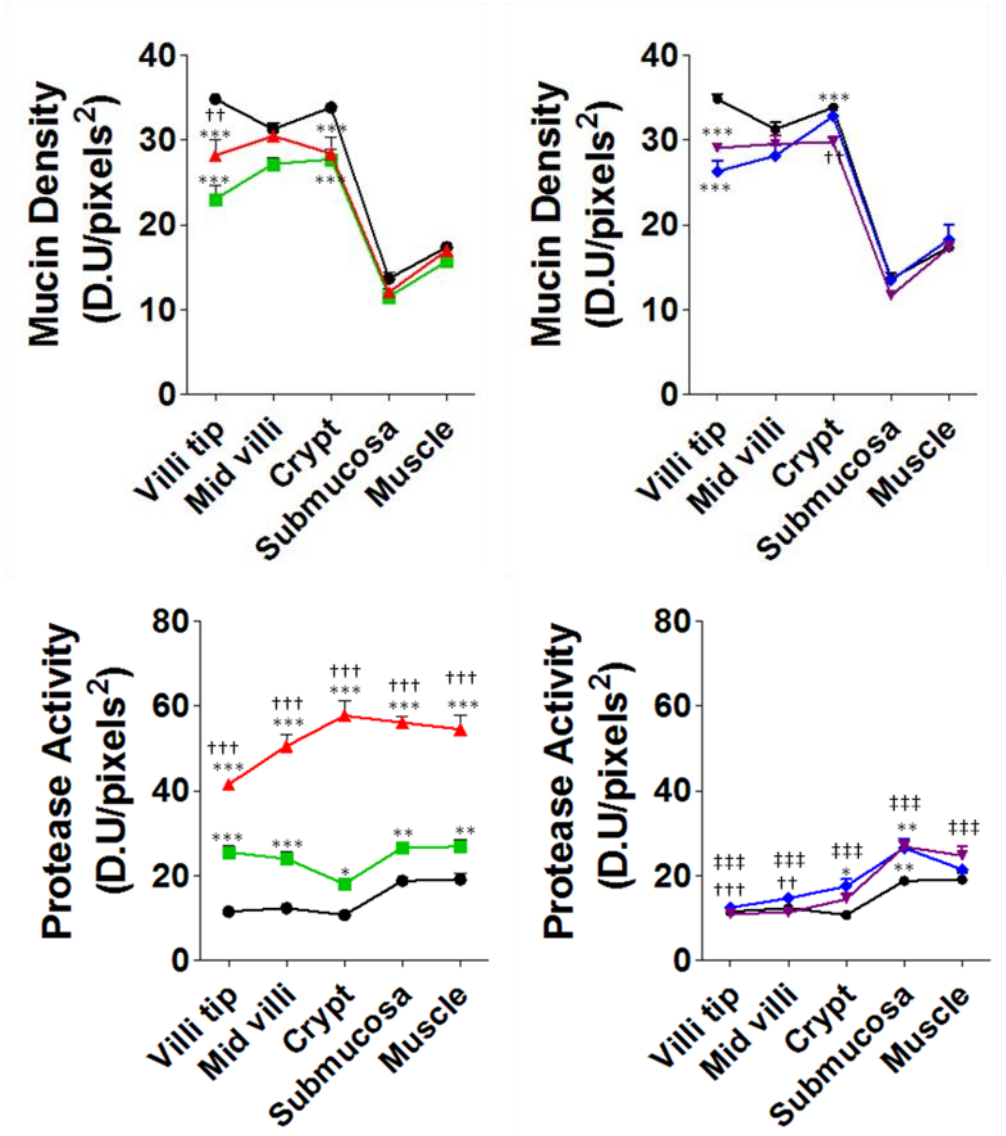

Figure 3.9 Serine protease activity and mucin density measurements at the villus tip, mid villus, crypt and muscle were measured as the mean light intensity after *in-situ* zymography cleavage of the Texas Red fluorophore by serine proteases and labeling with primary antibody against mucin2 and FITC secondary antibody. Values are mean±SEM (n=4). *P <0.05, **P<0.001, ***P<0.0001 compared to sham. ††P<0.001, ††P<0.001, †††P<0.0001 compared to 15 min SAO. ‡‡‡P<0.0001 compared to 30 min SAO, ##P<0.001, §§§P<0.0001 compared to 15 min SAO with TA. Figures are displayed as sham and SAO and sham and SAO plus TA for better visualization.

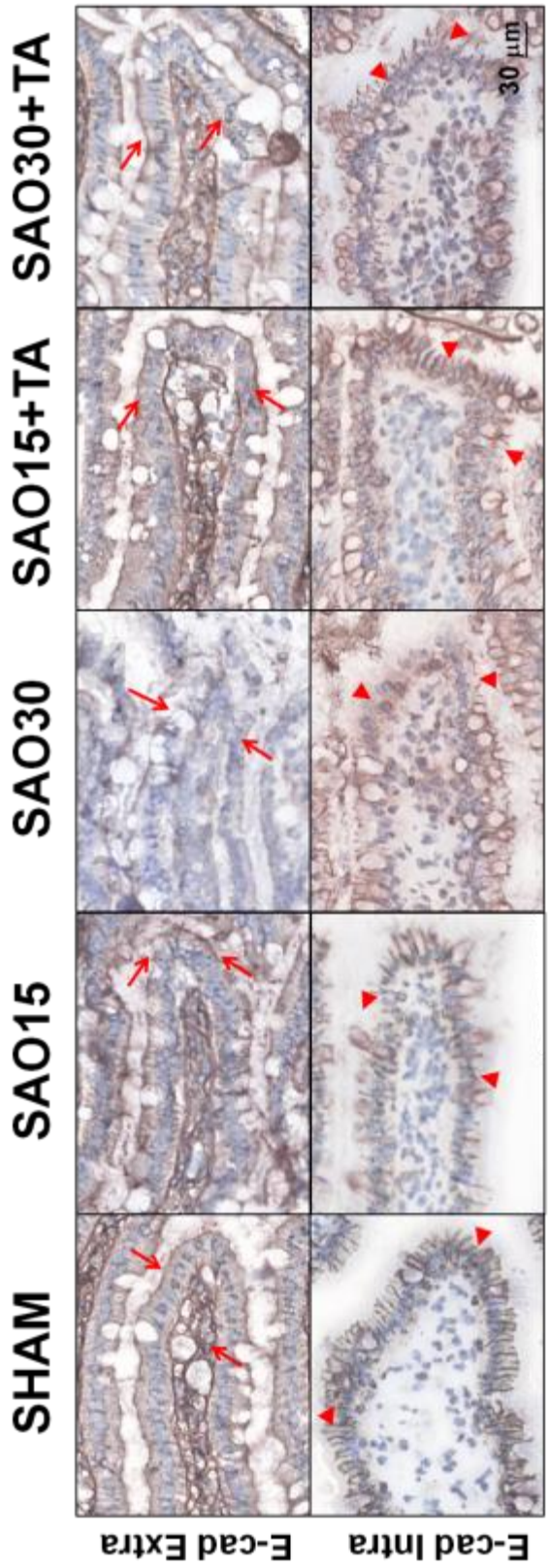

Figure 3.10 E-cadherin immunohistochcemistry. Representative micrographs of the villus tip from jejunal frozen sections oriented horizontally. Arrows represent immunoperoxidase staining against the extracellular domain of E-caherin and arrowheads represent staining agains intracellular domains of E-cadherin.

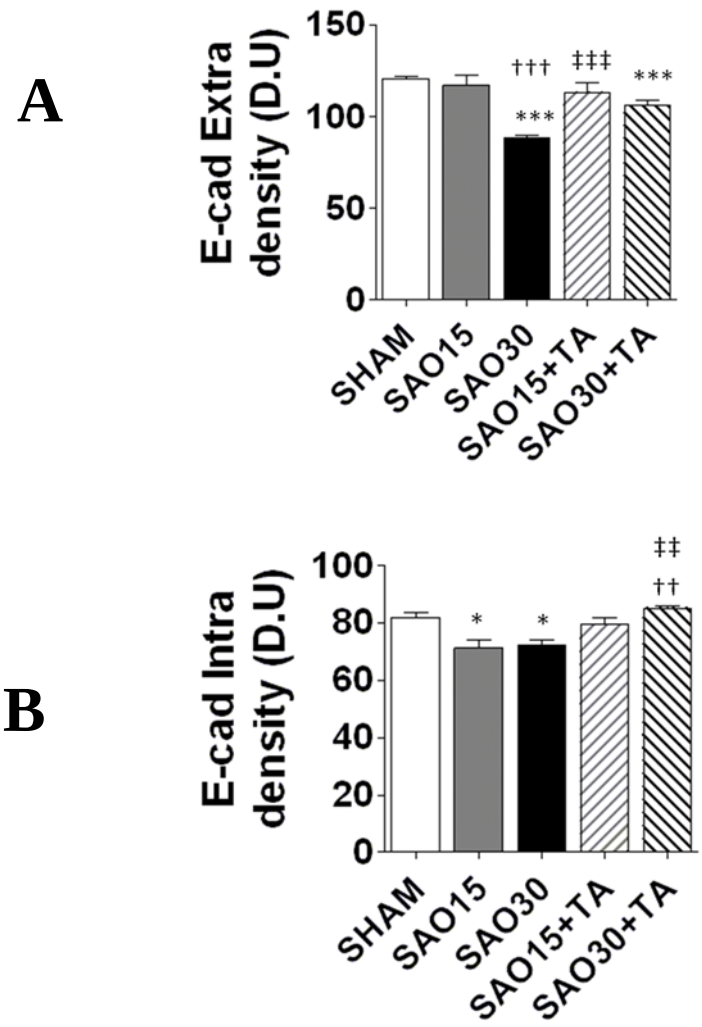

Figure 3.11 E-cadherin immunohistochemistry density measurements: measured as the mean light intensity after labeling with primary antibody against extracellular **(A)** and intracellular domain **(B)** of E-cadherin and DAB substrate, values are mean±SEM (n=4)/group. *P <0.05, ***P<0.0001 compared to sham. ††P<0.001, †††P<0.0001 compared to 15 min SAO. ‡‡P<0.001, ‡‡‡P<0.0001 compared to 30 min SAO, §§§P<0.0001 compared to 15 min SAO with TA.

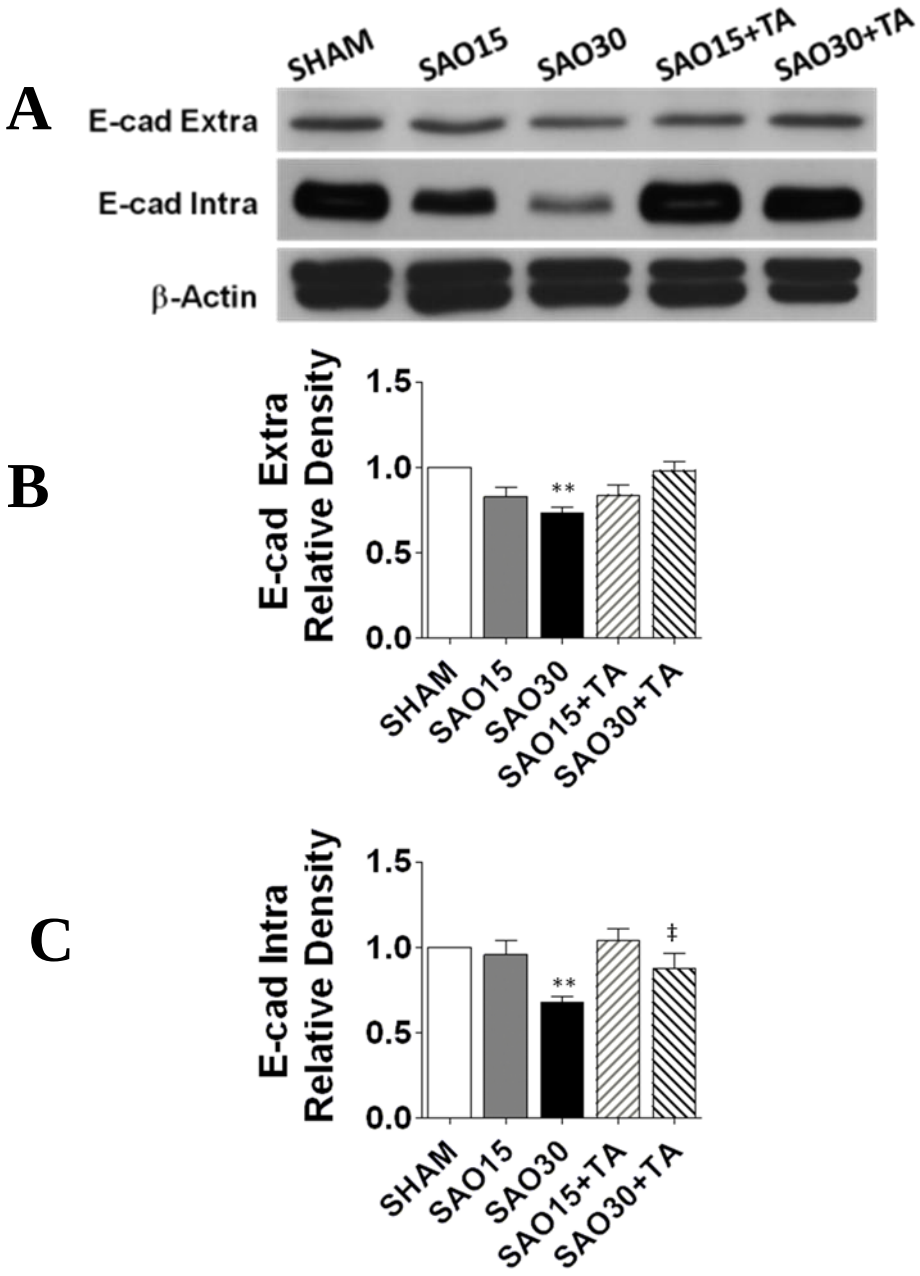

Figure 3.12 E-cadherin western blots: intra- and extra-cellular domains in intestine homogenates with removal of luminal contents **(A)**. Relative density of intra-cellular **(B)** and extra-cellular domains **(C)** of E-cadherin with respect of β-actin. Values are mean±SEM (n=4)/group. *P <0.05, ***P<0.0001 compared to sham. ††P<0.001, †††P<0.0001 compared to 15 min SAO. ‡‡P<0.001, ‡‡‡P<0.0001 compared to 30 min SAO, §§§P<0.0001 compared to 15 min SAO with TA.

3.8 References

1. Bounous G, McArdle AH, Hodges DM, Hampson LG, & Gurd FN (1966) Biosynthesis of intestinal mucin in shock: relationship to tryptic hemorrhagic enteritis and permeability to curare. (Translated from eng) *Ann Surg* 164(1):13-22 (in eng).

2. Albanese CT, *et al.* (1994) Role of intestinal mucus in transepithelial passage of bacteria across the intact ileum in vitro. *Surgery* 116(1):76.

3. Maxson RT, Dunlap JP, Tryka F, Jackson RJ, & Smith SD (1994) The role of the mucus gel layer in intestinal bacterial translocation. *Journal of Surgical Research* 57(6):682-686.

4. Nimmerfall F & Rosenthaler J (1980) Significance of the goblet-cell mucin layer, the outermost luminal barrier to passage through the gut wall. *Biochemical and biophysical research communications* 94(3):960-966.

5. Bansil R, Stanley E, & LaMont JT (1995) Mucin biophysics. (Translated from eng) *Annu Rev Physiol* 57:635-657 (in eng).

6. Qin X, Caputo FJ, Xu DZ, & Deitch EA (2008) Hydrophobicity of mucosal surface and its relationship to gut barrier function. (Translated from eng) *Shock* 29(3):372-376 (in eng).

7. Lidell M, Moncada D, Chadee K, & Hansson G (2006) Entamoeba histolytica cysteine proteases cleave the MUC2 mucin in its C-terminal domain and dissolve the protective colonic mucus gel. *Proceedings of the National Academy of Sciences* 103(24):9298.

8. Dekker J, Rossen J, Büller H, & Einerhand A (2002) The MUC family: an obituary. *Trends in biochemical sciences* 27(3):126-131.

9. Wang H, Lillehoj E, & Kim K (2004) MUC1 tyrosine phosphorylation activates the extracellular signal-regulated kinase. *Biochemical and biophysical research communications* 321(2):448-454.

10. Rahn J, Shen Q, Mah B, & Hugh J (2004) MUC1 initiates a calcium signal after ligation by intercellular adhesion molecule-1. *Journal of Biological Chemistry* 279(28):29386.

11. Meerzaman D, Shapiro P, & Kim K (2001) Involvement of the MAP kinase ERK2 in MUC1 mucin signaling. *American Journal of Physiology- Lung Cellular and Molecular Physiology* 281(1):86.

12. McNeill J, Stark R, & Greenway C (1970) Intestinal vasoconstriction after hemorrhage: roles of vasopressin and angiotensin. *American Journal of Physiology--Legacy Content* 219(5):1342-1347.

13. Chiu CJ, McArdle AH, Brown R, Scott HJ, & Gurd FN (1970) Intestinal mucosal lesion in low-flow states. I. A morphological, hemodynamic, and metabolic reappraisal. (Translated from eng) *Arch Surg* 101(4):478-483 (in eng).

14. Haglund U, Abe T, Ahren C, Braide I, & Lundgren O (1976) The intestinal mucosal lesions in shock. I. Studies on the pathogenesis. (Translated from eng) *Eur Surg Res* 8(5):435-447 (in eng).

15. Russell D, Barreto J, Klemm K, & Miller T (1995) Hemorrhagic shock increases gut macromolecular permeability in the rat. *Shock (Augusta, Ga.)* 4(1):50.

16. Wang W, Smail N, Wang P, & Chaudry IH (1998) Increased gut permeability after hemorrhage is associated with upregulation of local and systemic IL-6. *Journal of Surgical Research* 79(1):39-46.

17. Shute K (1976) Effect of intraluminal oxygen on experimental ischaemia of the intestine. *Gut* 17(12):1001.

18. Yang R, *et al.* (2002) Effect of hemorrhagic shock on gut barrier function and expression of stress-related genes in normal and gnotobiotic mice. *American Journal of Physiology-Regulatory, Integrative and Comparative Physiology* 283(5):R1263-R1274.

19. Rupani B, *et al.* (2007) Relationship between disruption of the unstirred mucus layer and intestinal restitution in loss of gut barrier function after trauma hemorrhagic shock. (Translated from eng) *Surgery* 141(4):481-489 (in eng).

20. Gawlak M, *et al.* (2009) High resolution in situ zymography reveals matrix metalloproteinase activity at glutamatergic synapses. (Translated from eng) *Neuroscience* 158(1):167-176 (in eng).

21. Bush KT, Tsukamoto T, & Nigam SK (2000) Selective degradation of E-cadherin and dissolution of E-cadherin-catenin complexes in epithelial ischemia. (Translated from eng) *Am J Physiol Renal Physiol* 278(5):F847-852 (in eng).

Chapter 4

Effect of Protease Inhibitors in Mucin Degradation

4.1 Introduction

The mucus layer is the first barrier lining the intestine for protection against invading organisms. Mucins are the main element responsible for the rheologic properties and barrier properties by the mucus layer. The viscoelasticity of mucus depends on mucin hydration, cross-linking and on the mucin concentration (1). Mucins are glycoproteins; therefore, they may be targets for diverse proteolytic and glycolytic enzymes. Partial or complete degradation of mucin molecules by microbial enzymes is often a fundamental step in disruption of defensive mucosal barriers, as these constitute direct interfaces between internal and external environments. The possible contribution of mucin degrading enzymes to the pathogenesis of infection is, therefore, not to be underestimated. Recent evidence suggests that enzymes able to digest mucin (mucinases) in particular may play a vital part in the etiology of certain conditions and/or infections (2). The carbohydrate component of the mucin molecule is particularly important in mucin susceptibility to enzymatic digestion as the majority of degradative enzymes that

have been studied affect carbohydrate side chains. The traditional view is that carbohydrate side chains protect the central protein core from attack by proteolytic enzymes.

4.2 Enzymes that may Degrade Mucins:

In a normal intestine, the protective role of mucin is maintained despite the abundant pancreatic digestive proteases. This protection is possible because its two large mucin domains are highly O-glycosylated and thus resistant to proteolytic cleavage because the glycans prevent access of the proteases to the protein core (3). In contrast, the N- and C-terminal cysteine-rich domains are less glycosylated, and the protein core is probably more exposed (3, 4). However, studies on the recombinant N-terminal cysteine-rich domain of mucin2 have revealed that the N-terminal trimers are held together within a core that is resistant to proteolytic enzymes. The protease resistance is likely due to the high number of intramolecular disulfide bonds that shield potential cleavage sites from the pancreatic enzymes (4). Reduction of the mucin polymer does not only dissolves the mucus gel but also renders the protein core outside of the mucin domains sensitive to proteolytic cleavages (5-7). Many proteases or glycosidases including those produced by bacteria are known to degrade components of mucus (2, 8). Theses enzymes may exert effects on the physical barrier and enhance bacterial adhesion and colonization as well as transport of noxius material from the intestinal lumen such as digestive enzymes.

4.2.1 Proteases: Proteases are likely to exhibit two modes of action in mucin degradation: The first mode is by initial cleavage at non-glycosylated regions, leading to

reduced viscoelasticity and disruption of gel structure (9, 10); and the second mode is by final disruption of exposed protein core after deglycosylation by other enzymes (9, 10).

4.2.2 Glycosidases: β-D-galactosidase, N-acetyl-β-D-galactosaminidase, α-fucosidases, sialidase and N-acetyl-β-D-glucosaminidase cleave sugars from mucin oligosaccharides (9, 11, 12). These enzymes may act in conjunction with each other enzymes to promote complete degradation of the glycoprotein (9, 11-13).

4.2.3 Sulphatases: Several organisms are known to produce sulphatases which act upon respiratory and gastrointestinal mucins (14). The loss of terminal sulphate residues may be an important rate-limiting factor in mucin degradation as this may expose underlying sugars to further enzymatic attack.

4.2.4 Sialidases: Sialidases have been subject to much investigation since their discovery in the 1940s (15), and their occurrence in bacteria and viruses is widespread. Sialidases cleave terminal sialic acids from glycoproteins and glycolipids, unmasking other sugars on their carbohydrate side chains. Sialidases tend to be highly substrate specific. They may target particular types of specific sugar linkages; or may be sensitive to the nature of the linkage sugar itself (D-galactose, N-acetyl-D-galactosamine, etc). Sialidases are most commonly secreted, but may be cell bound (11).

4.3 Mucin Degradation in Different Organs

Under normal conditions mucus adheres to many epithelial surfaces, where it serves as a diffusion barrier against contact with noxious substances and as a lubricant to minimize shear stresses; such mucus coatings are particularly prominent on the epithelia

of the respiratory, genital and gastrointestinal tracts. Disruption of mucin in different organs has been associated with disease states.

4.3.1 Airway mucin degradation in vitro: Airway mucins are important in the lung. Airway mucin concentration is decreased in cystic fibrosis (CF). The effect of mucin degradation in vitro was done by incubating freshly collected sputum and mucus without protease inhibitors from cystic fibrotic patients (16). Henke et al demonstrated that airway mucins can be degraded by synthetic human neutrophil elastase (HNE) and P. aeruginosa elastase B (psudolysin) and that degradation was inhibited by serine proteases inhibitors (diisopropyl flurophospahtes [DFP], phenylmethylsulfonyl fluoride [PMSF], and 1-choro-3-tosylamido-7amino-2-heptanone HCl [TLCK]). Their data indicate that the loss of the mucin barrier in the airways is most likely due to degradation by serine proteases contributing to the chronic infection in the CF airway (16).

4.3.2 Degradation of cervical mucins: In the female reproductive tract a primary function of the cervical mucus is the defense of the upper reproductive tract from microbial invasion. Physical clearance of microbes by mucosal secretions is the most effective line of defense. Microbial mucin degrading enzymes are either significantly associated with certain genital tract conditions and sexually transmitted infections or are known to be produced by the offending micro-organisms (10).

4.3.3 Degradation of gastric mucins: Previous rheological studies on gastric mucin indicate that this material is pH dependent, transitioning from a viscous solution at neutral pH to a gel in acidic conditions (17, 18). This feature of mucin is believed to play a crucial role in its protective function from damage by the stomach acidic secretions and

other insults. Bulk rheology measurements on porcine gastric mucin (PGM) show that H. pylori elevates the pH by secretion of urease, which catalyses hydrolysis of urea present in the stomach to yield NH_3 and CO_2 (18). This induces a dramatic decrease in viscoelastic moduli by altering the rheological properties of mucin (18).

4.3.4 Degradation of colonic mucins: In order for enteric pathogens to invade and make contact with the colonic epithelium, they must penetrate the thick protective mucus barrier (19). The ability of the cysteine proteases to dissolve mucus gels was confirmed by treating mucins from a MUC2-producing cell line with amoeba proteases (3). Cysteine proteases secreted from the amoeba disrupts the mucin polymeric network, thereby overcoming the protective mucus barrier (3).

4.4 Aims in this Chapter

Mucin is believed to protect the epithelial surface of the small intestine from luminal digestive enzymes, abrasion by food particles, and pathogens by forming a barrier between the lumen and the intestinal epithelium (20-23). The hypothesis of the study presented in this chapter is that that during intestinal ischemia mucin is subject to enzymatic digestion, resulting in mucin degradation and breakage of the intestinal epithelial barrier. Thus this chapter examines the effect of digestive enzymes on mucin disruption by luminal amylase inhibition with acarbose and serine protease inhibition with tranexamic acid and nafamostat mesilate.

4.5 Materials and Methods

4.5.1. Animal groups and SAO model: All animal protocols were reviewed and approved by the University of California San Diego Animal Subjects Committee. Male Wistar rats (300-350g, Harlan Sprague Dawley Inc, Indianapolis, IN) were randomly assigned to one of five groups (n=4 per group): a sham group (SHAM), and four groups subjected to 30min splanchnic ischemia without enteral protease inhibition (SAO30) and with enteral amylase inhibition by acarbose (SAO30+ACA), protease inhibition by tranexamic acid (SAO30+TA) and nafamostat mesilate (ANGD, [6-amidino-2-naphthyl p-guanidinobenzoate dimethanesulfonate]) (SAO+ANGD). Rats were kept on solid food restriction for 12 hours prior to surgery with water ad libitum. After general anesthesia (Ketamine/Xylazine, 75 mg/kg BW / 20 mg/kg BW, IM) all groups were injected 0.9% saline (3ml/100g BW) into the lumen of the intestine either alone (SHAM or SAO30 groups) or mixed with one of three enzyme inhibitors (SAO30+ACA, SAO30+TA, or SAO30+ANGD groups). The concentration of the enzyme inhibitors was as follows: acarbose (0.5mg/100g BW) and tranexamic acid (0.1g/100g BW) (Sigma-Aldrich, St Louis, MO) or nafamostat mesilate (5mg/ 100g BW, Torii Pharmaceutical Co. Ltd., Tokyo, Japan). 30 min after saline or saline/inhibitor injection, the superior mesenteric and celiac arteries were isolated and occluded for 30 min for the ischemic groups or isolated without occlusion in the sham group. After 30 min SAO or sham surgery the animals were euthanized with Beuthanasia® 0.22 ml/kg BW, IV.

4.5.2 Tissue cryosections: After euthanasia, jejunal sections (~1 cm in length) were excised without removal of luminal contents and suspended in Tissue-Tek O.C.T.

Compound (Sakura Finetek, Torrance, CA), snap frozen in isopentane/liquid nitrogen, and stored at -80^{o}C for analysis. Cryosections (5 µm thickness) along the longitudinal axis of the villi were used throughout all experiments. Cryosections were fixed in 10% formalin solution and processed in a non-blinded fashion.

4.5.3 In-situ tissue zymography and immunohistochemistry: In-situ zymography for trypsin activity in cryosections was assessed by measurement of fluorescence resulting from the proteolytic cleavage of the substrate (1mM, Nα-benzoyl-L-arginine-7-amido-methylcoumarin hydrochloride; Sigma-Aldrich) as described elsewhere (24). For immunohistochemical analysis, primary antibodies were diluted as followed: Trypsin 1:300 and mucin2 1:200 (Santa Cruz Biotechnology, Santa Cruz, CA); the extracellular domain of TLR4 1:250 (Abcam, Cambridge, MA), and the intracellular domain of TLR4 1:250 (Invitrogen, Carlsbad, CA, USA). Secondary antibodies were as follows: FITC (Santa Cruz Biotechnology) and HRP (ImmPRESS, Vector Lab; Burlingame, CA). The slides were developed using 3, 3´-diaminodbenzidine substrate and counterstained with hematoxylin or DAPI (Vector Lab) or propidium iodine (Sigma-Aldrich). Slides were observed in a non-blinded fashion under an inverted microscope (20X and 60X objectives).

4.5.4 Homogenates of intestine and luminal contents: Jejunal segments were excised without removal of luminal contents. For enzyme activity measurements, segments of intestine were homogenized with CelLytic™ (Sigma-Aldrich) without addition of protease inhibitors. For Western blot assays the intestine segments were homogenized as above in the presence of protease inhibitors (5mM EDTA, 5mM N-Ethylmaleimide,

25mM iodoacetamide, 5mM benzamidine, 300mM acarbose, 5mM 6-aminocaproic acid, 1mM protease inhibitor cocktail, (Sigma-Aldrich).

In separate experiments the small intestine of sham animals was excised, and the luminal contents were flushed with 20 ml saline. Homogenates or luminal contents were centrifuged (16,000g for 15 min at 4°C), the supernatant was collected and protein concentration was assessed with the bicinchoninic acid protein assay (Thermo Scientific).

4.5.5 Enzyme activity: Protease activity of intestinal homogenates (100μg of protein), homogenates of the luminal contents (50μg of protein), or 50μg/ml purified enzyme (porcine trypsin and amylase) was measured with substrates specific for trypsin and papain (50μM, Nα-benzoyl-L-arginine-7-amido-methylcoumarin hydrochloride) (25) and amylase (4mM, 2-Chloro-4-nitrophenyl-α-D-maltotrioside, Sigma-Aldrich) (26). The initial rates of hydrolysis were measured by the fluorescent intensity of 7-amido-4-methylcoumarin, 380/460 nm (excitation/emission) or the absorbance of 2-Chloro-4-nitrophenol at 405nm (SpectraMax Gemini XS, Molecular Devices, Sunnyvale, CA). The enzymatic inhibitory properties of acarbose and nafamostat mesilate were confirmed by incubation of amylase or trypsin with different concentrations of inhibitors for 30 minutes, followed by incubation with the specific substrates. The initial velocity of the reaction was expressed as the rate of change of relative units (RU) per minute and per μg of protein. The data was fitted with a non-linear regression of the Michaelis-Menten or Lineweaver-Burk equations and kinetic constants (maximum enzyme velocity, V_{max}, Michaelis-Menten constant, K_m,, and inhibitory constant, K_i) were computed (GraphPad Prism, Graphpad Software, San Diego, CA).

4.5.6 Quantitative PCR (qPCR): Total-RNA was isolated from jejunal segments (SHAM (n=6) and SAO30; n=4 for SAO30+ACA, SAO30+TA and SAO30+ANGD) using RNeasy kit (Qiagen, Valencia, CA), and the total RNA was quantified by optical density. cDNA was generated (iScript cDNA synthesis kit, BioRad Laboratories, Richmond, CA) and qPCR reactions were performed (SYBR Green, Biorad). The primer sequences used for rat mucin 2 (MUC2) were designed from the fragment of *Rattus norvegicus* mucin mRNA (GI 506641): 5'-CAGAGTGCATCAGTGGCTGT-3' (forward) and 5'-CCCGTCGAAGGTGATGTAGT-3' (reverse). ß-actin was used as a reference gene, chosen and designed from the ß-actin mRNA (GI 42475962): 5'-AACTGGGACGATATGGAGAAGATTT-3' (forward) and 5'-TGGGCACAGTGTGGGTGA-3' (reverse). The efficiencies of the primers were determined and used for calculating the change in MUC2 mRNA expression relative to β-actin mRNA expression.

4.5.7. Western blot: Tissue homogenate (20μg) were separated by SDS-PAGE. Membranes were incubated with primary antibodies as follows: mucin2, mucin13 and trypsin 1:1000 (Santa Cruz Biotechnology), pancreatic amylase 1:1000 (GeneTex, San Antonio, TX), intra- and extra-cellular domains of E-cadherin and TLR4 1:1000 (Abcam), intracellular domain of TLR4 1:1000 (Invitrogen). Secondary antibodies were diluted 1:20000 (Santa Cruz Biotechnology) and detected with enhanced chemiluminescent (ECL) substrate for horseradish peroxidase (HRP) (Super Signal West Pico, Thermo Scientific). The exposed x-ray films were scanned and label intensity was measured using digital gel analysis (NIH ImageJ software).

4.5.8. Statistical Analysis: Results are presented as mean±SEM. Unpaired comparisons of mean values between groups were carried out by one-way ANOVA followed by Bonferroni post-hoc comparisons. $P<0.05$ was considered significant.

4.6 Results

4.6.1. Inhibitory profile of acarbose and nafamostat mesilate: In order to determine the role of digestive enzymes in mucin disruption during ischemia, we used three inhibitors: acarbose, an α-glucosidase and pancreatic α-amylase inhibitor (27), tranexamic acid, a trypsin and plasminogen inhibitor (24, 28, 29); and nafamostat mesilate, a broad spectrum serine protease inhibitor (30)). Acarbose inhibited amylase non-competitively with an inhibitory constant K_i = 0.48mM (Figure 4.1) and nafamostat mesilate inhibited trypsin competitively with K_i = 0.78μM (Figure 4.2) Tranexamic acid inhibited trypsin competitively with K_i = 56.5mM (24)

4.6.2 Amylase and trypsin activity and protein levels after SAO. The activity levels of amylase and trypsin in intestine homogenates during ischemia were significantly higher compared to levels in sham animals (SHAM) and this activity was decreased in the groups treated with their respective inhibitors (Figure 4.3). The activity of luminal contents (LUM CONT) alone in the sham group was significantly elevated as compared to the activity of tissue homogenates of all groups (Figures 4.3).

Western blot for amylase and trypsin in intestinal homogenates for all groups showed no change in the amount of protein, implying that the enzymes are being activated during ischemia (Figure 4.4).

In-situ zymography of trypsin activity in the intestinal wall (Figure 4.5) revealed no trypsin activity in the SHAM group and high levels of trypsin activity for the ischemic group without protease inhibitors (SAO30) and for the ischemic group with acarbose treatment (SAO30+ACA). Ischemic groups treated with tranexamic acid (SAO30+TA) and nafamostat mesilate (SAO30+ANGD) had undetectable levels of trypsin activity in the intestinal wall.

4.6.3 Mucin2 degradation during SAO: To determine whether digestive enzymes mediate mucin degradation, we visualized mucin 2 and trypsin with immunohistochemical techniques. In the sham group (SHAM) mucin 2 had the appearance of an intact layer (Figure 4.6) while in the ischemic group without protease inhibitors (SAO30) this layer was discontinuous. The tips of the villi were destroyed and trypsin penetrated into the intestinal wall. In the presence of inhibitors, the mucin 2 layer also appeared less dense as compared to the sham group.

The protein levels of mucin 2 in intestine homogenates, as determined by Western blot (Figure 4.7A, B), were significantly decreased in the ischemic group as well as in the ischemic groups treated with tranexamic acid (SAO30+TA) and nafamostat mesilate (SAO30+ANGD). This evidence suggests that trypsin may not mediate mucin 2 degradation. Mucin 2 density in the ischemic group treated with acarbose (SAO30+ACA) was also decreased as compared to the sham group and was on average slightly greater than in the other ischemic groups (not significant).

4.6.4 Mucin2 mRNA levels after SAO: In order to determine whether ischemia affects MUC2 mRNA synthesis we performed real-time quantitative PCR; the results show that

mRNA relative levels in intestinal tissues were higher after 30 min of ischemia. mRNA levels in ischemic group without protease inhibition (SAO30) were significantly elevated compared to SHAM while the mRNA relative levels for the ischemic groups with luminal inhibitor treatments (SAO30+ACA, SAO30+TA, SAO30+ANGD) were not significantly increased compared to sham (Figure 4.7C).

4.6.5. Mucin13 fragmentation during SAO: Western blot analysis indicates that the digestive enzymes were not associated with a significant shift in the density levels of the intact molecule of mucin 13 (56kDa) in any of the groups (Figure 4.7A). Low molecular weight bands were observed in addition to the band corresponding to the whole molecule. The sham group (SHAM) had low molecular weight bands around 24kDa and to lesser degree at 20kDa. The density of these bands was significantly decreased in the ischemic group without luminal inhibitors (SAO30) and in the groups with trypsin inhibition by either tranexamic acid (SAO30+TA) or nafamostat mesilate (SAO30+ANGD) (Figure 4.8). The ischemic group with amylase inhibition by acarbose (SAO30+ACA) had higher density levels of these bands. There was also another band around 17kDa that was not present in the sham group and appeared during ischemia (Figure 4.7A). Density of this band was significantly greater in the ischemic group alone and in the groups with luminal inhibition by tranexamic acid or nafamostat mesilate compared to sham, and was present to a lesser degree in the acarbose group (not significant) (Figure 4.8).

4.7 Discussion

The importance of mucin during breakdown of the intestinal mucosal barrier in ischemia and hemorrhagic shock was first suggested in the 1960s (31). Since then a

number of investigators have established a correlation between the loss of the intestinal mucus layer and increased intestinal injury during hemorrhagic shock (32) and sepsis (33, 34). In the previous chapters it was shown that 30 minutes of intestinal ischemia results in mucin disruption and transport of digestive enzymes from the lumen of the intestine into the intestinal wall and subsequently into the systemic circulation (24).

In this study we showed in-vivo that mucin disruption during early periods of intestinal ischemia is not directly mediated by trypsin. Mucin 2 and mucin 13 are degraded during ischemia but this disruption is not prevented by the inhibition of trypsin with tranexamic acid or nafamostat mesilate (Figure 5). Thus, there is a possibility that another protease may be involved in mucin degradation. There is some preservation of mucin 2 and mucin13 by amylase inhibition with acarbose, which may suggest an indirect role of pancreatic amylase; the role of amylase remains to be further investigated.

Furthermore the ischemic groups treated with luminal injection of enzyme inhibitors had reduced enzymatic activity and these groups had less visible injury as compared to the ischemic group without inhibitors. These results suggest that individual digestive enzymes or a combination of them mediate epithelial cell disruption but not mucin disruption.

Goblet cell-derived mucin (mucin 2) in the mucus layer has been proposed to be the major barrier against passage of high-molecular weight compounds across the intestinal barrier (35). The level of the mucus layer is determined by a balance between secretion and degradation of this protein. A variety of stimuli in different pathologies may lead to mucin over-secretion or cessation of secretion (36-40). In the current results

we show that after 30min ischemia the level of MUC2 mRNA is significantly increased as compared to the sham group. This rapid response after a relatively short period of ischemia may serve to replenish mucin 2 in the mucus layer, which may be a critical protection mechanism to prevent the escape of luminal digestive enzymes. Further studies are necessary to determine whether MUC2 mRNA is translated if longer periods of ischemia and reperfusion are present and if under these conditions the rate of mucin degradation is greater than the rate of secretion, resulting in irreversible injury.

In conclusion, the results presented here confirm that during ischemia mucin isoforms are degraded, which may stimulate synthesis of new mucin to restore the damaged barrier. As mucin is degraded digestive enzymes in the lumen of the intestine enter across the intestinal epithelium initiating autodigestion.

Chapter 4 in full is submitted material to Plos One as it appears in “Breakdown of Mucin as Barrier to Digestive Enzymes in the Ischemic Rat Small Intestine” by Chang M., Alsaigh T., Kistler E. B., Schmid-Schönbein G.W. The dissertation author is the primary author of this manuscript.

A

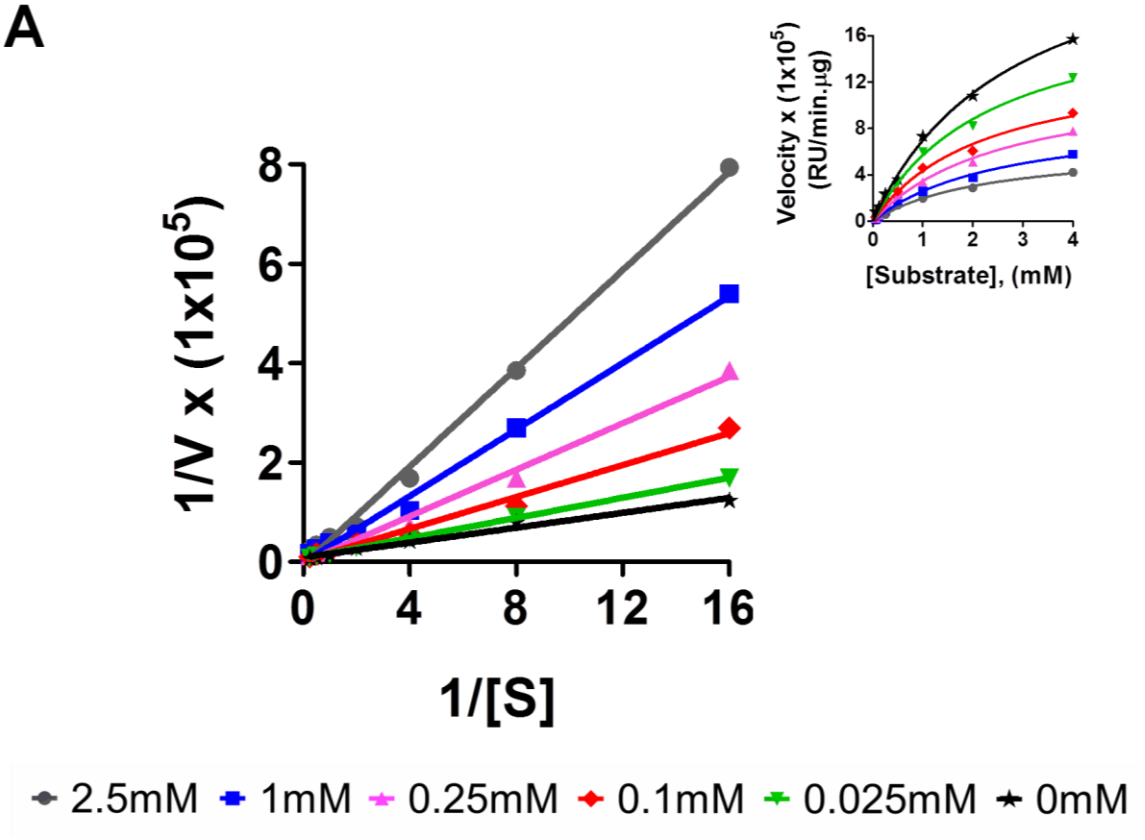

B

[ACA] x(1x10^5)	2.5mM	1mM	0.25mM	0.1mM	0.025mM	0mM
VMAX	6.5	9.2	12.6	14.2	19.4	26.6
KM	2.3	2.5	2.6	2.2	2.4	2.8
R^2	0.991	0.990	0.990	0.987	0.994	0.996

Figure 4.1 Inhibitory profile of acarbose. Lineweaver-Burk Plot with inset Michaelis-Menten plot of amylase activity with different concentrations of acarbose **(A).** Enzyme kinetic parameters, maximum enzyme velocity (V_{max}, RFU/min.µg), Michaelis-Menten constant (K_m, mM or µM) for amylase with different concentrations of inhibitors calculated after non-linear regression **(B).**

A

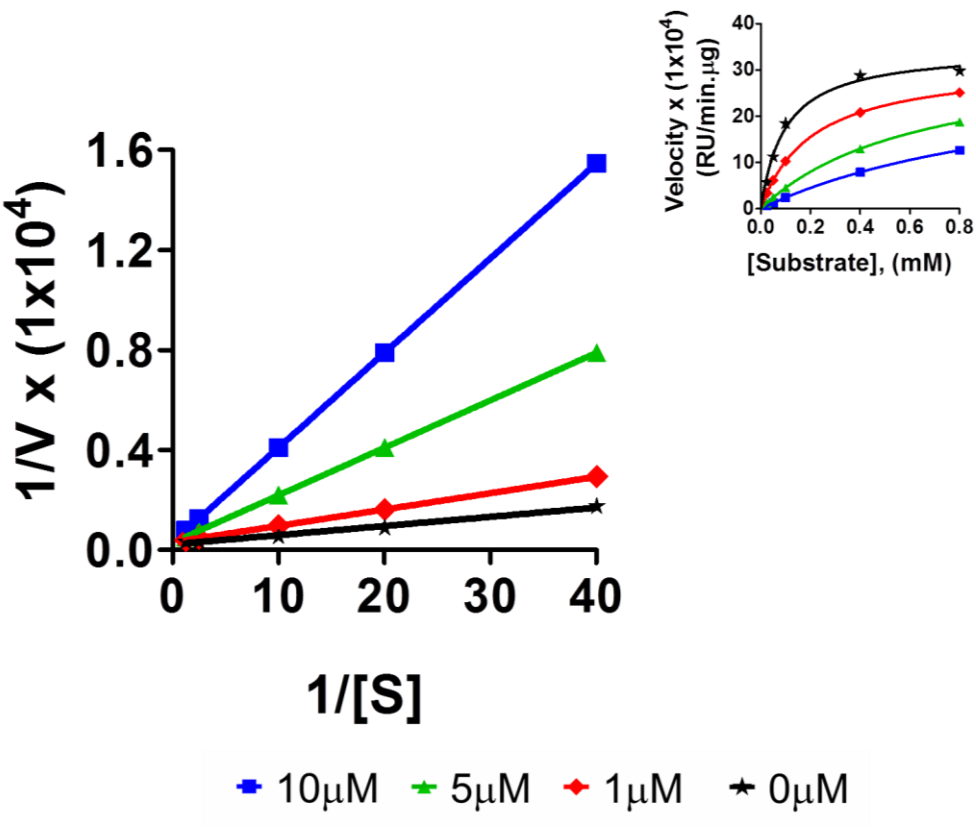

B

[ANGD] x(1x10⁴)	10µM	5µM	1µM	0µM
VMAX	31.5	33.8	31.5	34.5
KM	1.194	0.642	0.206	0.098
R^2	0.999	0.996	0.998	0.988

Figure 4.2 Inhibitory profile of nafamostat mesilate. Lineweaver-Burk Plot with inset Michaelis-Menten plot of amylase activity with different concentrations of nafamostat mesilate **(A)**. Enzyme kinetic parameters, maximum enzyme velocity (V_{max}, RFU/min. µg), Michaelis-Menten constant (K_m, mM or µM) for trypsin with different concentrations of inhibitors calculated after non-linear regression **(B)**.

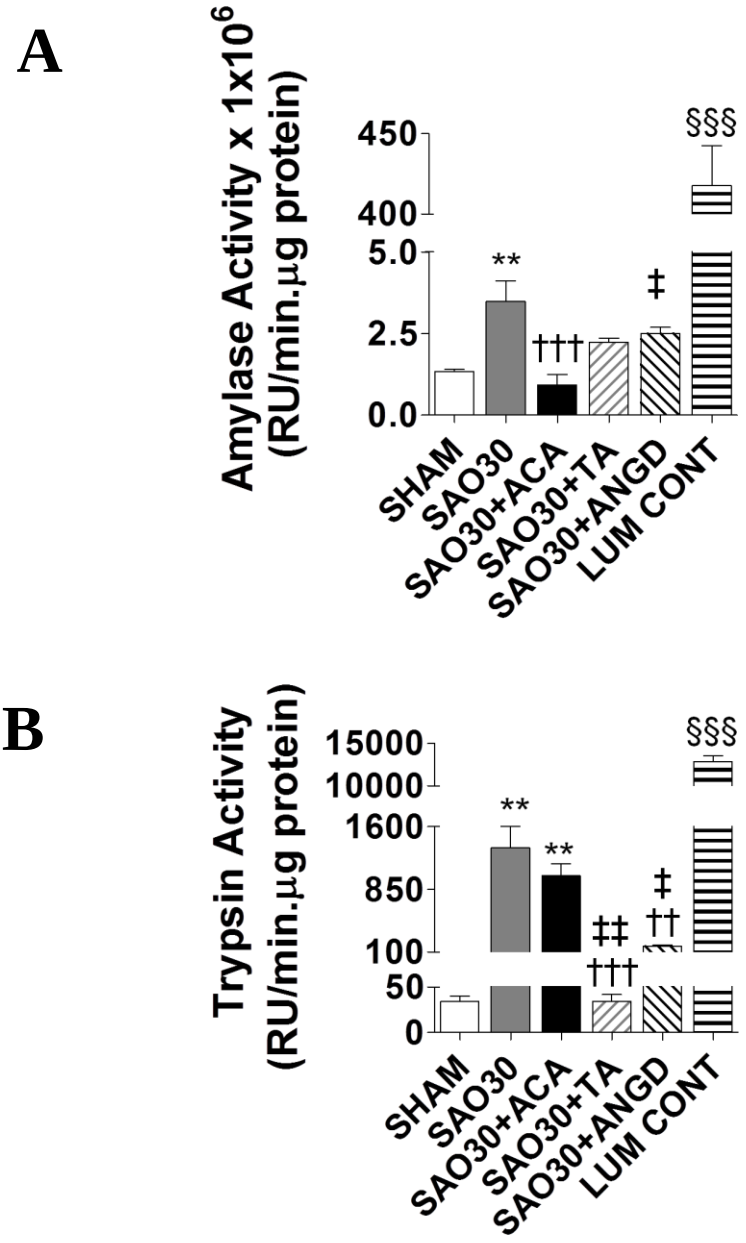

Figure 4.3 Amylase and trypsin activity in intestine homogenates during SAO. Enzyme activity of amylase **(A)** and trypsin **(B)** in intestine homogenates of SHAM animals or animals subjected to SAO protocol with luminal inhibition with acarbose (ACA), tranexamic acid (TA) or nafamostat mesilate or without (NI). Activity of luminal contents of SHAM intestines for each enzyme is shown at the end of the graphs. Values are mean±SEM (n=4)/group ** P<0.001 compared to SHAM, ††† P<0.0001 compared to SAO30, ‡ P<0.05 and ‡‡P<0.001 compared to ACA, §§§ P<0.0001 compared to all the other groups.

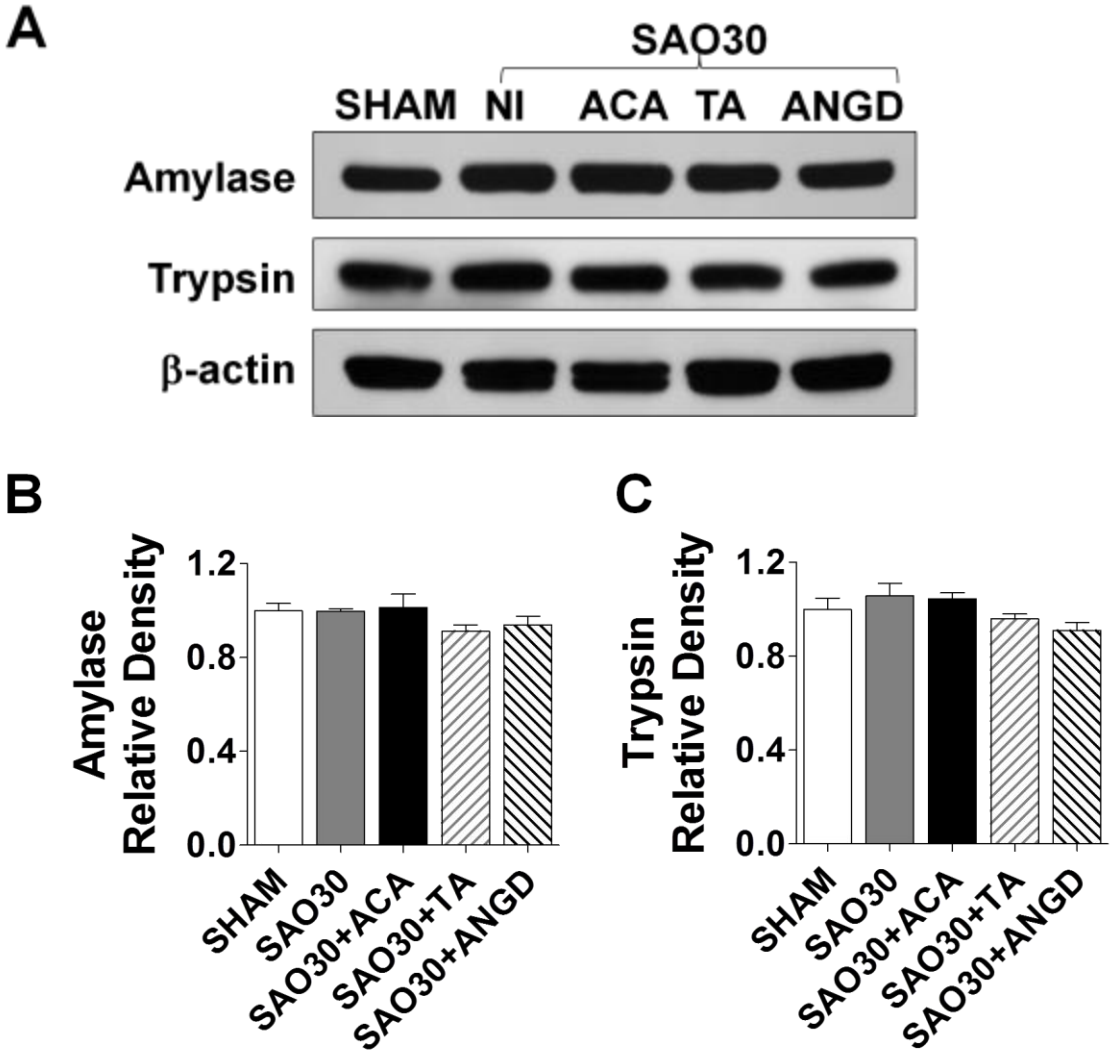

Figure 4.4 Western blots for amylase and trypsin and β-actin in intestine homogenates **(A)** with corresponding density levels measurements **(B, C)**. Values are mean±SEM (n=4)/group.

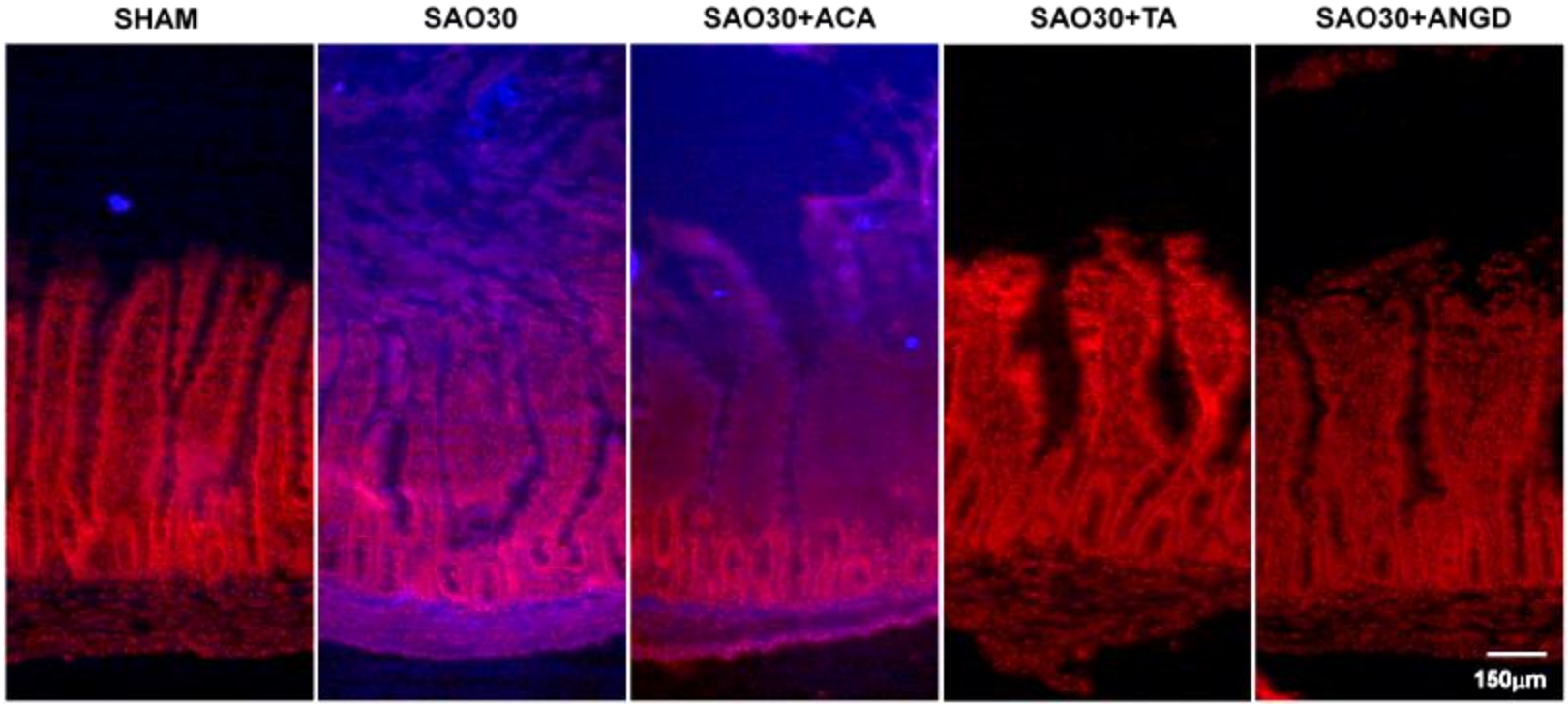

Figure 4.5 In situ zymography for trypsin in jejunal sections. Representative micrographs of trypsin activity as observed by fluorescence of specific substrate (blue), nuclei counterstaining with propidum iodine (red) in SHAM animals or animals subjected to SAO protocol with luminal inhibition with acarbose (ACA), tranexamic acid (TA) or nafamostat mesilate or without (NI).

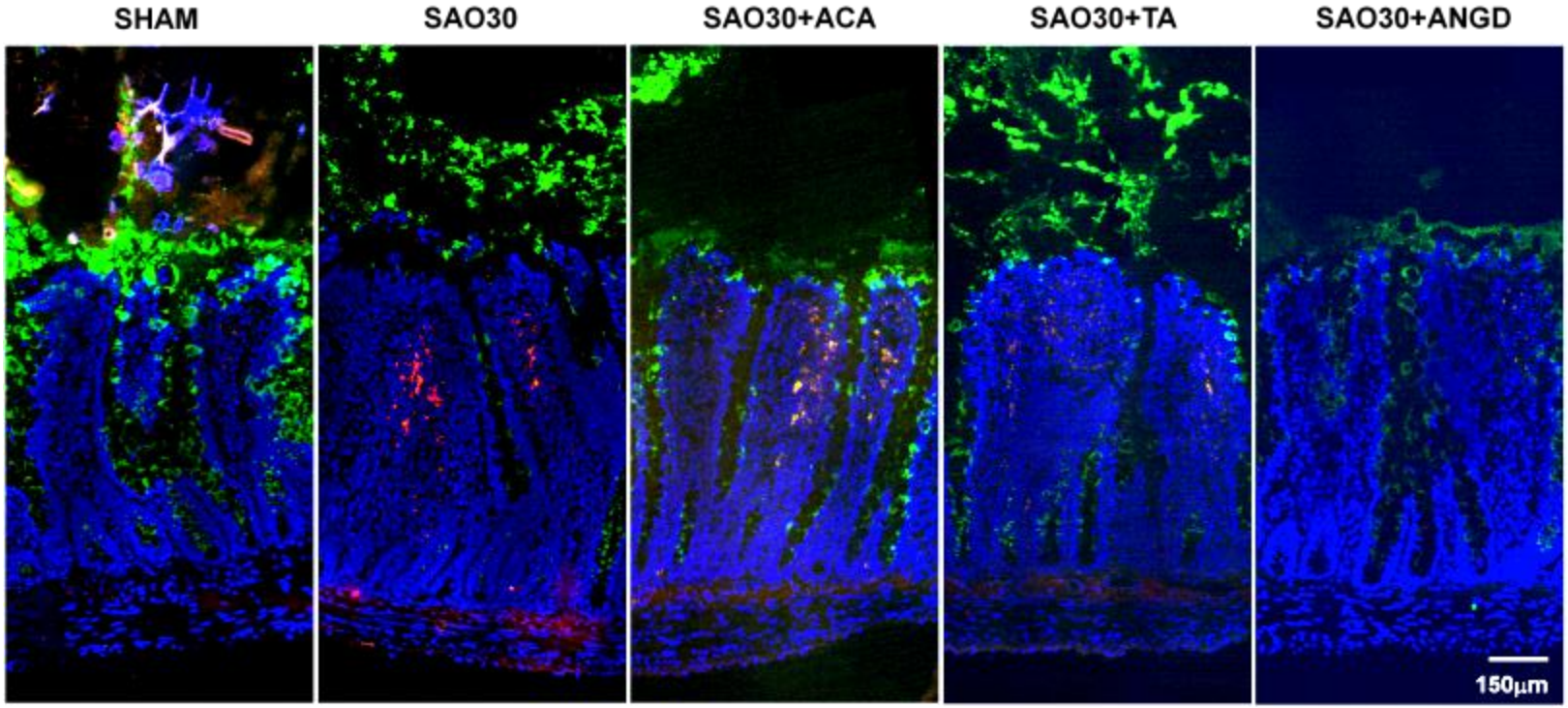

Figure 4.6 In situ zymography for trypsin in jejunal sections. Representative micrographs of trypsin activity as observed by fluorescence of specific substrate (blue), nuclei counterstaining with propidum iodine (red) in SHAM animals or animals subjected to SAO protocol with luminal inhibition with acarbose (ACA), tranexamic acid (TA) or nafamostat mesilate or without (NI).

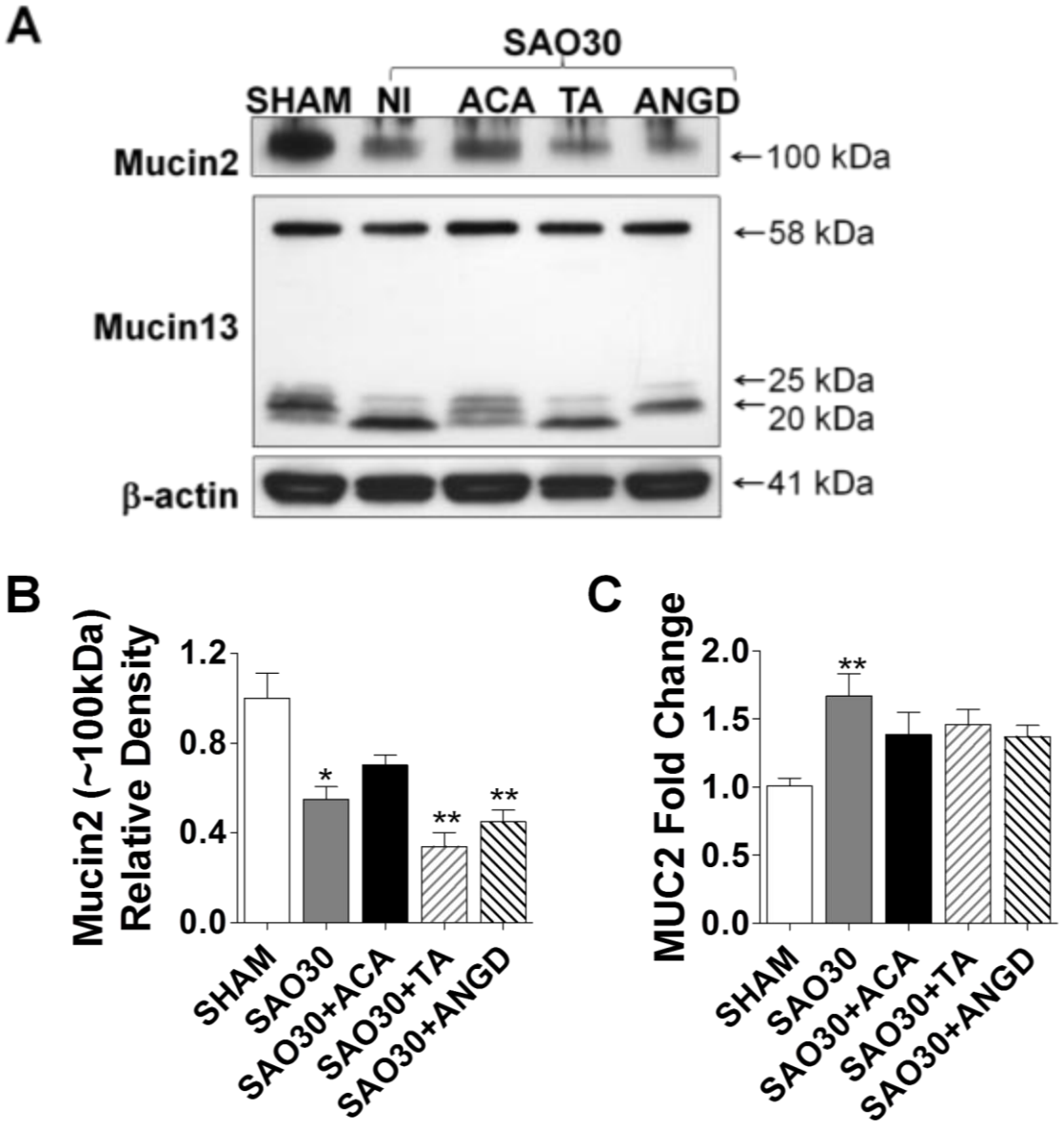

Figure 4.7 Western blot for mucin 2 and mucin 13 in jejunal homogenates of SHAM animals or animals subjected to SAO protocol with luminal inhibition with acarbose (ACA), tranexamic acid (TA) or nafamostat mesilate or without (NI) **(A)**. Density levels measurement of mucin 2 **(B)** and mRNA expression of MUC2 **(C)**. Values are mean±SEM (n=4)/group ** P<0.001 compared to SHAM, ††† P<0.0001 compared to SAO30, ‡ P<0.05 and ‡‡ P<0.001 compared to ACA.

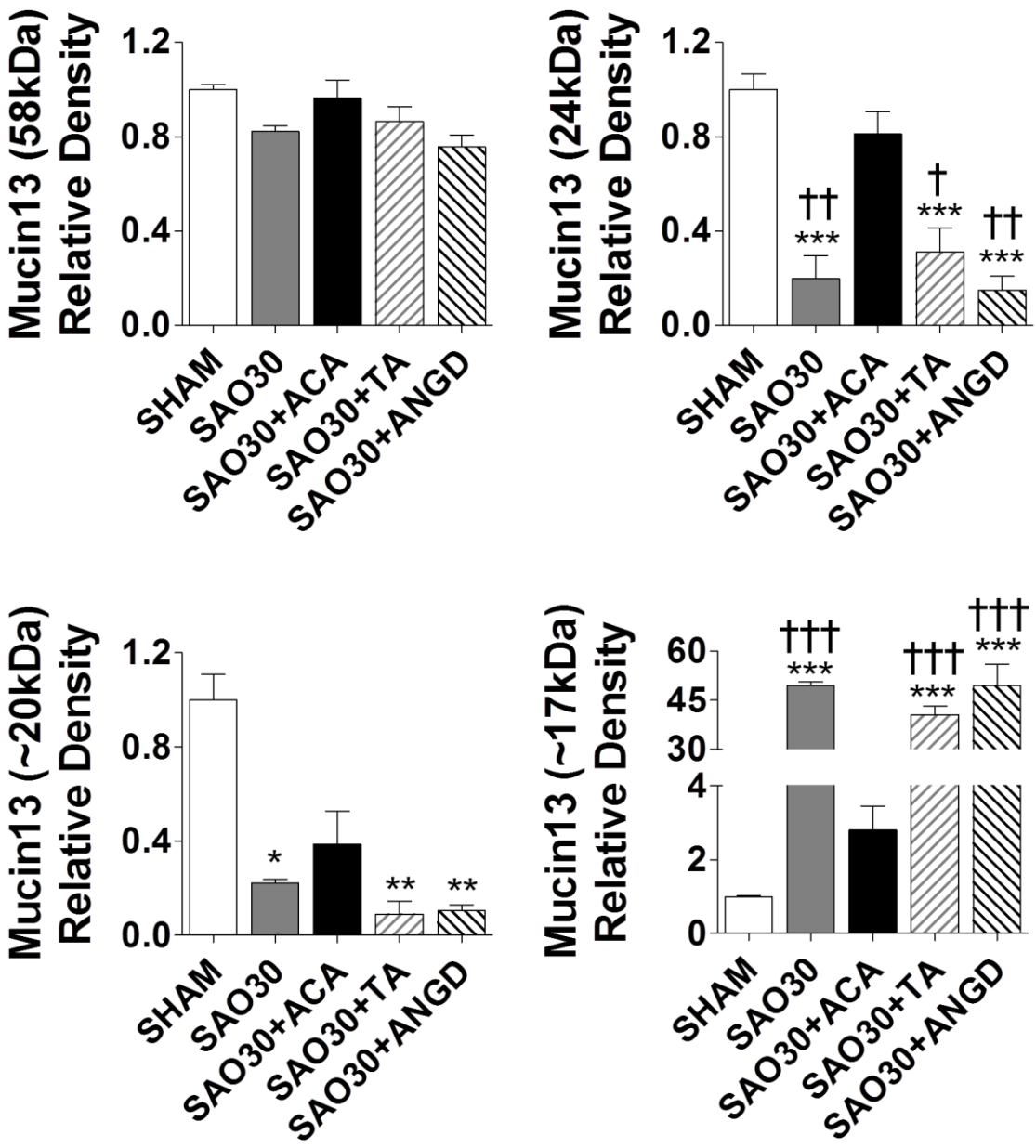

Figure 4.8 Mucin 13 density levels of different fragments. Values are mean±SEM (n=4)/group ** P<0.001 compared to SHAM, ††† P<0.0001 compared to SAO30, ‡ P<0.05 and ‡‡ P<0.001 compared to ACA.

4.8 References

1. Wolf D, Blasco L, Khan M, & Litt M (1977) Human cervical mucus: I. Rheological characteristics. *Fertil. Steril* 28:41-46.

2. Kilian M, Reinholdt J, Lomholt H, Poulsen K, & Frandsen EVG (1996) Biological significance of IgA1 proteases in bacterial colonization and pathogenesis: critical evaluation of experimental evidence*. *Apmis* 104(1-6):321-338.

3. Lidell M, Moncada D, Chadee K, & Hansson G (2006) Entamoeba histolytica cysteine proteases cleave the MUC2 mucin in its C-terminal domain and dissolve the protective colonic mucus gel. *Proceedings of the National Academy of Sciences* 103(24):9298.

4. Godl K, *et al.* (2002) The N terminus of the MUC2 mucin forms trimers that are held together within a trypsin-resistant core fragment. *Journal of Biological Chemistry* 277(49):47248-47256.

5. Carlstedt I, *et al.* (1993) Characterization of two different glycosylated domains from the insoluble mucin complex of rat small intestine. *Journal of Biological Chemistry* 268(25):18771-18781.

6. Karlsson NG, *et al.* (1997) The glycosylation of rat intestinal Muc2 mucin varies between rat strains and the small and large intestine. *Journal of Biological Chemistry* 272(43):27025-27034.

7. Herrmann A, *et al.* (1999) Studies on the "insoluble" glycoprotein complex from human colon. *Journal of Biological Chemistry* 274(22):15828-15836.

8. Alugupalli KR & Kalfas S (1996) Degradation of lactoferrin by periodontitis-associated bacteria. *FEMS microbiology letters* 145(2):209-214.

9. Dwarakanath A, *et al.* (1995) Faecal mucinase activity assessed in inflammatory bowel disease using 14C threonine labelled mucin substrate. *Gut* 37(1):58-62.

10. Wiggins R, Hicks S, Soothill P, Millar M, & Corfield A (2001) Mucinases and sialidases: their role in the pathogenesis of sexually transmitted infections in the female genital tract. *Sexually transmitted infections* 77(6):402-408.

11. Howe L, *et al.* (1999) Mucinase and sialidase activity of the vaginal microflora: implications for the pathogenesis of preterm labour. *International journal of STD & AIDS* 10(7):442-447.

12. Stewart-Tull D, Ollar R, & SCOBIE TS (1986) Studies on the Vibrio cholerae mucinase complex. I. Enzymic activities associated with the complex325. *Journal of medical microbiology* 22(4):325-333.

13. Connaris S & Greenwell P (1997) Glycosidases in mucin-dwelling protozoans. *Glycoconjugate journal* 14(7):879-882.

14. Robertson A & Wright DP (1997) Bacterial glycosulphatases and sulphomucin degradation. *Canadian journal of gastroenterology= Journal canadien de gastroenterologie* 11(4):361.

15. Corfield T (1992) Bacterial sialidases—roles in pathogenicity and nutrition. *Glycobiology* 2(6):509-521.

16. Henke MO, *et al.* (2011) Serine proteases degrade airway mucins in cystic fibrosis. *Infection and immunity* 79(8):3438-3444.

17. Bhaskar K, *et al.* (1992) Viscous fingering of HCl through gastric mucin. *Nature* 360(6403):458-461.

18. Celli JP, *et al.* (2009) Helicobacter pylori moves through mucus by reducing mucin viscoelasticity. *Proceedings of the National Academy of Sciences* 106(34):14321-14326.

19. Atuma C, Strugala V, Allen A, & Holm L (2001) The adherent gastrointestinal mucus gel layer: thickness and physical state in vivo. *Am J Physiol-Gastr L* 280(5):G922-G929.

20. Gum Jr J (1995) Human mucin glycoproteins: Varied structures predict diverse properties and specific functions. *Biochemical Society Transactions* 23(4):795.

21. Strous GJ & Dekker J (1992) Mucin-type glycoproteins. *Critical reviews in biochemistry and molecular biology* 27(1-2):57-92.

22. Allen A & Snary D (1972) The structure and function of gastric mucus. *Gut* 13(8):666.

23. Lamont JT (1992) Mucus: the front line of intestinal mucosal defense. *Annals of the New York Academy of Sciences* 664(1):190-201.

24. Chang M, Kistler EB, & Schmid-Schönbein GW (2011) Disruption of the Mucosal Barrier during Gut Ischemia Allows Entry of Digestive Enzymes into the Intestinal Wall. *Shock*.

25. Zimmerman M, Ashe B, Yurewicz EC, & Patel G (1977) Sensitive assays for trypsin, elastase, and chymotrypsin using new fluorogenic substrates. (Translated from eng) *Anal Biochem* 78(1):47-51 (in eng).

26. Henkel E, Morich S, & Henkel R (1984) 2-Chloro-4-nitrophenyl-ß-D-maltoheptaoside: A New Substrate for the Determination of α-Amylase in Serum and Urine. *Clinical Chemistry and Laboratory Medicine* 22(7):489-496.

27. Kim MJ, *et al.* (1999) Comparative Study of the Inhibition of [alpha]-Glucosidase,[alpha]-Amylase, and Cyclomaltodextrin Glucanosyltransferase by Acarbose, Isoacarbose, and Acarviosine-Glucose. *Archives of biochemistry and biophysics* 371(2):277-283.

28. Andersson L, *et al.* (1965) Experimental and Clinical Studies on AMCA, the Antifibrinolytically Active Isomer of p Aminomethyl Cyclohexane Carboxylic Acid. *Scandinavian Journal of Haematology* 2(3):230-247.

29. Dubber AHC, McNicol G, & Douglas A (1965) Amino methyl cyclohexane carboxylic acid (AMCHA), a new synthetic fibrinolytic inhibitor. *British Journal of Haematology* 11(2):237-245.

30. Fujii S & Hitomi Y (1981) New synthetic inhibitors of C1r [combining macron], C1 esterase, thrombin, plasmin, kallikrein and trypsin. *Biochimica et Biophysica Acta (BBA)-Enzymology* 661(2):342-345.

31. Bounous G, McArdle AH, Hodges DM, Hampson LG, & Gurd FN (1966) Biosynthesis of intestinal mucin in shock: relationship to tryptic hemorrhagic enteritis and permeability to curare. (Translated from eng) *Ann Surg* 164(1):13-22 (in eng).

32. Rupani B, *et al.* (2007) Relationship between disruption of the unstirred mucus layer and intestinal restitution in loss of gut barrier function after trauma hemorrhagic shock. (Translated from eng) *Surgery* 141(4):481-489 (in eng).

33. Albanese CT, *et al.* (1994) Role of intestinal mucus in transepithelial passage of bacteria across the intact ileum in vitro. *Surgery* 116(1):76.

34. Maxson RT, Dunlap JP, Tryka F, Jackson RJ, & Smith SD (1994) The role of the mucus gel layer in intestinal bacterial translocation. *Journal of Surgical Research* 57(6):682-686.

35. Nimmerfall F & Rosenthaler J (1980) Significance of the goblet-cell mucin layer, the outermost luminal barrier to passage through the gut wall. *Biochemical and biophysical research communications* 94(3):960-966.

36. Kemper AC & Specian RD (1991) Rat small intestinal mucins: a quantitative analysis. *The Anatomical record* 229(2):219-226.

37. Forstner JF, Roomi NW, Fahim R, & Forstner GG (1981) Cholera toxin stimulates secretion of immunoreactive intestinal mucin. *Am J Physiol-Gastr L* 240(1):G10-G16.

38. LaMont JT, Turner BS, DiBenedetto D, Handin R, & Schafer AI (1983) Arachidonic acid stimulates mucin secretion in prairie dog gallbladder. *Am J Physiol-Gastr L* 245(1):G92-G98.

39. Faure M, *et al.* (2005) Dietary threonine restriction specifically reduces intestinal mucin synthesis in rats. *The Journal of nutrition* 135(3):486.

40. Merlin D, *et al.* (1994) ATP-stimulated electrolyte and mucin secretion in the human intestinal goblet cell line HT29-C1. 16E. *Journal of Membrane Biology* 137(2):137-149.

Chapter 5

Mucin as Barrier to Digestive Enzymes in-vivo and in-vitro

5.1 Introduction

The intestinal epithelium covering the gastrointestinal tract consists of a monolayer of enterocytes covered by a mucus gel layer. Together these two layers provide a dynamic and regulated barrier allowing selective passage of luminal contents into the intestinal wall. Loss of the epithelial/mucus layer integrity is a common feature in gastrointestinal diseases (1, 2) and intestinal ischemia encountered in different forms of shock (3-5).

The mucus gel layer, which ranges in thickness from 50-300μm (6), is a hydrated polymeric gel composed of carbohydrates, lipids and protein (7). The major protein component of the mucus layer is mucin, which consists of several isoforms, both secreted and membrane associated. Mucin is believed to protect the epithelial surface of the small intestine from luminal digestive enzymes, abrasion by food particles, and pathogens by forming a barrier between the lumen and the intestinal epithelium (8-11). The epithelial cells also form a selective barrier to molecules found in the lumen; this barrier depends

on the integrity of intercellular junctions and the extracellular plasma membrane proteins. Changes in the environment of epithelial cells make these molecules targets for proteolytic attack (12), cause disruption of cell structure components influencing intracellular signaling (13-15), and impair epithelial barrier function (16).

Intestinal epithelial cells express numerous membrane proteins on the plasma membrane whose fate after disruption of the mucin layer is uncertain and may be determined by the access of digestive enzymes. In the previous chapters I reported that E-cadherin, which plays a major role in maintaining the intercellular junctions between epithelial cells (17), is degraded during intestinal ischemia (3). Conversely the fate of other membrane molecules, e.g. toll-like receptor 4 (TLR4), which is usually associated with infection and sepsis (18, 19) and recently has been linked to hemorrhagic shock and intestinal ischemia (20, 21), remains unknown.

5.2 Intestinal Permeability

The epithelial barrier is composed of enterocytes interspersed with goblet cells; enterocytes are attached to each other by adherent junctions and tight junctions. There is now substantial evidence that the integrity of the intestinal epithelial barrier regulates permeability by influencing paracellular flow of fluid and solutes. The epithelial barrier depends on a complex of proteins composing different intercellular junctions, including tight junctions, adherens junctions, and desmosomes, which allow passage of small molecules but prevent the passage of large molecules forming a closed seal (22, 23). E-cadherin is primarily found at the adherens junctions and plays a critical role in cell-cell adhesions that are fundamental to formation of the intestinal epithelial barrier (24). The

intestinal epithelium represents the largest interface between the external environment and the internal host milieu and constitutes the major barrier through which molecules can either be absorbed or secreted. Bidirectional permeability assays are commonly used to compare basolateral to apical permeability (secretory direction) with apical to basolateral permeability (absorptive direction). By examining the absorptive/uptake ratio of permeability, direction of transport of a molecule can be determined.

5.3 Aims in this Chapter

As reported in the previous chapters, disruption of mucin2 (secreted) and mucin13 (membrane bound) after intestinal ischemia is accompanied by transport of digestive enzymes into the intestinal wall. Thus the hypothesis in this chapter is that mucin is a barrier to luminal digestive enzymes under normal physiological conditions. Digestive enzymes make contact with the epithelium in to the absence or during degradation of mucin results in receptor destruction and loss of epithelial cell integrity and function. In this chapter it is investigated whether mucin disruption observed during intestinal ischemia is accompanied by impaired epithelial cell integrity and function. Using a rat model of intestinal ischemia by splanchnic arterial occlusion (SAO) the fate of two two selected membrane proteins (E-cadherin and TLR4) is studied. Furthermore rat intestinal epithelial cell cultures were utilized to demonstrate that addition of a mucin layer on the apical side protects epithelial cells against trypsin-mediated disruption.

5.4 Materials and Methods

5.4.1 Animal groups and SAO model: All animal protocols were reviewed and approved by the University of California San Diego Animal Subjects Committee. Male

Wistar rats (300-350g, Harlan Sprague Dawley Inc, Indianapolis, IN) were randomly assigned to one of five groups (n=4 per group): a sham group (SHAM), and four groups subjected to 30min splanchnic ischemia without enteral protease inhibition (SAO30) and with enteral amylase inhibition by acarbose (SAO30+ACA), protease inhibition by tranexamic acid (SAO30+TA) and nafamostat mesilate (ANGD, [6-amidino-2-naphthyl p-guanidinobenzoate dimethanesulfonate]) (SAO+ANGD). Rats were kept on solid food restriction for 12 hours prior to surgery with water ad libitum.

After general anesthesia (Ketamine/Xylazine, 75 mg/kg BW / 20 mg/kg BW, IM) all groups were injected 0.9% saline (3ml/100g BW) into the lumen of the intestine either alone (SHAM or SAO30 groups) or mixed with one of three enzyme inhibitors (SAO30+ACA, SAO30+TA, or SAO30+ANGD groups). The concentration of the enzyme inhibitors was as follows: acarbose (0.5mg/100g BW) and tranexamic acid (0.1g/100g BW) (Sigma-Aldrich, St Louis, MO) or nafamostat mesilate (5mg/ 100g BW, Torii Pharmaceutical Co. Ltd., Tokyo, Japan). 30 min after saline or saline/inhibitor injection, the superior mesenteric and celiac arteries were isolated and occluded for 30 min for the ischemic groups or isolated without occlusion in the sham group. After 30 min SAO or sham surgery the animals were euthanized with Beuthanasia® 0.22 ml/kg BW, IV.

5.4.2 Assessment of intestinal permeability in-Vivo: In separate experiments, rat jejunal sections were assayed for in-vivo FITC-dextran transport (20kDa, Sigma-Aldrich) from the lumen of the intestine into the intestinal wall. Groups were the same as described above with FITC-dextran (100mg/ml) added to saline or saline/inhibitor

solution prior to injection in the lumen of the intestine followed by 30 minutes ischemia or sham surgery and euthanasia.

5.4.3 Tissue cryosections: After euthanasia, jejunal sections (~1 cm in length) were excised without removal of luminal contents and suspended in Tissue-Tek O.C.T. Compound (Sakura Finetek, Torrance, CA), snap frozen in isopentane/liquid nitrogen, and stored at -80^{o}C for analysis. Cryosections (5 µm thickness) along the longitudinal axis of the villi were used throughout all experiments. Cryosections were fixed in 10% formalin solution and processed in a non-blinded fashion.

5.4.4 Immunohistochemistry: For immunohistochemical analysis, primary antibodies were diluted as followed: extracellular domain of TLR4 1:250 (Abcam, Cambridge, MA), and the intracellular domain of TLR4 1:250 (Invitrogen, Carlsbad, CA, USA). Secondary antibodies were as follows: FITC (Santa Cruz Biotechnology) and HRP (ImmPRESS, Vector Lab; Burlingame, CA). The slides were developed using 3, 3´-diaminodbenzidine substrate and counterstained with hematoxylin or DAPI (Vector Lab) or propidium iodine (Sigma-Aldrich). Slides were observed in a non-blinded fashion under an inverted microscope (20X and 60X objectives).

5.4.5 Intestine homogenates: Jejunal segments were excised without removal of luminal contents. For Western blot measurements, segments of intestine were homogenized with CelLytic™ (Sigma-Aldrich) in the presence of protease inhibitors (5mM EDTA, 5mM N-Ethylmaleimide, 25mM iodoacetamide, 5mM benzamidine, 300mM acarbose, 5mM 6-aminocaproic acid, 1mM protease inhibitor cocktail, (Sigma-Aldrich). Homogenates

were centrifuged (16,000g for 15 min at 4°C), the supernatant was collected and protein concentration was assessed with the bicinchoninic acid protein assay (Thermo Scientific).

5.4.6 Epithelial cell culture: IEC-18 cells (CRL-1589; ATCC, Manassas, VA), a cell line derived from the ileum of rat intestine, were grown in Dulbecco's modified Eagle's medium (DMEM) supplemented with 4 mM L-glutamine, 1.5 g/L sodium bicarbonate, 4.5 g/L glucose, 0.1 Unit/ml bovine insulin, 95%; and fetal bovine serum, 5%.

5.4.7 Immunocytochemistry: IEC-18 cells were grown in 8-well culture slides (BD Biosciences, San Jose, CA) until 100% confluency was reached. On the day of the experiment the media was removed and cells were rinsed three times with PBS followed by incubation with serum free media (SFM) with or without porcine trypsin (5μM, Sigma-Aldrich) for 60 min. Cells were fixed with 4% paraformaldehyde in PBS followed by blocking and permeabilization in 2% BSA in 0.1% PBS-T for 1 hour at room temperature. The slides were incubated overnight with primary antibody E-cadherin 1:250 (Abcam) followed by incubation with FITC secondary antibody (Santa Cruz Biotechnology) and Alexa Fluor® 568 phalloidin (Invitrogen). Slides were observed using an inverted microscope (20X objective) using the appropriate fluorescent filters.

5.4.8 Mucin layer addition to epithelial cells in-vitro: IEC-18 cells were grown in 10ml Transwell dishes (0.4-μm filter; Corning-Costar Corp) until 100% confluency. For the experiment the media was removed and cells were rinsed three times with phosphate buffered saline (PBS), the basolateral side was filled with serum free medium and the apical side was covered with or without a mucin film (~400μm, 10% in SFM, porcine

stomach; Sigma-Aldrich, St. Louis, MO). Serum free medium with or without 5μM trypsin was carefully added to the apical side. Cells were incubated for 60min at 37°C.

5.4.9 Cell lysis: After completion of the mucin layer assay, cell media was removed and the cells were rinsed three times with PBS, scraped and lysed for Western blot analysis in RIPA buffer (Thermo Scientific, Rockford, IL) containing 1mM proteinase (Sigma-Aldrich) and phosphatase (Thermo Scientific) inhibitors cocktail. Cells were transferred to Eppendorf tubes followed by incubation with agitation for 10 min at 4 °C and centrifugation at 4 °C for 10 min at 13,000 rpm. Total protein concentration in the supernatant was determined with the bicinchoninic acid protein assay.

5.4.10 Paracellular flux measurement: The cells were seeded on 12-well Transwell plates (0.4-μm filter; Corning-Costar Corp, Cambridge, MA) to 100% confluency. FITC-dextran (20kDa, 50mg/ml, Sigma-Aldrich) in serum free medium with or without trypsin was added to the apical side of the epithelial cells with or without a mucin layer (see above). Cells were incubated for 60min at 37 °C, media from the bottom chamber was collected every 10min and the amount of dextran in the basolateral side was measured (SpectraMax Gemini XS) at 492/520 nm (excitation/emission). Three independent experiments per group were performed.

5.4.11 Western blot: 20μg of protein of cell lysate or tissue homogenate were separated by SDS-PAGE. Membranes were incubated with primary antibodies as follows: intra- and extra-cellular domains of E-cadherin and TLR4 1:1000 (Abcam), intracellular domain of TLR4 1:1000 (Invitrogen). Secondary antibodies were diluted 1:20000 (Santa Cruz Biotechnology) and detected with Super Signal West Pico (Thermo Scientific). The

exposed x-ray films were scanned and label intensity was measured using digital gel analysis (NIH ImageJ software).

5.4.12 Statistical analysis: Results are presented as mean±SEM. Unpaired comparisons of mean values between groups were carried out by one-way ANOVA followed by Bonferroni post-hoc comparisons. $P<0.05$ was considered significant.

5.5 Results

5.5.1 FITC-dextran transport into the intestinal wall during SAO: FITC-dextran (20 kDa) transport measurements show that in the sham group (SHAM) FITC-dextran remained intraluminal, lining the villi with negligible transfer from the lumen of the intestine into the intestinal wall (Figure 5.1). In contrast, the ischemic groups without luminal inhibitors (SAO30) had erosion at the villi tips with detectable FITC-dextran infiltration into the intestinal wall. Although the ischemic groups with enzyme inhibitors (SA030+ACA, SAO30+TA, SAO30+ANGD) had a preserved villus structure as seen on frozen sections, there was some penetration of FITC-dextran into the intestinal wall.

5.5.2 Intestinal ischemia is accompanied by E-cadherin Degradation: In order to determine whether mucin disruption during intestinal ischemia is accompanied by disruption of epithelial cell integrity, we determined the levels of both intra- and extra-cellular domains of E-cadherin by Western blot (Figure 5.2). Both domains of E-cadherin were degraded after 30 min ischemia without protease inhibitor (SAO30). Inhibition of amylase (SAO30+ACA) and trypsin (SAO30+TA and SAO30+ANGD) yielded levels of E-cadherin that were higher than those in the ischemic group alone. However, these differences were not statistically significant.

5.5.3 TLR4 degradation during intestinal ischemia: Immunolabeling in the sham animals (SHAM) demonstrated both domains of TLR4 along the villi. In contrast, after 30min ischemia without luminal inhibition of digestive enzymes (SAO30), visible morphological damage was accompanied by disruption of both domains of TLR4 (Figure 5.3). Ischemic groups with luminal inhibition of amylase or trypsin (SA30+ACA, SAO30+TA, SAO30+ANGD) had preservation of the villus structure and greater staining than the ischemic group without inhibitors.

In order to determine whether mucin disruption is also accompanied by the degradation of typical membrane surface proteins, we measured the levels of the intra- and extra-cellular domains of TLR4 (Figure 5.4A). Western blot analysis reveals that both domains of TLR4 were degraded after 30 min ischemia (SAO30) and this was not significantly reversed by inhibition of amylase (SAO30+ACA) and trypsin (SAO30+TA, SAO30+ANGD) (Figure 5.4A, B).

5.5.4 Trypsin-mediated E-cadherin degradation in-vitro: To determine whether trypsin disrupts the epithelial cells in a like manner observed in-vivo in the rat model of intestinal ischemia and whether addition of a mucin layer prevents this, we studied an in-vitro model using a monolayer of rat intestinal epithelial cells. After incubation of IEC-18 cells for 1hour with 5μM trypsin, E-cadherin immunohistochemical labeling was decreased without alteration in cell shape or the monolayer (Figure 5.5). At higher trypsin concentrations, the epithelial actin cytoskeleton started to disappear, the cells retracted and the monolayer began to disintegrate.

5.5.5 Mucin layer reduces trypsin-mediated FITC-dextran transport: In order to assess the ability of the mucin layer to act as a barrier against trypsin-mediated epithelial cell permeability increases, we measured the rate at which FITC-dextran (20kDa) diffused across the epithelial cell monolayer (Figure 5.6). The addition of 5μM trypsin in serum free media (group SFM+Tryp) to the apical side of the IEC-18 cell monolayer resulted in significantly increased FITC-dextran levels on the basolateral side of the cell monolayer as compared to cells without apical trypsin (SFM). When a mucin layer was added on the apical side prior to addition of serum free media with or without trypsin, the levels of FITC-dextran measured on the basolateral side were not significantly different between the groups. In addition, diffusion of FITC-dextran across the epithelial cell monolayer in cultures not exposed to protease, but containing a mucin layer, was significantly reduced as compared to cells that did not have a mucin layer.

5.5.6 Mucin layer reduces E-cadherin and TLR4 degradation in vitro: Western blot for both intra- and extra-cellular domains of E-cadherin revealed degradation of this protein in whole-cell lysates after one hour incubation with serum free media containing 5μM trypsin (SFM+Try) (Figure 5.7). This is supported by reduced density of the whole molecule as seen with antibodies against both intra- and extra-cellular domains as well as the appearance of lower molecular weight bands. Application of a layer of 10% mucin on the apical side of the cells prior to the addition of the serum free media with trypsin resulted in higher density of the whole molecule of both intra- and extra-cellular domains of E-cadherin and decreased density of their corresponding lower molecular weight bands (Figure 5.8). Similarly, density levels for the extracellular domain of TLR4 were reduced

in intestinal epithelial cells that were treated with serum free media containing trypsin (SFM+Try) as compared to those without trypsin treatment (SFM) (Figure 5.9). A mucin layer on the apical side of the cells reduced degradation of the TLR4 extra-cellular domain. Density levels of the intra-cellular domain of TLR4 remained unchanged in all groups (Figure 5.10).

5.6 Discussion

In this study we demonstrated *in-vivo* with ischemic bowel and endogenous digestive enzymes in the intestinal lumen, as well as *in-vitro* using intestinal epithelial cell cultures and trypsin in the culture media, that degradation or absence of mucin results in loss of epithelial function as a barrier. In both cases we observed loss of E-cadherin, increased permeability to FITC-dextran, and degradation of TLR4.

Trypsin concentration in the rat intestinal lumen has been reported to be between 1 to 40μM (25, 26); the typical trypsin concentration used to pass cells in cell culture is 0.5g/L (22μM) (27). In the present studies, we show that incubation of intestinal epithelial cells with 5μM trypsin for one hour is sufficient to degrade E-cadherin and TLR4 without destroying the monolayer (Figure 5.5). We demonstrated in vivo that sham animals have an intact mucin layer with preserved epithelial cell integrity and function; similarly we showed in-vitro that having a mucin layer on the apical side of the cell monolayer protects the intestinal epithelial cells against trypsin-mediated disruption (Figures 5.7-10). Collectively these results suggest that if digestive enzymes such as trypsin are given the opportunity to come in contact with enterocytes at concentrations

normally found in the intestinal lumen the result will be loss of integrity and function of the epithelial barrier.

An intact mucin layer in normal intestine is essential to protect epithelial membrane proteins against enzymatic hydrolysis and loss of function; for instance, degradation of E-cadherin junctions results in increased epithelial permeability. Degradation of membrane receptors, such as TLR4, disrupts the pathway for TLR4 signaling after binding of lipopolysaccharides after as little as 30 min of ischemia. It remains to be investigated whether degradation of the extracellular domain of TLR4 may in itself initiate a signaling cascade, as has been reported for TLR5 and TLR15 (28, 29).

While the importance of the epithelial barrier in intestinal homeostasis is well recognized, the significance of the mucus layer with regard to passage of digestive enzymes remains less certain. We show here *in-vitro* that addition of an exogenous layer of mucin to the apical side of intestinal epithelial cells significantly reduces trypsin-mediated disruption of E-cadherin and TLR4 but does not completely prevent it. One explanation could be that the exogenous mucin as used in the current experiment is of gastric origin, which contains MUC5 instead of MUC2. Although from different origins these two mucin isoforms have similar general characteristics (30, 31). In addition, it may be that complete protection against trypsin degradation by an exogenous mucin layer on an epithelial monolayer is not achieved because the mucin used in this experiment is partially purified and may not form a complete barrier as is found *in-vivo*.

Degradation of E-cadherin and TLR4 in-vivo was not prevented by inhibition of luminal trypsin using two different blockers. This evidence suggests that other

mechanisms may play a role in mucin degradation during intestinal ischemia. This hypothesis is consistent with the basic concept that the mucin layer may be degraded only minimally during normal digestion in the non-ischemic intestine. In an ischemic intestine depleted of ATP, new intracellular and extracellular degrading processes may start in the epithelium; this issue requires further investigation.

In conclusion, the results presented here confirm that mucin in the mucus layer is a barrier that protects the intestinal epithelium against enzymatic auto-digestion. During ischemia mucin isoforms are degraded, which may stimulate synthesis of new mucin to restore the damaged barrier. As mucin is degraded and the barrier function of the mucus layer is thus compromised, digestive enzymes in the lumen of the intestine are allowed to come into contact with the epithelium with consequent loss of epithelial cell integrity and function. This cascade of events results in intestinal injury, transport of digestive enzymes into the systemic circulation and subsequent shock.

Chapter 5 in full is submitted material to Plos One as it appears in “Breakdown of Mucin as Barrier to Digestive Enzymes in the Ischemic Rat Small Intestine” by Chang M., Alsaigh T., Kistler E. B., Schmid-Schönbein G.W. The dissertation author is the primary author of this manuscript.

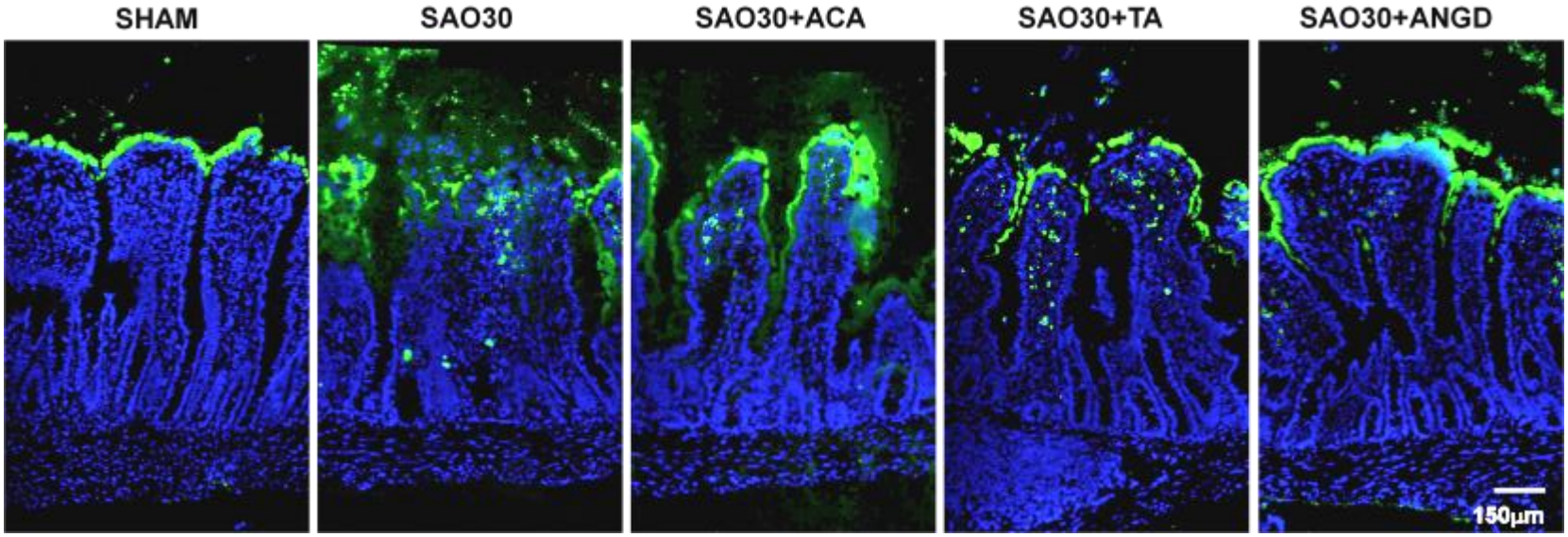

Figure 5.1 FITC-dextran transport during SAO. Representative micrographs of jejunal sections of SHAM animals or animals subjected to SAO protocol with luminal inhibition with acarbose (ACA), tranexamic acid (TA) or nafamostat mesilate or without-(SAO30), showing localization of FITC-dextran (green) with nuclei counterstaining (blue)

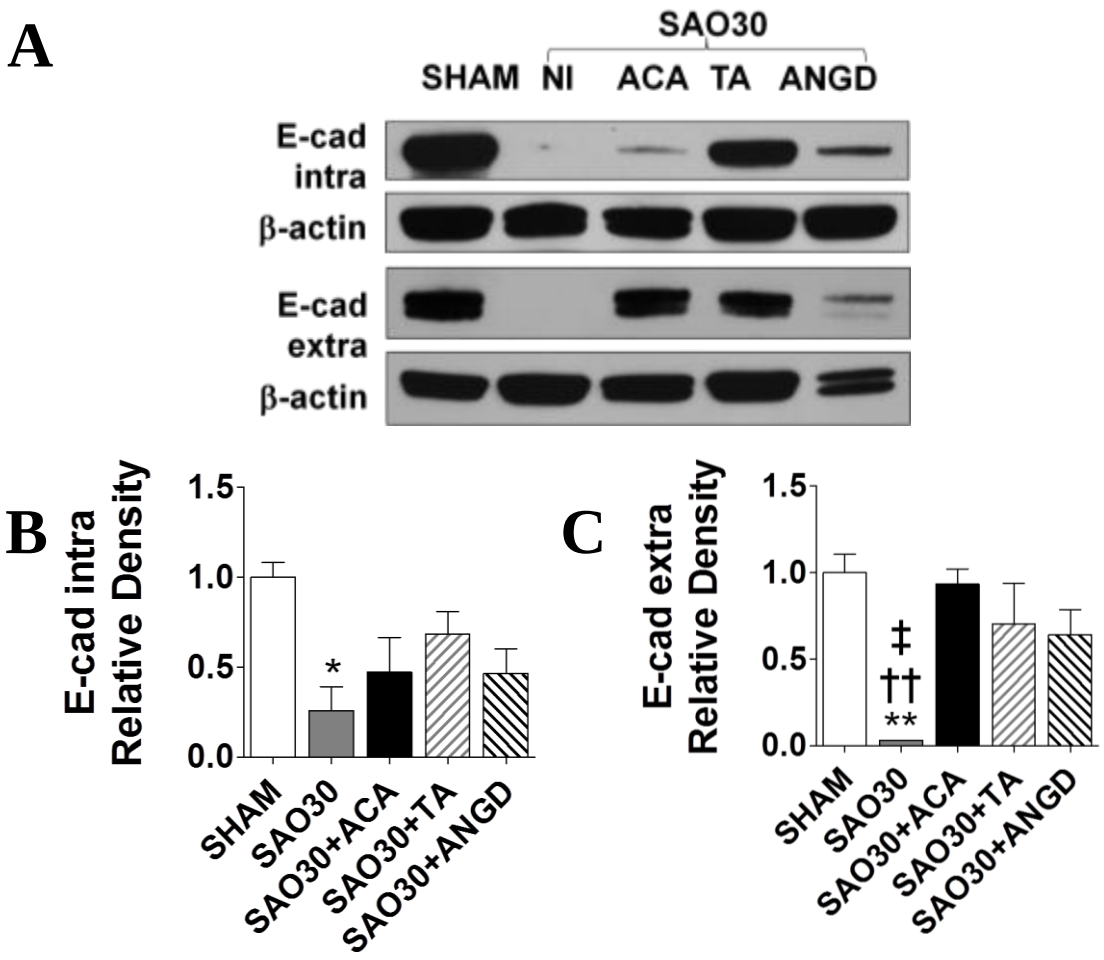

Figure 5.2 E-cadherin protein levels after SAO. Western blot for intra- and extra-cellular domains of E-cadherin **(A)** in jejunal homogenates of SHAM animals or animals subjected to SAO protocol with luminal inhibition with acarbose (ACA), tranexamic acid (TA) or nafamostat mesilate or without (SAO30). Relative density of **(B)** intra- and **(C)** extracellular domains of E-cadherin. Values are mean±SEM (n=4)/group * P<0.01 compared to sham, †† P<0.001 as compared to ACA, ‡ P<0.01 as compared to TA

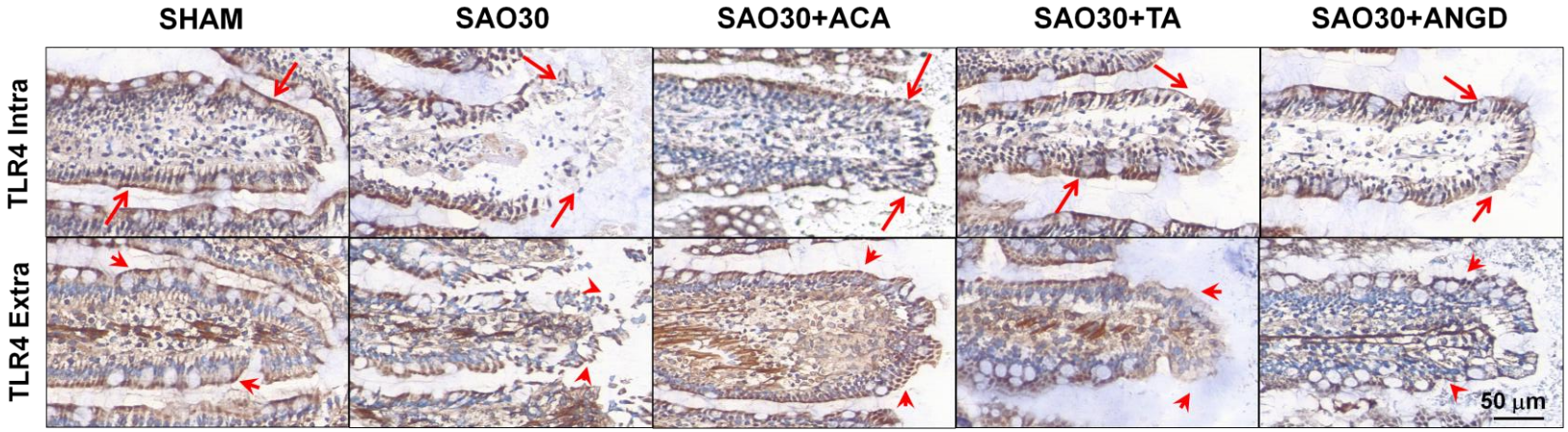

Figure 5.3 TLR4 immunohistochcemistry. Immunohistochemistry of intra- and extra-cellular domains of TLR4 (brown) and nuclei counterstaining with hematoxylin (blue). Arrows show location of TLR4.

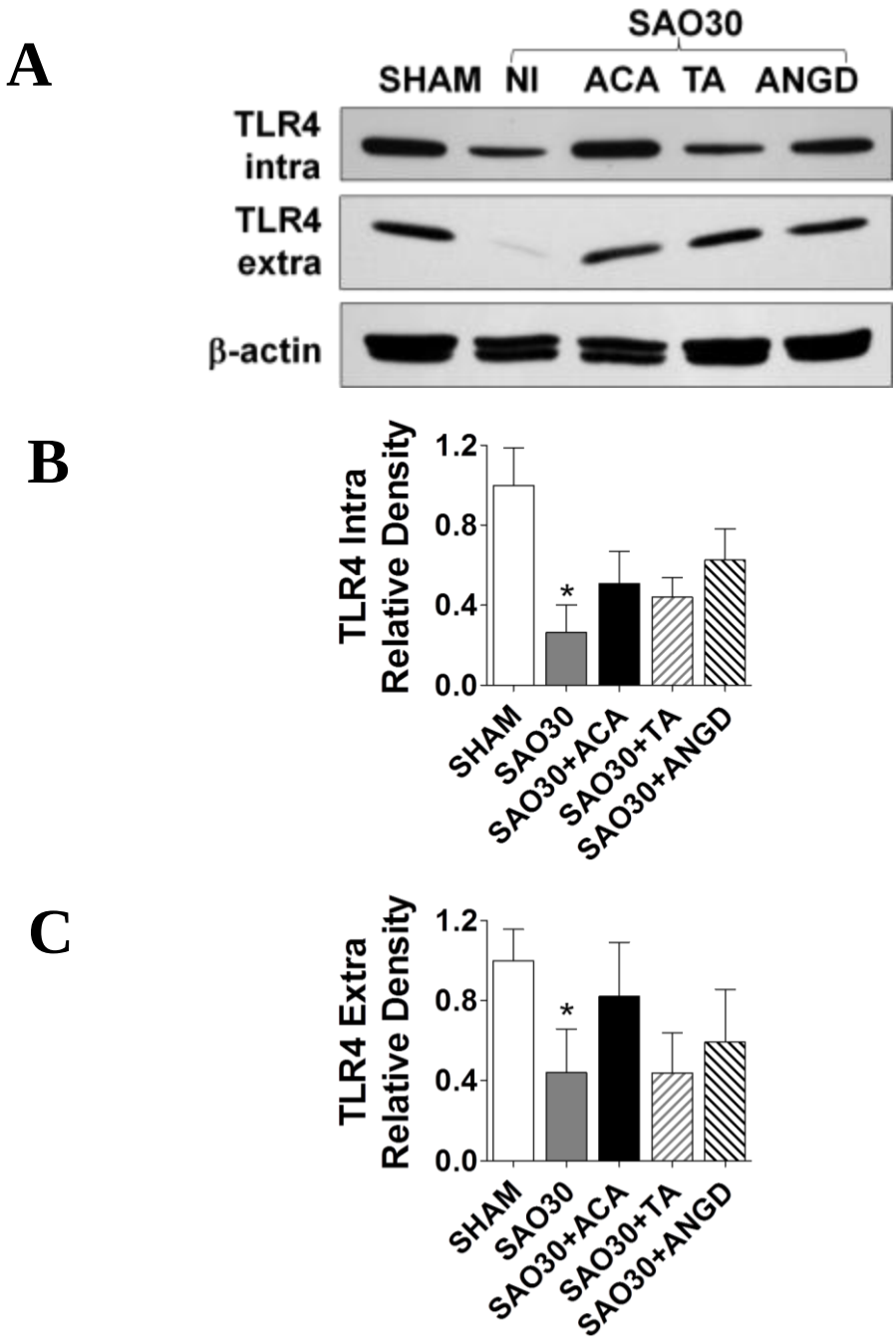

Figure 5.4 TLR4 protein levels after intestinal ischemia. Western blot for intra- and extra-cellular domains of TLR4 **(A)** in jejunal homogenates of SHAM animals or animals subjected to SAO protocol with luminal inhibition with acarbose (ACA), tranexamic acid (TA) or nafamostat mesilate or without (NI) (A) with corresponding density level measurements **(B, C)** . Values are mean±SEM (n=4)/group *P<0.05 compared to SHAM.

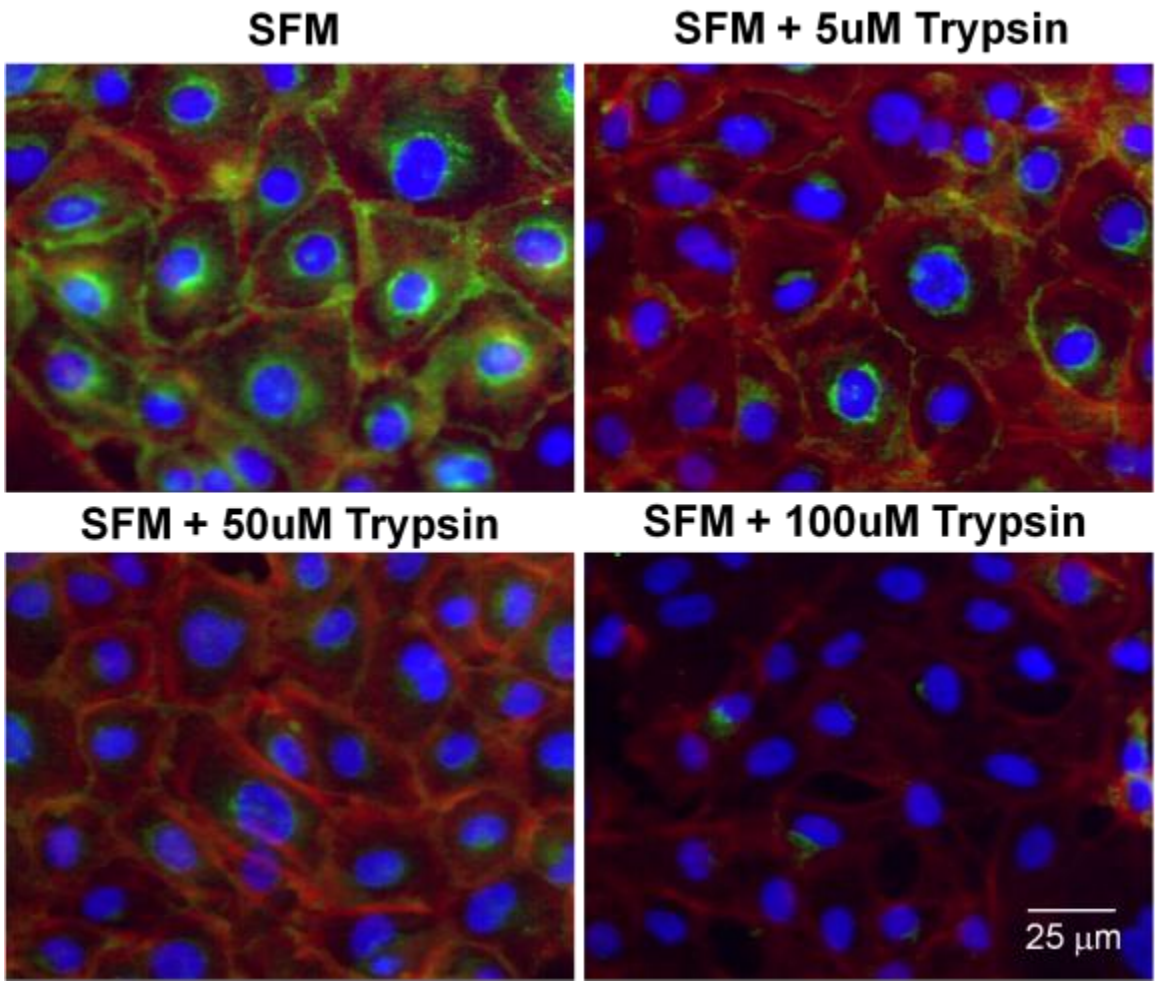

Figure 5.5 E-cadherin localization in intestinal epithelial cells after trypsin exposure. Representative micrographs of IEC-18 cells immunostained for the intra-cellular domain of E-cadherin (green), actin (red), and nuclei (blue) after exposure to serum free medium (SFM) with different trypsin concentrations.

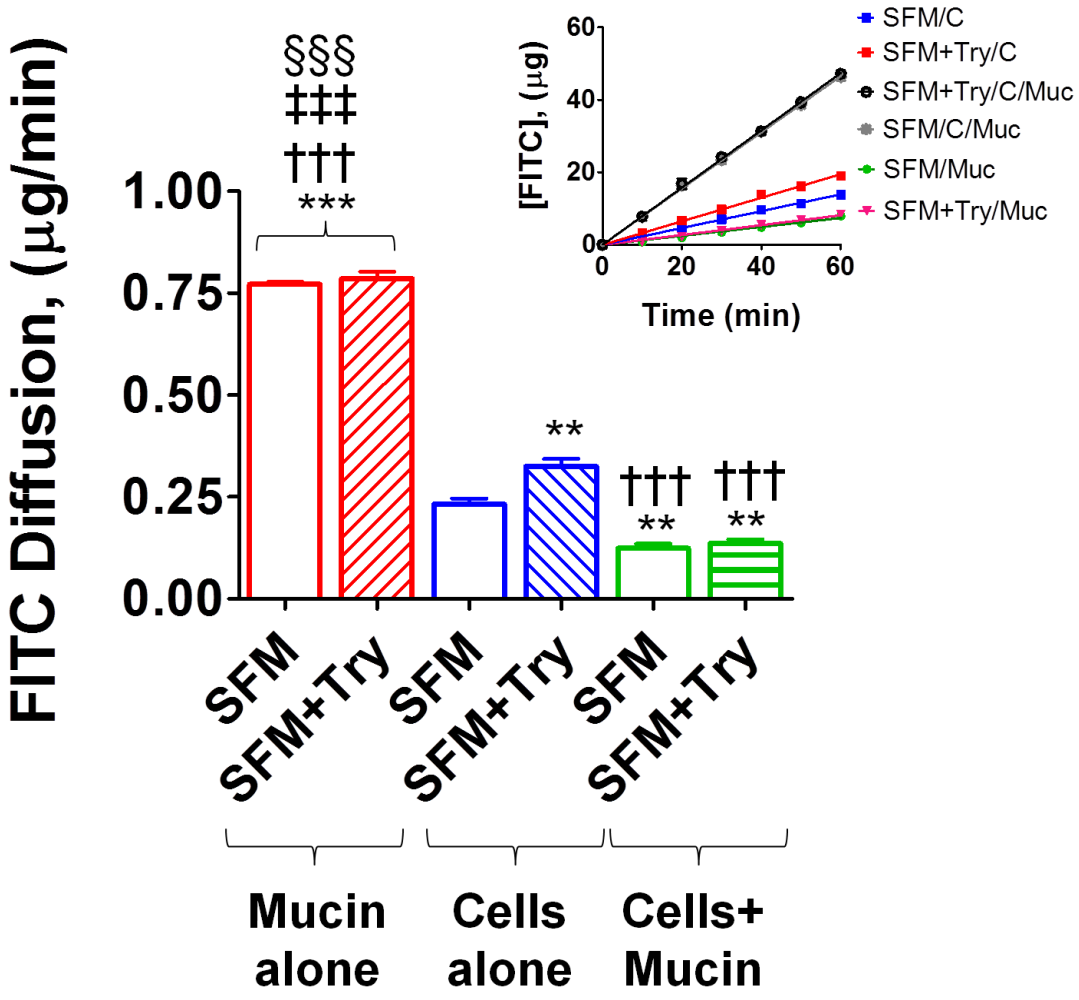

Figure 5.6 FITC-dextran diffusion across the intestinal epithelial cells monolayer. Rate of diffusion of FITC-dextran across mucin alone, IEC-18 cell monolayer alone or IEC-18 cell monolayer with a mucin layer after exposure to serum free media alone (SFM) or serum free media with trypsin (SFM+Try).

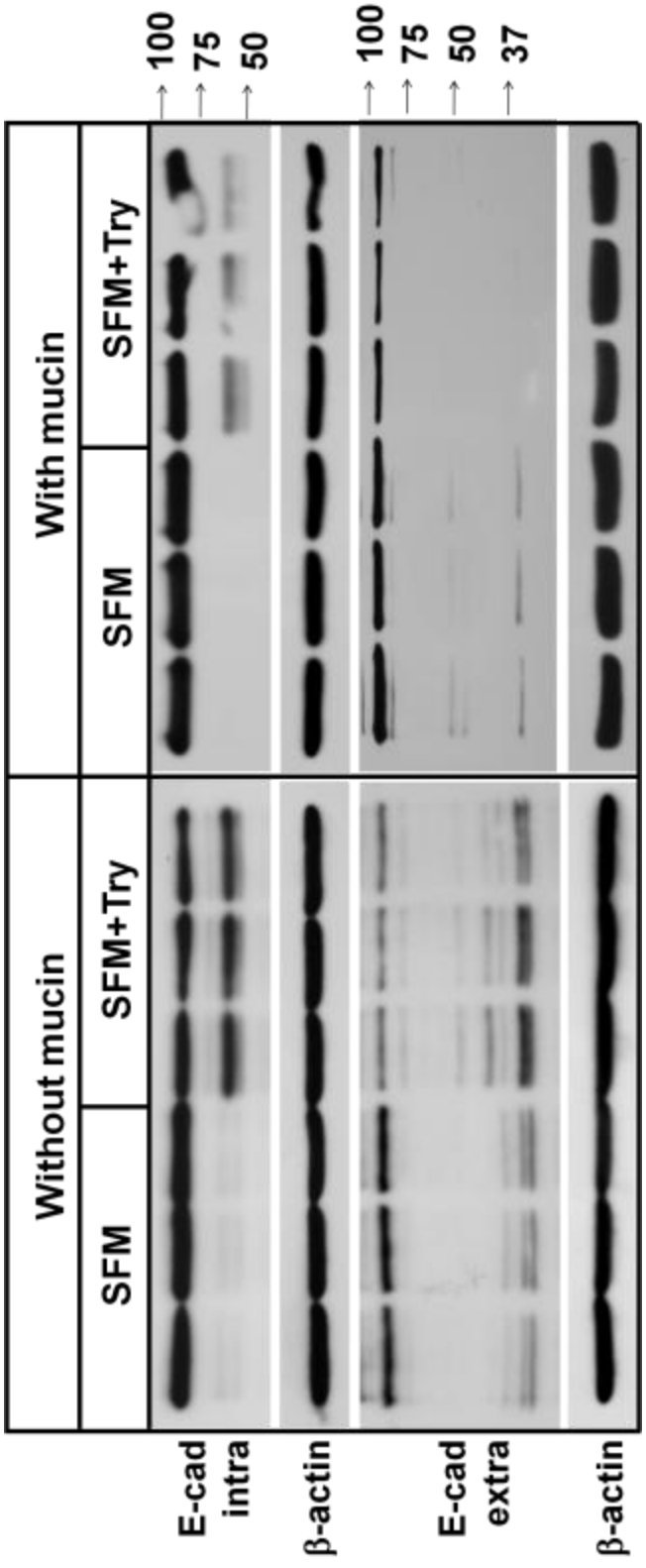

Figure 5.7 E-cadherin protein levels in IEC-18. Western blot for intra- and extra-cellular domains of E-cadherin of IEC-18 cells without a mucin layer after exposure with serum free without and with trypsin (SFM and SFM+Try respectively) and IEC-18 cell with a mucin layer after exposure to serum free media with or without trypsin (SFM+Mucin and SFM+Mucin +Try)

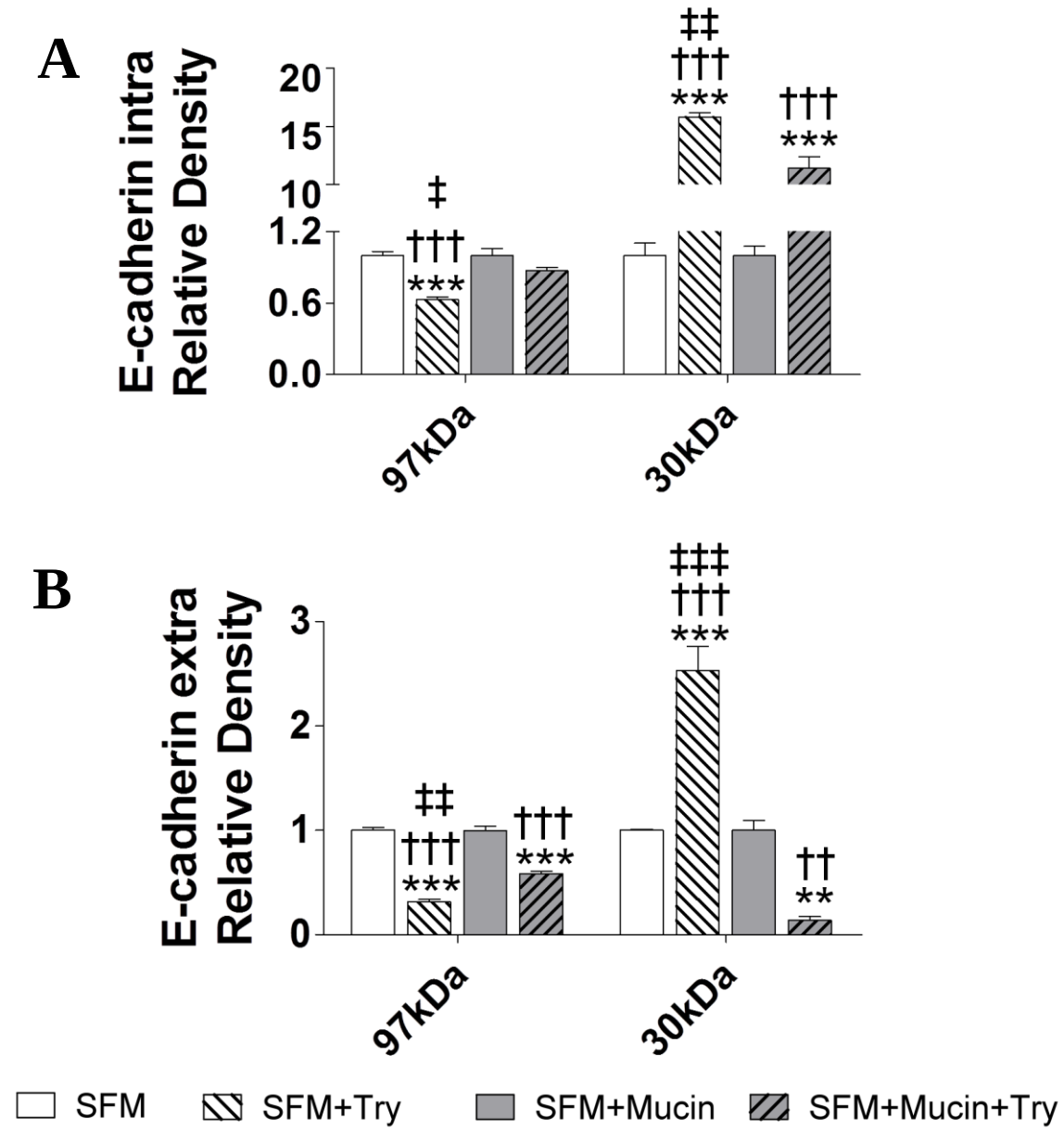

Figure 5.8 E-cadherin relative densities in IEC-18. corresponding density levels measurements of intra- **(A)** and extra-cellular domains of E-cadherin **(B)**. Values are mean±SEM (n=4)/group, ** P<0.001 and *** P<0.0001 compared to SFM; †† P<0.001, ††† P<0.0001 compared to SFM+Mucin; and ‡‡ P<0.001, ‡‡‡ P<0.0001 compared to SFM+Mucin+Try.

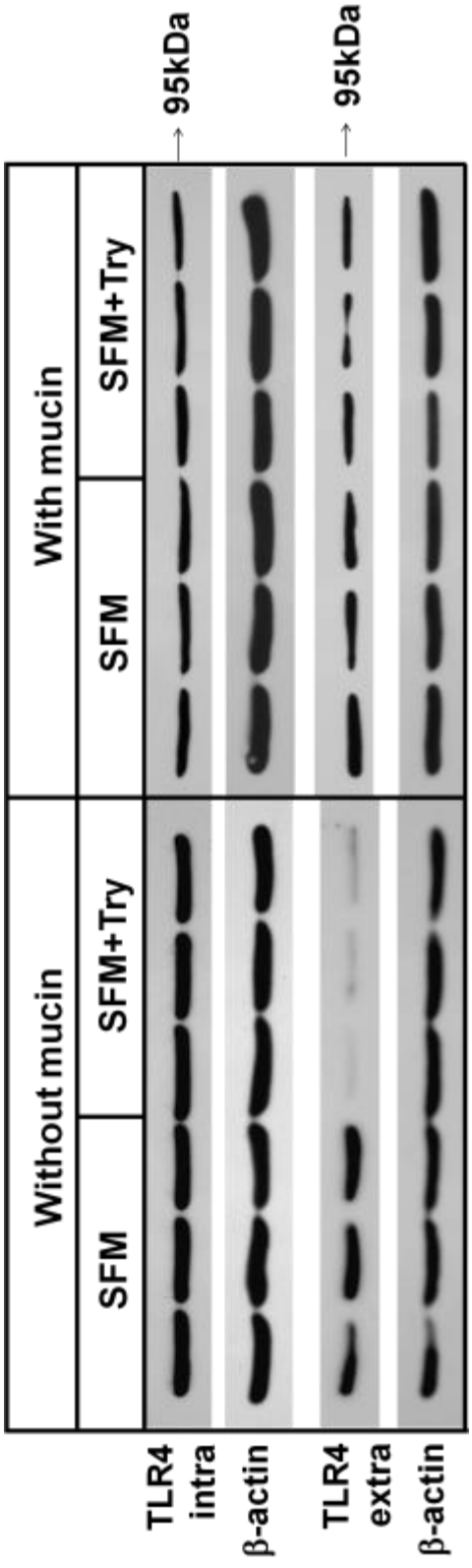

Figure 5.9 TLR4 protein levels in IEC-18. Western blot for intra- and extra-cellular domains of E-cadherin of TLR4 cells without a mucin layer after exposure with serum free without and with trypsin (SFM and SFM+Try respectively) and IEC-18 cell with a mucin layer after exposure to serum free media with or without trypsin (SFM+Mucin and SFM+Mucin +Try)

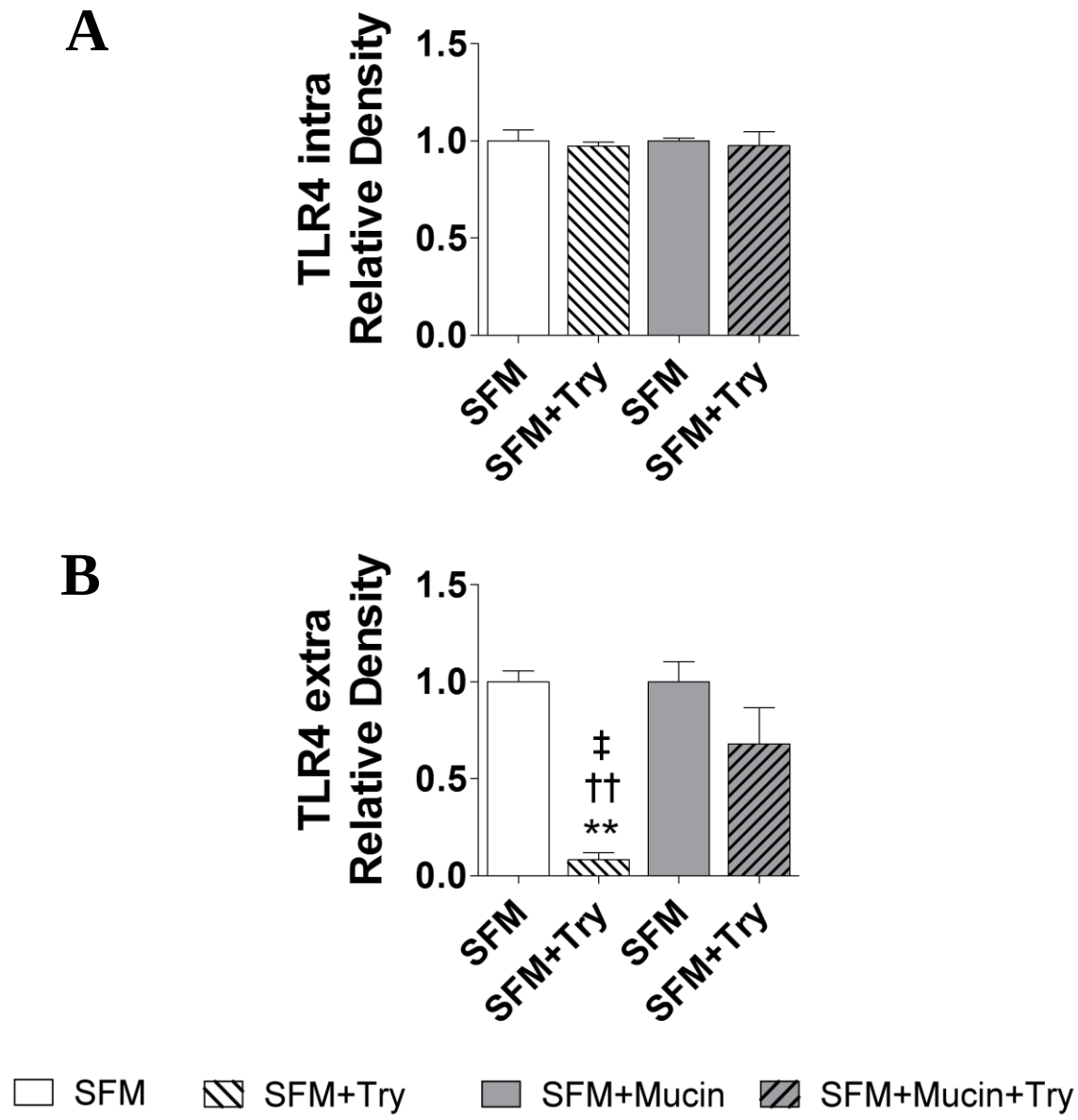

Figure 5.10 TLR4 relative densities in IEC-18. corresponding density levels measurements of intra- **(A)** and extra-cellular domains of TLR4 **(B)**. Values are mean±SEM (n=4)/group, ** P<0.001 and *** P<0.0001 compared to SFM; †† P<0.001, ††† P<0.0001 compared to SFM+Mucin; and ‡‡ P<0.001, ‡‡‡ P<0.0001 compared to SFM+Mucin+Try.

5.7 References

1. Corfield A, *et al.* (2000) Mucins and mucosal protection in the gastrointestinal tract: new prospects for mucins in the pathology of gastrointestinal disease. *Gut* 47(4):589.

2. Corfield AP, Carroll D, Myerscough N, & Probert C (2001) Mucins in the gastrointestinal tract in health and disease. *Front Biosci* 6(10):D1321-1357.

3. Chang M, Kistler EB, & Schmid-Schönbein GW (2011) Disruption of the Mucosal Barrier during Gut Ischemia Allows Entry of Digestive Enzymes into the Intestinal Wall. *Shock*.

4. Rupani B, *et al.* (2007) Relationship between disruption of the unstirred mucus layer and intestinal restitution in loss of gut barrier function after trauma hemorrhagic shock. (Translated from eng) *Surgery* 141(4):481-489 (in eng).

5. Haglund U, Abe T, Ahren C, Braide I, & Lundgren O (1976) The intestinal mucosal lesions in shock. I. Studies on the pathogenesis. (Translated from eng) *Eur Surg Res* 8(5):435-447 (in eng).

6. Atuma C, Strugala V, Allen A, & Holm L (2001) The adherent gastrointestinal mucus gel layer: thickness and physical state in vivo. *Am J Physiol-Gastr L* 280(5):G922-G929.

7. Lichtenberger L (1995) The hydrophobic barrier properties of gastrointestinal mucus. *Annual review of physiology* 57(1):565-583.

8. Gum Jr J (1995) Human mucin glycoproteins: Varied structures predict diverse properties and specific functions. *Biochemical Society Transactions* 23(4):795.

9. Strous GJ & Dekker J (1992) Mucin-type glycoproteins. *Critical reviews in biochemistry and molecular biology* 27(1-2):57-92.

10. Allen A & Snary D (1972) The structure and function of gastric mucus. *Gut* 13(8):666.

11. Lamont JT (1992) Mucus: the front line of intestinal mucosal defense. *Annals of the New York Academy of Sciences* 664(1):190-201.

12. Werb Z (1997) ECM and Cell Surface Proteolysis: Minireview Regulating Cellular Ecology. *Cell* 91:439-442.

13. Coughlin SR (2000) Thrombin signalling and protease-activated receptors. *Nature* 407(6801):258-264.

14. Giannelli G, Falk-Marzillier J, Schiraldi O, Stetler-Stevenson WG, & Quaranta V (1997) Induction of cell migration by matrix metalloprotease-2 cleavage of laminin-5. *Science* 277(5323):225.

15. Yu Q & Stamenkovic I (2000) Cell surface-localized matrix metalloproteinase-9 proteolytically activates TGF-β and promotes tumor invasion and angiogenesis. *Genes & development* 14(2):163.

16. Epstein FH, Fish EM, & Molitoris BA (1994) Alterations in epithelial polarity and the pathogenesis of disease states. *New England Journal of Medicine* 330(22):1580-1588.

17. Man Y, Hart VJ, Ring CJ, Sanjar S, & West MR (2000) Loss of epithelial integrity resulting from E-cadherin dysfunction predisposes airway epithelial cells to adenoviral infection. *American journal of respiratory cell and molecular biology* 23(5):610.

18. Hotchkiss RS & Karl IE (2003) The pathophysiology and treatment of sepsis. *New England Journal of Medicine* 348(2):138-150.

19. Lorenz E, Mira JP, Frees KL, & Schwartz DA (2002) Relevance of mutations in the TLR4 receptor in patients with gram-negative septic shock. *Arch Intern Med* 162(9):1028.

20. Sodhi C, *et al.* (2011) DNA attenuates enterocyte Toll-like receptor 4-mediated intestinal mucosal injury after remote trauma. *Am J Physiol-Gastr L* 300(5):G862-G873.

21. Moses T, Wagner L, & Fleming SD (2009) TLR4-mediated Cox-2 expression increases intestinal ischemia/reperfusion-induced damage. *Journal of leukocyte biology* 86(4):971-980.

22. Nusrat A, Turner J, & Madara J (2000) Molecular Physiology and Pathophysiology of Tight Junctions: IV. Regulation of tight junctions by extracellular stimuli: nutrients, cytokines, and immune cells. *American Journal of Physiology- Gastrointestinal and Liver Physiology* 279(5):851.

23. Gonzalez-Mariscal L, Betanzos A, Nava P, & Jaramillo B (2003) Tight junction proteins. *Progress in biophysics and molecular biology* 81(1):1-44.

24. Clayburgh D & Le Shen J (2004) A porous defense: the leaky epithelial barrier in intestinal disease. *Laboratory investigation* 84(3):282-291.

25. Green G & Nasset E (1980) Importance of bile in regulation of intraluminal proteolytic enzyme activities in the rat. *Gastroenterology* 79(4):695-702.

26. Miyasaka K & Green G (1984) Effect of partial exclusion of pancreatic juice on rat basal pancreatic secretion. *Gastroenterology* 86(1):114.

27. Helgason CD & Miller CL (2005) *Culture of Primary Adherent Cells and a Continuously Growing Nonadherent Cell Line* (Humana Pr Inc, Totowa, New Jersey) 3rd Ed.

28. Choi YJ, Im E, Pothoulakis C, & Rhee SH (2010) TRIF modulates TLR5-dependent responses by inducing proteolytic degradation of TLR5. *Journal of Biological Chemistry* 285(28):21382.

29. de Zoete MR, Bouwman LI, Keestra AM, & van Putten JPM (2011) Cleavage and activation of a Toll-like receptor by microbial proteases. *Proceedings of the National Academy of Sciences* 108(12):4968.

30. Guzman K, Bader T, & Nettesheim P (1996) Regulation of MUC5 and MUC1 gene expression: correlation with airway mucous differentiation. *American Journal of Physiology-Lung Cellular and Molecular Physiology* 270(5):L846-L853.

31. Gendler S & Spicer A (1995) Epithelial mucin genes. *Annual review of physiology* 57(1):607-634.

Chapter 6

Effect of Ischemic Factors in Mucin Degradation

6.1 Introduction

During early ischemic states the integrity of the intestinal mucosa becomes compromised (1-7), which makes the intestinal wall potentially accessible to pancreatic digestive enzymes normally present in the intestinal lumen (8, 9). Hemorrhagic lesions in the small intestinal mucosa have been reported in dogs (10-13), cats (14-16) and similar mucosal lesions have also been reported in patients dying in shock (1-7). A characteristic feature is that these lesions are visible first at the tip of the villi, and in cases in which the entire villus is destroyed the deeper layers of the intestinal wall are still free from inflammatory changes (13, 14). During mesenteric ischemia, the perfusion of the different layers of the intestine is redistributed disproportionately, favoring the more metabolically active areas, evident by relatively smaller decreases in flow in the superficial villus region. However, because of increased metabolic demand at the villus tip, and the countercurrent shunting of oxygen at the villus base the villus tip remains

preferentially susceptible to ischemic injury; thus under ischemic conditions, the gut dies progressively from the inside out.

6.2 Ischemic Factors Affecting Intestinal and Mucosal Properties.

Previous studies have shown that the mucosal barrier is disrupted in shock (17, 18); mucin is the main component of this barrier and the mechanism leading to loss of function is yet to be determined. Mucin is a glycoprotein consisting of a carbohydrate and protein core that due to its dual nature serves as a barrier. Loss of the mucosal barrier, and especially mucin, will permit leakage of cytotoxic mediators as well as digestive enzymes. Mucin properties could be affected as a result of ischemia due to hypoxia, decrease of ATP or luminal pH which have been shown to affect mucin both in-vitro and in-vivo (19-21) or by enzymatic degradation of its outer glyco-domain and/or its inner core protein domain.

6.2.1 Hypoxia: In hemorrhagic shock and ischemia/reperfusion injury, intestinal blood flow is reduced and the intestinal villi are damaged. However, providing an extracellular source of oxygen to enterocytes (by perfusing the lumen of the gut with gaseous oxygen, oxygenated crystalloid or perfluorocarbon solutions) ameliorates mucosal injury induced by ischemia and maintains mucosal barrier function (22-27). Perfluorocarbons (PFC) has a high oxygen delivery capacity, is nontoxic and is biochemically inert capable of dissolving up to 40 percent oxygen by volume (28, 29). This remarkable and reversible oxygen solubility has encouraged investigations into therapeutic application in situations where tissue oxygen delivery is impaired, such as in intestinal ischemia.

6.2.2 ATP depletion: Exposing an intact epithelial monolayer to a variety of physiologic insults, including nitric oxide donor (30), acidosis (31), and prolonged hypoxia (32), has been linked to increased permeability and reduction in total cellular ATP levels (33). Exposing Caco-2_{BBc} intestinal epithelial monolayers to hypoxic conditions for prolonged period depletes cellular ATP levels and increases paracellular permeability to macromolecules (32). Acute and profound ATP depletion to approximately 10% of normal levels has been shown to impair the structure and function of tight junctions in cultured epithelial monolayers (34). Normal airway mucus hydration (and their viscoelasticity) is regulated by at least two signaling systems mediated by ATP and adenosine (35). Both signaling systems are present in epithelia of cystic fibrotic patients, but the adenosine signaling system is nonfunctional because its effector component, the cystic fibrosis transmembrane conductance regulator (CFTR) is either missing or nonfunctional.

The normal cystic fibrosis transmembrane conductance regulator (CFTR) acts as a cAMP-activated Cl− channel and also helps regulate Na+ reabsorption by the epithelial Na+ channel (ENaC). To hydrate airway mucus, the adenosine system normally regulates CFTR to inhibit Na+ reabsorption and initiate Cl− secretion. Since mutant CFTR cannot perform these functions, Na+ reabsorption causes water reabsorption by osmosis, leading to mucus dehydration, flattened cilia, and stasis (35). The CFTR is also critical to intestinal anion secretion in the small intestine (36).

6.2.3 pH changes: Previous studies on gastric mucin indicate that the rheology of this material is pH dependent, transitioning from a viscous solution at neutral pH to a gel in

acidic conditions. Bulk rheology measurements on porcine gastric mucin (PGM) show that pH elevation by H. pylori induces a dramatic decrease in viscoelastic moduli (37).

In the small intestine the proximal duodenum is unique in that it is the only leaky epithelium regularly exposed to concentrated gastric acid. To prevent injury from occurring, numerous duodenal defense mechanisms have evolved. The most studied is bicarbonate secretion, which is presumed to neutralize luminal acid. Less well studied in their protective roles are the mucus gel layer and blood flow (38). Exposure of the mucosa to physiologic acid solutions promptly lowers intracellular pH (pHi), followed by recovery after acid is removed; indicating that acid at physiologic concentrations readily diffuses into, but does not damage duodenal epithelial cells. Cellular acid then exits the cell via an amiloride-inhibitable process, presumably sodium-proton exchange (NHE). Mucus gel thickness and blood flow increase promptly during acid perfusion; both decrease after acid challenge and are inhibited by vanilloid receptor antagonists or by sensory afferent denervation (38). Bicarbonate secretion is not affected by acid superfusion but increases after challenge. With continued acid exposure, a new steady state with thickened mucus gel, increased blood flow, and a higher cellular buffering power protects against acid injury (38).

6.3 Aims in this Chapter

The mucus that covers the intestinal tract forms a physical barrier between the intestinal lumen and the underlying epithelia. It has been reported that one of mucin's function is to form a transport barrier for the apical cell surfaces and to participate in intracellular signaling (17, 18, 39). In this study I will determine whether the disruption

of the mucus layer, such that it results in penetration of digestive enzymes into the wall of the ischemic intestine, is due to hypoxia, ATP depletion or acidosis. I hypothesize that oxygen depletion and ATP depletion are a requirement for mucin degradation and supplementation with enteral oxygen or ATP serve to minimize the mucin degradation. The aims in this chapter are to determine whether hypoxia, ATP depletion and pH change in the lumen of the intestine lead to the disruption of the mucosal layer and degradation of mucin during intestinal ischemia.

6.4 Materials and Methods

6.4.1. Animal groups and SAO model: All animal protocols were reviewed and approved by the University of California San Diego Animal Subjects Committee. Male Wistar rats (250-300g, Harlan Sprague Dawley Inc, Indianapolis, IN) were randomly assigned to one of the following groups (n=4 per group): two groups with saline injection in the lumen of the intestine with either sham surgery (SHAM) or 30min splanchnic ischemia (SAO). In order to study the effect of hypoxia two groups with perfluorocarbon (Sigma-Aldrich, St Louis, MO) without oxygen injected in the lumen of the intestine with either SHAM or SAO surgery (SHAM+PFC, SAO+PFC) and two groups with oxygenated perfluorocarbon, bubbled for 10min with either SHAM or SAO surgery (SHAM+PFC+O2, SAO+PFC+O2). To study the effect of free radicals, dimethylthiourea (DMTU, Sigma-Aldrich), 2.0 mg/g BW was injected in the lumen of the intestine of SAO animals (SAO+DMTU). To study the effect of ATP supplementation two groups with ATP-$MgCl_2$ (Sigma-Aldrich), 25mg/kg BW was injected in the lumen of the intestine with SHAM or SAO surgery (SHAM+ATP, SAO+ATP). To study the effect of pH a

SHAM group with saline at pH 5.5 and a SHAM and SAO with HEPES buffer. Rats were kept on solid food restriction for 12 hours prior to surgery with water ad libitum. After general anesthesia (Ketamine/Xylazine, 75 mg/kg BW / 20 mg/kg BW, IM) 30 min after saline, PFC, ATP or HEPES injection, the superior mesenteric and celiac arteries were isolated and occluded for 30 min for the ischemic groups or isolated without occlusion in the sham group. After 30 min SAO or sham surgery the animals were euthanized with Beuthanasia® 0.22 ml/kg BW, IV.

6.4.2 Tissue cryosections: After euthanasia, jejunal sections (~1 cm in length) were excised without removal of luminal contents and suspended in Tissue-Tek O.C.T. Compound (Sakura Finetek, Torrance, CA), snap frozen in isopentane/liquid nitrogen, and stored at -80^{o}C for analysis. Cryosections (5 µm thickness) along the longitudinal axis of the villi were used throughout all experiments. Cryosections were fixed in 10% formalin solution and processed in a non-blinded fashion.

6.4.3 In-situ tissue zymography and immunohistochemistry: In-situ zymography for trypsin activity in cryosections was assessed by measurement of fluorescence resulting from the proteolytic cleavage of the substrate (1mM, Nα-benzoyl-L-arginine-7-amido-methylcoumarin hydrochloride; Sigma-Aldrich) as described elsewhere (40). For immunohistochemical analysis, primary antibodies were diluted as followed: Trypsin 1:300 and mucin2 1:200 (Santa Cruz Biotechnology, Santa Cruz, CA); the extracellular domain of TLR4 1:250 (Abcam, Cambridge, MA), and the intracellular domain of TLR4 1:250 (Invitrogen, Carlsbad, CA, USA). Secondary antibodies were as follows: FITC (Santa Cruz Biotechnology) and HRP (ImmPRESS, Vector Lab; Burlingame, CA). The

slides were developed using 3, 3´-diaminodbenzidine substrate and counterstained with hematoxylin or DAPI (Vector Lab) or propidium iodine (Sigma-Aldrich). Slides were observed in a non-blinded fashion under an inverted microscope (20X and 60X objectives).

6.4.4 Mucin and lectin staining: The simultaneous visualization of lectins and mucin was carried out using Lectin GS-II From Griffonia simplicifolia, Alexa Fluor® 594 Conjugate (EnzChek®, Invitrogen, Carlsbad, CA) and specific antibody for mucin2 with FITC secondary antibody (1:10000, Santa Cruz Biotechnology) and nuclei counterstaining with DAPI. Sections were observed on an inverted microscope (20X objective) using the appropriate fluorescent filters.

6.4.5 Hypoxia staining: In separate experiments, the level of tissue hypoxia was detected with Hypoxyprobe™-1 Kit (Natural Pharmacia International, Burlington, MA, USA). This method utilizes a small molecular marker, pimonidazole, which after intravenous injection forms adducts with thiol containing proteins only in oxygen-starved cells.

After general anesthesia, as described above, pimonidazole-HCl (6 mg/100 g) was injected intravenously 30 min before SAO or SHAM; at 30 min the animal was euthanized and the jejuna section removed, embedded in O.C.T and frozen in liquid nitrogen. Then cryosections were immunostained using a rabbit antibody that binds to protein adducts of pimonidazole in hypoxic cells.

6.4.6 Homogenates of intestine and luminal contents: Jejunal segments were excised without removal of luminal contents. For enzyme activity measurements, segments of

intestine were homogenized with CelLytic™ (Sigma-Aldrich) without addition of protease inhibitors. For Western blot assays the intestine segments were homogenized as above in the presence of protease inhibitors (5mM EDTA, 5mM N-Ethylmaleimide, 25mM iodoacetamide, 5mM benzamidine, 300mM acarbose, 5mM 6-aminocaproic acid, 1mM protease inhibitor cocktail, (Sigma-Aldrich). In separate experiments the small intestine of sham animals was excised, and the luminal contents were flushed with 20 ml saline. Homogenates or luminal contents were centrifuged (16,000g for 15 min at 4°C), the supernatant was collected and protein concentration was assessed with the bicinchoninic acid protein assay (Thermo Scientific).

6.4.7 Western blot: Tissue homogenate (20μg) were separated by SDS-PAGE. Membranes were incubated with primary antibodies as follows: mucin2, mucin13 and trypsin 1:1000 (Santa Cruz Biotechnology), pancreatic amylase 1:1000 (GeneTex, San Antonio, TX), intra- and extra-cellular domains of E-cadherin and TLR4 1:1000 (Abcam), intracellular domain of TLR4 1:1000 (Invitrogen). Secondary antibodies were diluted 1:20000 (Santa Cruz Biotechnology) and detected with Super Signal West Pico (Thermo Scientific). The exposed x-ray films were scanned and label intensity was measured using digital gel analysis (NIH ImageJ software).

6.4.8 ATP assay: ATP concentration in intestine homogenates was measured using ATP fluorometirc assay kit (BioVision, Mountain View, CA) according to the manufacturer's protocol. Briefly jejunal sections were homogenized with perchloric acid (BioVision), centrifuged at 15,000xG for 5 min at 4^{o}C. Samples were mixed with ATP reaction mix,

incubated for 30min protected from light and the fluorescence was measured with 535/587 (Ex/Em).

6.4.9 TBARS assay: Thiobarbituric Acid Reactive Substances (TBARS) was measured using a commercial kit (Zeptometrix, Buffalo, NY). Briefly jejunal sections were homogenized with perchloric acid (BioVision), centrifuged at 15,000xG for 5 min at 4^{o}C. Samples were mixed with thiobarbituric acid (TBA) reagent, incubated at 95^{o}C for 60 min, and cool down in ice bath for 10min. Samples were centrifuged at 3000rpm for 15min and the supernatant were read at 530/550 (Ex/Em).

6.4.10 Statistical Analysis: Results are presented as mean±SEM. Unpaired comparisons of mean values between groups were carried out by one-way ANOVA followed by Bonferroni post-hoc comparisons. $P<0.05$ was considered significant.

6.5 Results

6.5.1 Oxygenated PFC, DMTU and HEPES prevent elevation of trypsin activity in the intestinal wall: In-situ zymography of trypsin activity in the intestinal wall revealed no trypsin activity for the following SHAM groups (SHAM, SHAM+PFC, SHAM+PFC+O2) (Figure 6.1) and (SHAM+ATP, SHAM+HEPES) (Figure 6.2). High levels of trypsin activity were observed for the ischemic groups with saline in the lumen of the intestine (SAO) and for the ischemic group with deoxygenated perfluorocarbon (SAO30+PFC) (Figure 6.1). Moderate levels of trypsin activity were also observed for the ischemic groups with ATP supplementation (SAO+ATP) and SHAM with saline at pH 5.5 (Figure 6.2). Ischemic groups treated with oxygenated perfluorocarbon

(SAO30+PFC+O2) (Figure 6.1) or DMTU (SAO+DMTU) or HEPES (SAO+HEPES) (Figure 6.2) had undetectable levels of trypsin activity in the intestinal wall.

6.5.2 Carbohydrate and protein portion of mucin are reduced during SAO: Double labeling of lectin and mucin2 reveals that after 30min of ischemia (SAO) in addition to villi injury at the tip of the villi there is decrease in labeling of both lectins and mucin2 as compared to SHAM groups (SHAM, SHAM+PFC, SHAM+PFC+O2) (Figure 6.3) especially in the interface between the villi tip and the intestinal lumen. The same was observed in the ischemic group with deoxygenated perfluorocarbon (SAO+PFC).

Enteral injection of oxygenated perfluorocarbon (SAO+PFC+O2) not only preserved the villus structure but also preserved both lectin and mucin2 staining (Figure 6.3). ATP supplementation in both SHAM and ischemic group (SAO+ATP) resulted in more visible staining in the lumen (Figure 6.4). There was no apparent injury in the ischemic group with this treatment and no difference in lectin or mucin2 labeling as compared to SHAM group.

Luminal injection with DMTU during ischemia (SAO+DMTU) also resulted in undetectable villi injury or reduction of the staining levels of lectin or mucin2 (Figure 6.4). SHAM groups acidic saline (SHAM+pH5.5) or ischemic group with hepes buffer (SAO+HEPES) had also normal looking villi and lectin and mucin2 staining as compared to sham (SHAM+HEPES) (Figure 6.4).

6.5.3 Mucin2 and mucin13 degradation is mediated by ischemic factors: Western blots of mucin2 and mucin13 for SHAM and ischemic groups (SAO) with only saline in

the lumen of the intestine show that the mucin2 labeling density significantly increased after ischemia (Figures 6.5 and 6.6)**.** Mucin13 western analysis show that besides the full protein in the SHAM group there are low molecular weight bands at around 24kDa. But after ischemia those bands are not detected or present in lower quantities than SHAM and there was also appearance of a lower molecular weight band around 17kDa that was not present in the SHAM group (Figure 6.5 and 6.6). Injection of deoxygenated perfluorcarbon (SHAM+PFC, SAO+PFC) presented similar results as observed in groups with only saline injection. Mucin2 protein levels are reduced in the SAO group (SAO+PFC) as compared to sham (SHAM+PFC) (Figure 6.7 and 6.8).

Mucin13 was also detected in form of lower molecular weight fragments at 17kDa with the only difference that bands around 24kDa did not completely disappear in the ischemic group (SAO+PFC) as compared to the group with just saline (SAO). Injection of oxygenated perfluorocarbon (SHAM+PFC, SAO+PFC) resulted in mucin2 with levels in the ischemic group similar to the sham group (Figure 6.7. 6.8). Mucin13 levels in this group resulted in complete disappearance or at most very faint levels of the 17kDa band in the ischemic group (SAO+PFC+O2) as compared to sham (SHAM+PFC+O2). Injection of DMTU in the ischemic group (SAO+DMTU) resulted in reduced levels of mucin2 while mucin13 western blot reveal no appearance of the lower molecular weight band at 17kDA (Figure 6.7 and 6.8). This pattern was also observed in the groups with ATP injection in the lumen of the intestine where the ischemic group (SAO+ATP) had the same mucin2 and mucin13 protein levels as the sham (SHAM+ATP) (Figure 6.9 and 6.10). The same pattern was observed in the groups with

either hepes of acidic saline treatment. The sham group with acidic saline (SHAM+pH5.5) and ischemic group with hepes (SAO+HEPES) had similar levels of mucin2 and mucin13 as compared to sham (SHAM+HEPES).

6.5.4 Oxygenated Perfluorocarbon prevents intestinal hypoxia: Hypoxia staining revealed that after 30min ischemia markers of hypoxia are present in the intestinal villi (SAO, SAO+PFC) (Figure 6.11) and (SAO+ATP) (Figure 6.12) as compared to sham groups (SHAM, SHAM+PFC, SHAM+PFC+O2) (Figure 6.11) and (SHAM+ATP, SHAM+HEPES, SHAM+pH5.5). Ischemic groups with DMTU (SAO+DMTU) and hepes buffer (SAO+HEPES) presented some levels of hypoxic staining but not as strong as the previous groups (Figure 6.12). In contrast, the ischemic group with oxygenated perfluorocarbon (SAO+PFC+O2) injected in the lumen of the intestine presented no detectable sign of hypoxia staining (Figure 6.11).

6.5.5 ATP concentration in intestine homogenates decreases during SAO: The concentration of ATP in the intestinal tissue after 30min ischemia significantly decreased in the groups with only saline (SAO) and deoxygenated perfluorocarbon (SAO+PFC) as compared to SHAM or SHAM+PFC (Figure 6.13). Injection with oxygenated perfluorocarbon in ischemic intestine (SAO+PFC+O2) presented no reduction in ATP concentration as compared to SAO or SAO+PFC. Injection of ATP in the lumen of the intestine significantly increased the ATP concentration in the wall of both sham and ischemic intestines (SHAM+ATP and SAO+ATP) as compared to SHAM and SAO, there was no difference between SHAM+ATP or SAO+ATP (Figure 6.13). The ATP levels in ischemic intestine treated with DMTU (SAO+DMTU) were lower than SHAM

and higher than SAO but it was no statistically significant (Figure 6.13). Sham groups with hepes or acidic saline (SHAM+HEPES, SHAM+pH5.5) were not different than SHAM but were significantly different than SAO (Figure 6.13). The ischemic group with hepes buffer (SAO+HEPES) had levels similar to sham groups (SHAM and SHAM+HEPES) and it was significantly different from SAO (Figure 6.13)

6.5.6 Oxygenated perfluorocarbon reduces levels of thiobarbituric acid reactive substances: TBARS assay performed in intestine homogenates reveal a non-significant increase in MDA equivalent levels in the ischemic intestine with luminal saline injection (SAO) and deoxygenated perfluorocarbon (SAO+PFC) as compared to SHAM or SHAM+PFC (Figure 6.14). In contrast, groups with oxygenated perfluorocarbon (SHAM+PFC+O2 and SAO+PFC+O2) had lower levels of MDA equivalents (Figure 6.14). The levels of SAO+PFC+O2 were significantly lower as compared to SAO or SAO+PFC (Figure 6.14). Ischemic group with luminal ATP injection had no significantly lower levels of MDA equivalents as compare to sham (SHAM+ATP). MDA levels in the ischemic group with DMTU treatment (SAO+DMTU) were not statistically different from SHAM. There was no significant change in the MDA levels among the other groups (Figure 6.14).

6.6 Discussion

It has been reported that mucin's main function is to "protect" the apical cell surfaces and to participate in intracellular signaling [23, 31, 32]. Increases in intestinal permeability reported in patients with sepsis (41), burn victims (42), and trauma (32) is accompanied by gastrointestinal mucosal acidosis (32) and cellular hypoxia. The results

in this chapter show that ischemic factors such as hypoxia, ATP depletion and pH changes are directly involved in the disruption of mucin during intestinal ischemia.

It has been shown that hat MUC3 is selectively responsive to hypoxia through transcription-dependent pathways (43). The data presented in this chapter indicates that oxygen supplementation with oxygenated perfluorocarbon prevents ischemic injury, as well as enhanced trypsin activity in the intestinal wall. There is protection of mucin2 and mucin13 molecule, preserved levels of intestinal tissue ATP and significantly reduced levels of thiobarbituric acid reactive substances. Thus hypoxia directly mediates mucin disruption, but the mechanism by which this takes place still needs to be elucidated. For instance, it was shown that MUC3 expression is regulated by HIF-1, a member of the Per-ARNT-Sim (PAS) family of basic helix-loop-helix (bHLH) transcription factors (44). HIF-1 exists as an αβ heterodimer, the activation of which is dependent upon stabilization of an O_2-dependent degradation domain of the α subunit by the ubiquitin-proteasome pathway (45). Hypoxia can also increase anaerobic metabolism and the development of lactic acidosis (46). In addition ATP depletion is a consequence of ischemia and cellular hypoxia (46).

There is evidence that oxygen-derived free radicals play an important role in the pathogenesis of the injury of various tissues including the gastrointestinal system (47, 48) and ischemia-induced intestinal damage (49). The hydroxyl radical can damage virtually all types of macromolecules including carbohydrates, nucleic acids, lipids and amino acids (50, 51). The hydroxyl radical is the major contributor to ischemic damage; it has been hypothesized and a primary source of free radicals in ischemic lesions may be the

enzyme xanthine oxidase (49, 52) and that …… (53). Other potential sources of these radicals in the lumen of the intestine include food, bacteria and neutrophils. It has been reported that gastrointestinal mucins may function as oxygen radical scavangers due to their high concentration of carbohydrate moieties resulting in a drop in mucin viscosity, suggesting possible damage to the molecule (54). Thus dimethylthiourea (DMTU), a hydroxyl radical scavenger that is able to penetrate into the intracellular space (55) may be able to prevent mucin disruption as a result of hydroxyl radical damage. It has been reported that LPS-induced production of free radicals may be involved in activation of goblet cell secretion in intestinal epithelium and that DMTU administered prior to LPS application blocks this effect (56).

The results in this chapter show that TBARS assay yield no significant increase in MDA levels during ischemia; oxygen and ATP supplementation decreased MDA levels as compared to ischemic group with just saline. This result may suggest that the partial increase observed during ischemia is directly dependent on hypoxia and ATP depletion. The data presented in this chapter show protection of the intestine when DMTU was present in the lumen of the intestine after ischemia (SAO+DMTU). We also see no increased trypsin activity in the intestinal wall which may indicate a lack of trypsin transport. Mucin13 is protected with no appearance of lower molecular weight fragments, but there is reduction in mucin2 protein levels. Double labeling of lectin and mucin2 shows levels similar to the sham group, which may indicate partial protection of both carbohydrates and mucin2 protein by DMTU.

Mucus hydration (and viscoelasticity) in the airway mucosa has been shown to be regulated by ATP and adenosine signaling (35). Also it has been reported that as ATP tissue levels decrease during ischemia and reperfusion there is an increase in intestinal permeability (33); thus ATP may be indirectly affecting mucin properties and subsequently increasing intestinal permeability. The ischemic groups with ATP supplementation present less trypsin activity in the wall as compare to the ischemic group with only saline in the lumen. The lectin and mucin2 staining as well as protein levels of mucin2 and mucin13 are also preserved. Therefore the results suggest that ATP depletion mediates mucin degradation although the exact mechanism still needs to be identified. There are many possible pathways by which ATP may control mucin homeostasis. For instance there is a feedback involving surface pH and ATP concentration mediated by purinergic receptor (38, 57). Also ATP may regulate mucin hydration by chloride transmembrane conductance regulator (CFTR) or ENAC channels (33, 35).

It is known that mucin molecules in solution can cross-link to form aggregates via H-bonds, electrostatic and hydrophobic interactions, as well as Van der Waals forces (20). This cross-linking leads to the formation of a gel network that can be affected by disulfide bonds between lectins, mucin hydration, ionic strength or pH which can cause conformational changes from an isotropic random coil to an anisotropic extended random coil (58). A reduction in pH from 7.4 to 6.5 was seen to produce a significant decrease in the velocity of mucin swelling from the secretory granule matrix (59). However, when HCL is injected into solutions of gastric mucin, viscous fingers or channels dependent on pH and mucin concentration are formed, providing a possible explanation for the

transport of acid through the lumen of the stomach (58). It has been proposed that among the functions of the mucin-bound carbohydrates include protease resistance, large water-holding capacity and high charge density from sialic acid and sulfate residues, which are charged at neutral pH (60). A change of luminal pH in the lumen of the intestine will change the charge of the mucin molecule thus affecting mucin hydration. The results presented in this chapter show that when acidic saline (pH5.5) was injected into the lumen of a sham animal there was a slightly increase in trypsin activity in the wall of the intestine and a non-significant decrease in mucin2 density as compared to sham group with hepes buffer, mucin13 molecule appeared unaffected by addition of acidic saline. A possible explanation is that in the sham intestine the acidic saline in the lumen was buffered by the normal mechanisms thus preventing major injury, another experiment is needed in which sustained acidic conditions in the lumen of the intestine are sustained. When hepes buffer was added in the lumen of the intestine (SAO+HEPES) there was no significant decrease in mucin2 molecule as compared to sham (SHAM+HEPES) and there was no degradation of mucin13 which suggests that acidic pH does play a role in mucin degradation.

In conclusion, the results presented here confirm that during ischemia mucin isoforms are degraded and this process is the result of ischemia. The most likely sequence of events is that intestinal ischemia results in hypoxia, which subsequently results in ATP depletion and luminal acidosis. These combined events alter mucin structure making the molecule susceptible to enzymatic degradation. Treatment of ischemic factors with

oxygenated perfluorocarbon, ATP-MgCl2 supplementation, or a buffering agent such as hepes results in protection of mucin thus reducing intestinal injury.

Chapter 6 in full is currently being prepared for submission for publication of the material by Chang M., Cabrales P. and Schmid-Schönbein G.W. The dissertation author is the primary author of this manuscript.

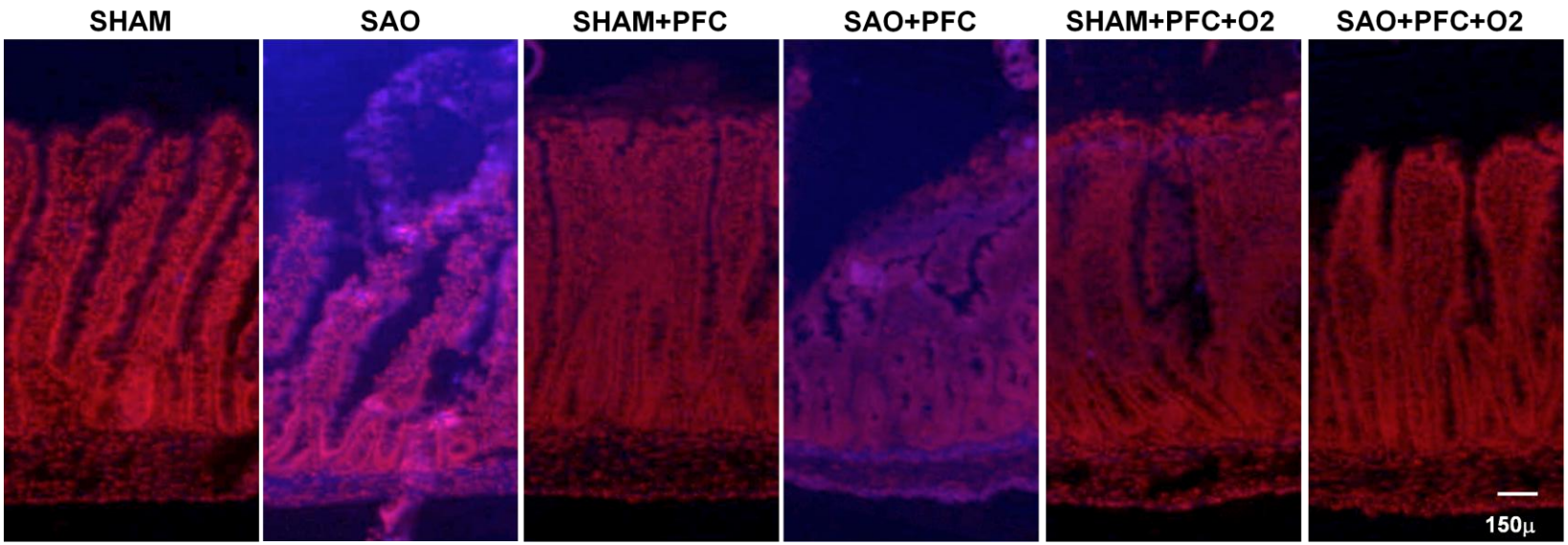

Figure 6.1 In situ zymography for trypsin in jejunal sections. Representative micrographs of trypsin activity as observed by fluorescence of specific substrate (blue), nuclei counterstaining with propidum iodine (red) in SHAM animals or animals subjected to SAO protocol with luminal injection of perfluorocarbons with or without oxygen.

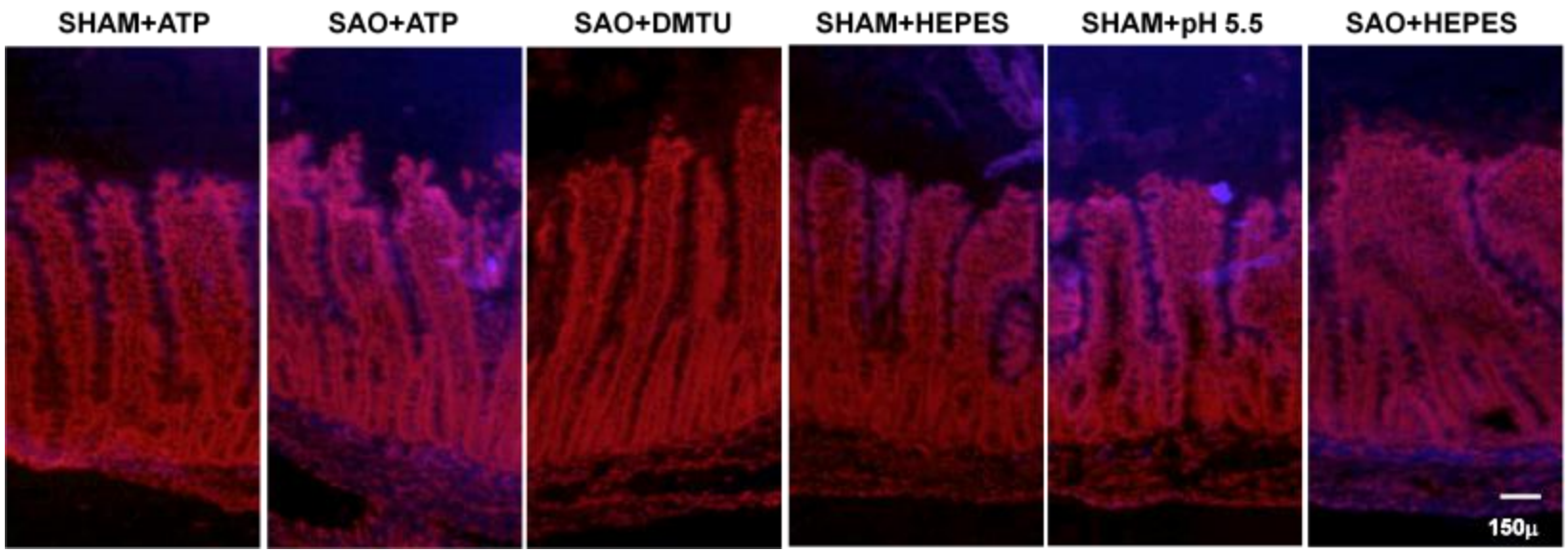

Figure 6.2 In situ zymography for trypsin in jejunal sections. Representative micrographs of trypsin activity as observed by fluorescence of specific substrate (blue), nuclei counterstaining with propidum iodine (red) in SHAM animals or animals subjected to SAO protocol with luminal injection of ATP or HEPES or saline at pH5.5.

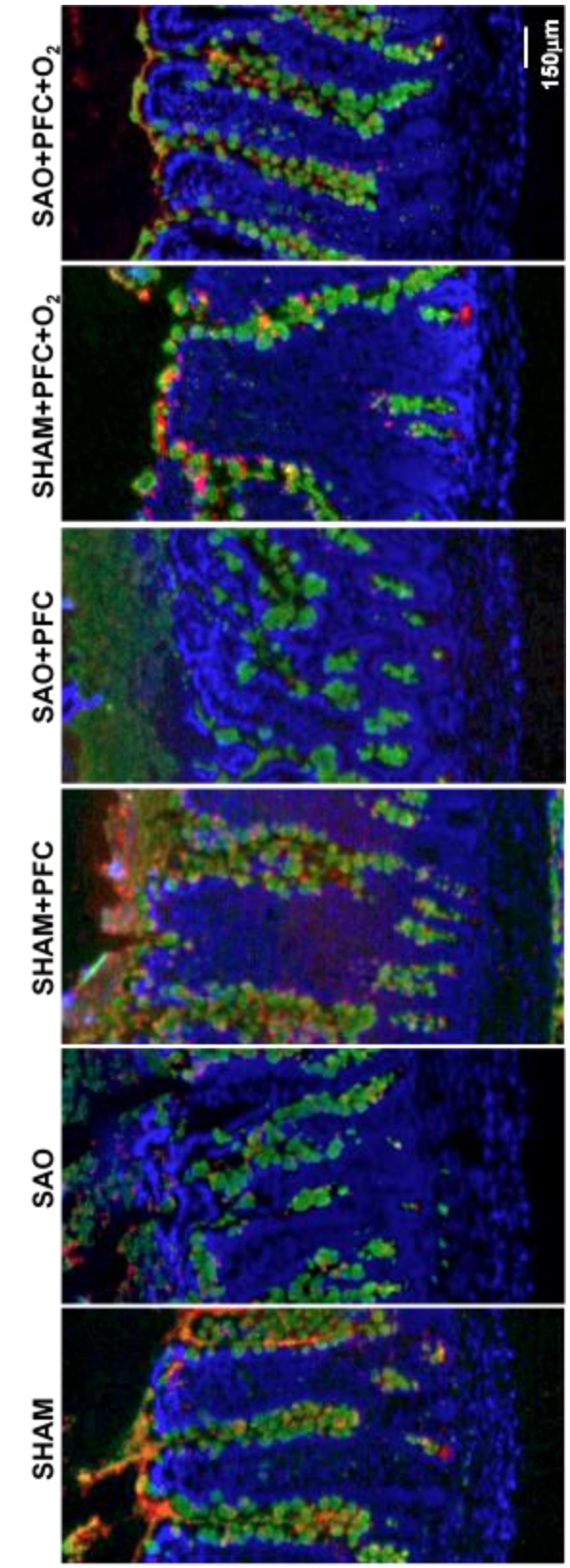

Figure 6.3 Mucin2 and lectin staining. Representative micrographs of mucin2 and lectin fluorescent staining for SHAM and SAO groups with saline in the lumen and with perfluorocarbons with or without oxygen. (blue) nuclcei, (red) lectin and (green) mucin2.

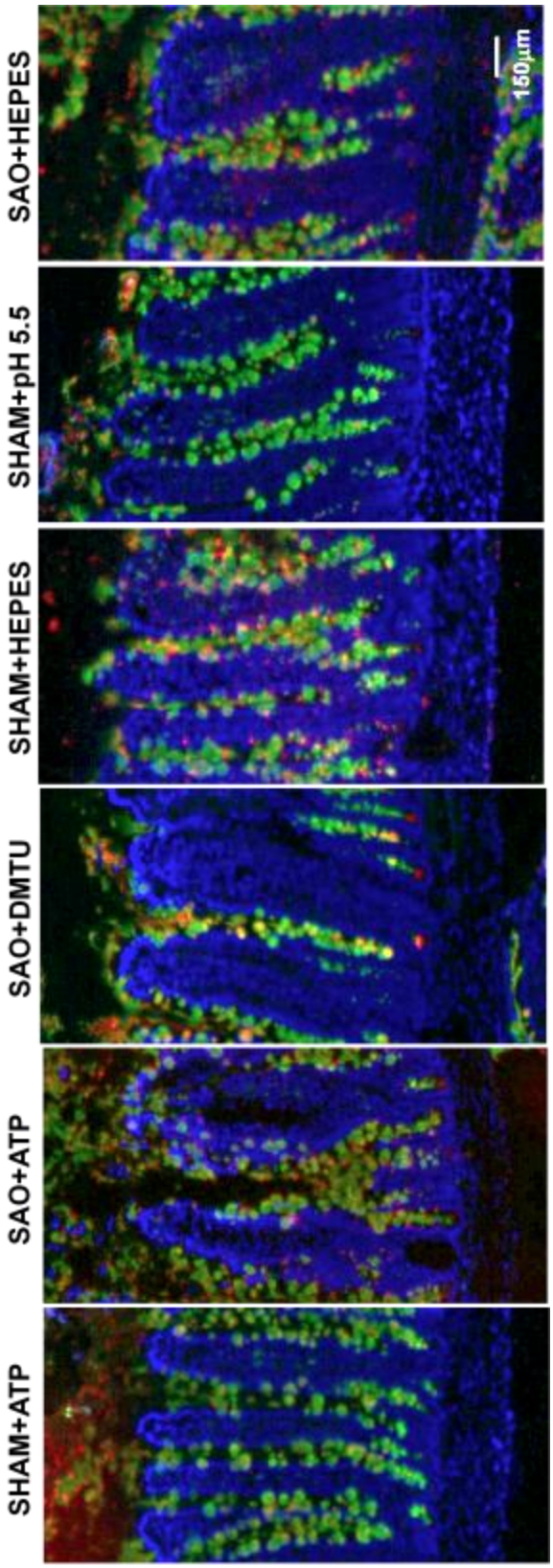

Figure 6.4 Mucin2 and lectin staining. Representative micrographs of mucin2 and lectin fluorescent staining for SHAM and SAO groups with ATP in the lumen and with DMTU or HEPES or saline at pH 5.5. (blue) nuclcei, (red) lectin and (green) mucin2.

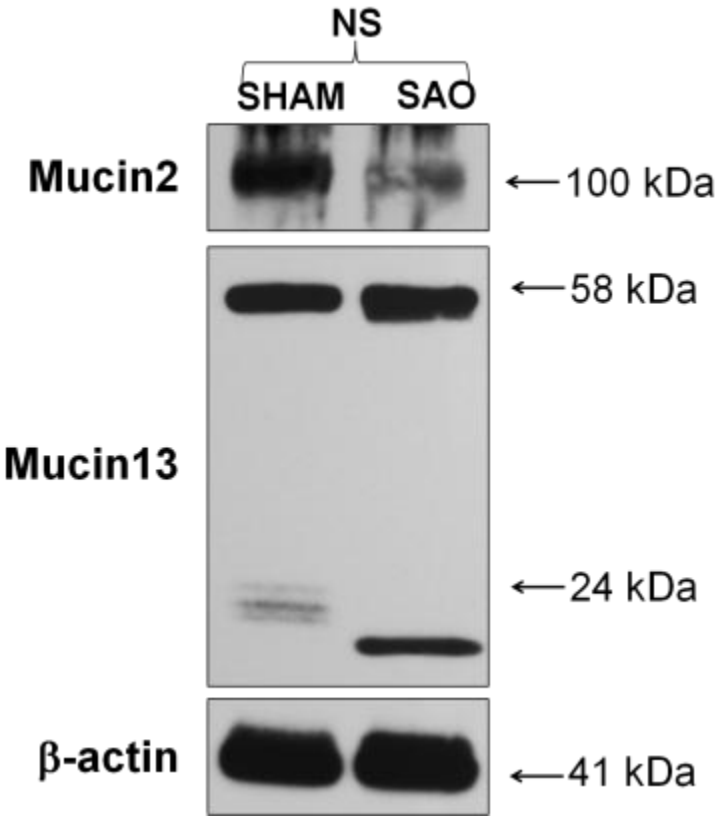

Figure 6.5 Western blots for mucin2 and mucin13 and β-actin of intestine homogenates of SHAM and SAO animals with normal saline in the lumen of the intestine.

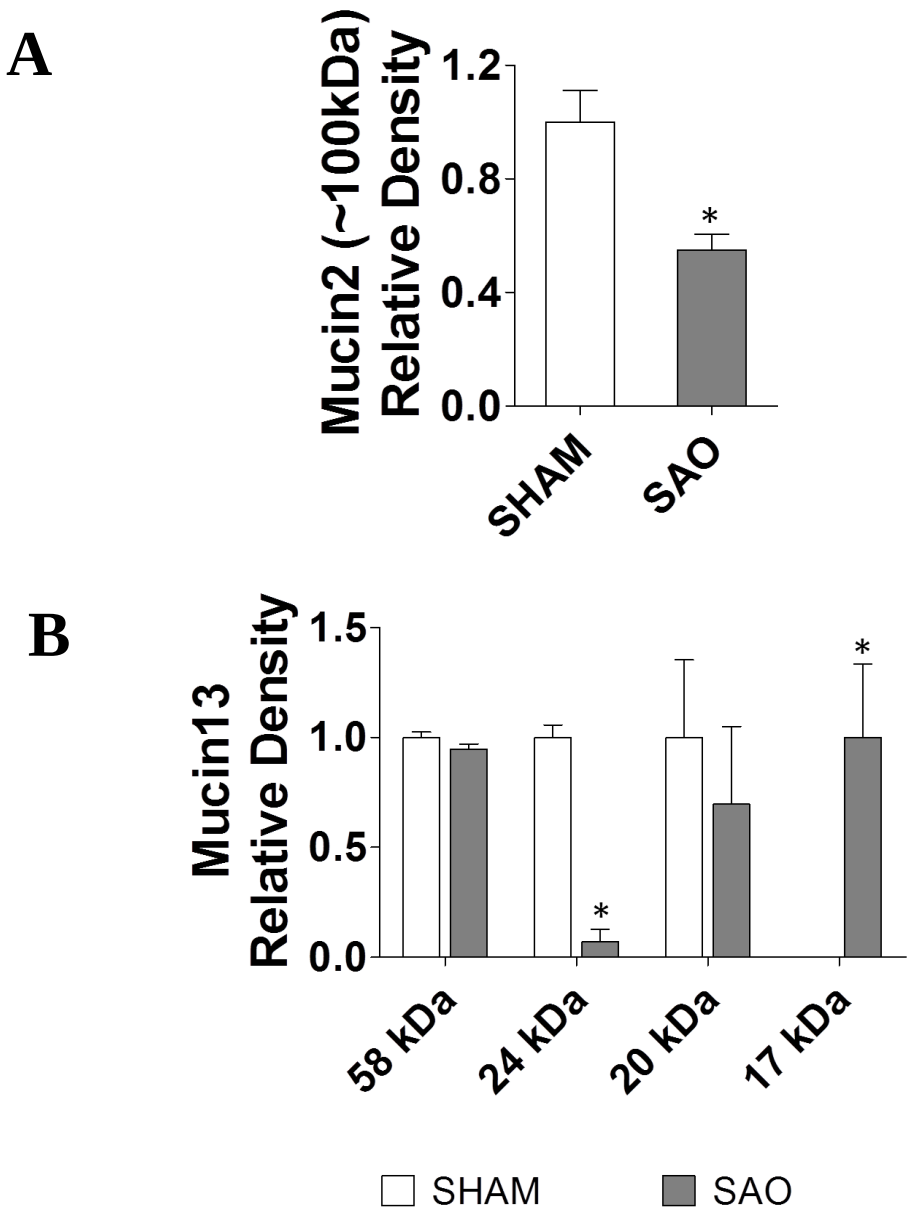

Figure 6.6 Relative densities of mucin2 and mucin13 with respect to β-actin **(A and B)**. Values are mean±SEM (n=4)/group * P<0.05 compared to SHAM.

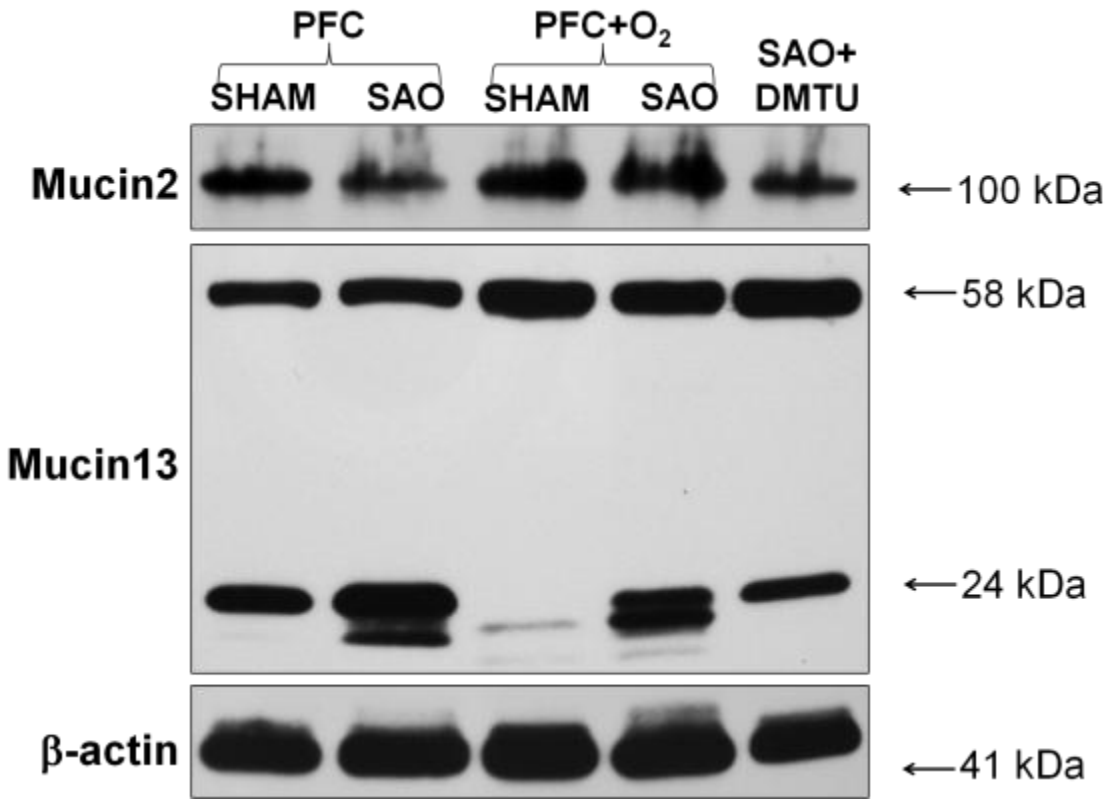

Figure 6.7 Western blots for mucin2 and mucin13 and β-actin of intestine homogenates of SHAM and SAO animals with perfluorocarbon with or without oxygen and SAO with DMTU treatment in the lumen of the intestine.

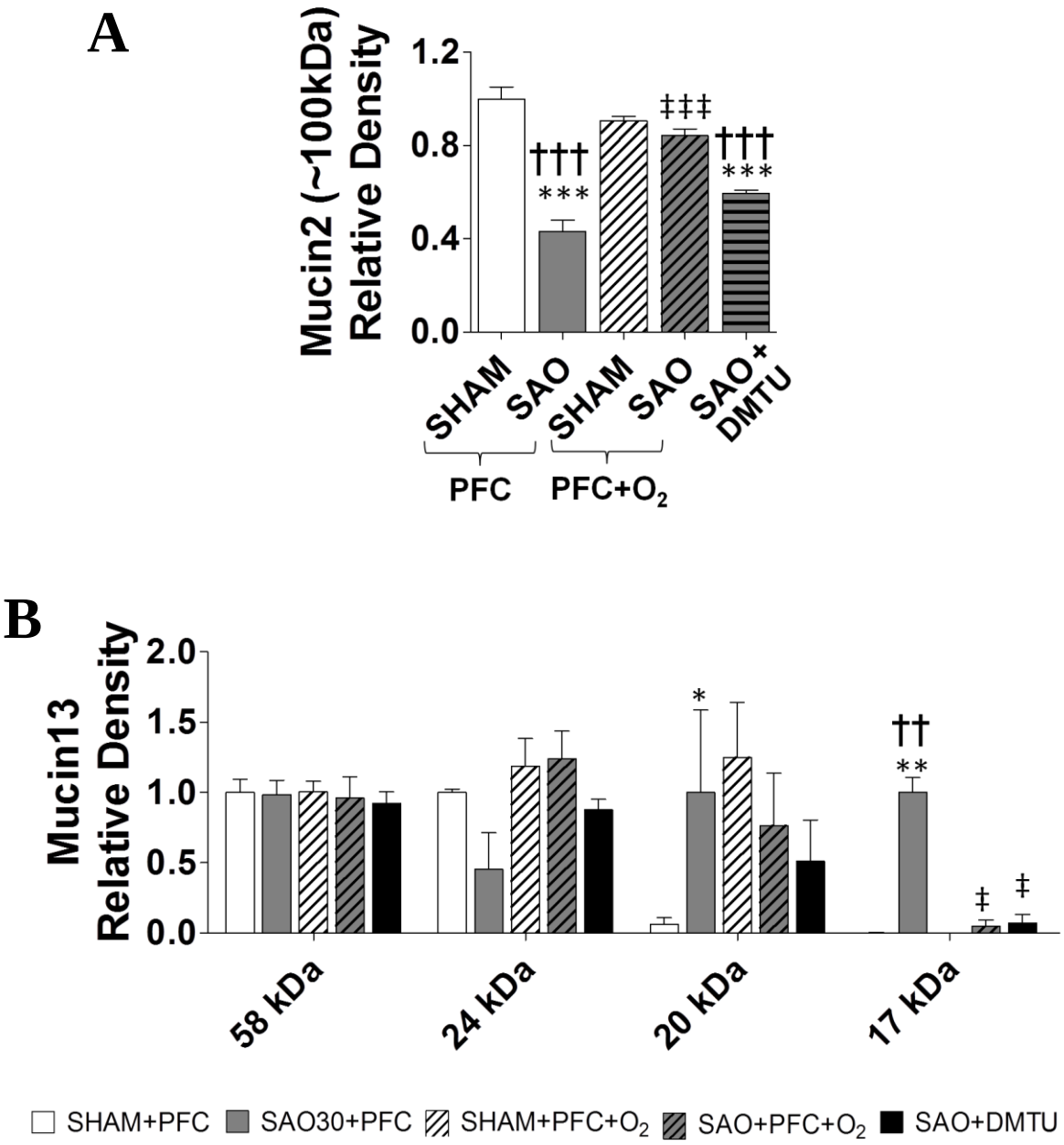

Figure 6.8 Relative densities of mucin2 and mucin13 with respect to β-actin **(A and B)**. Values are mean±SEM (n=4)/group * P<0.05 and ** P<0.001 compared to SHAM+PFC, †† P<0.001 compared to SHAM+PFC+O2, ‡ P<0.05 and ‡‡P<0.001 compared to SAO+PFC.

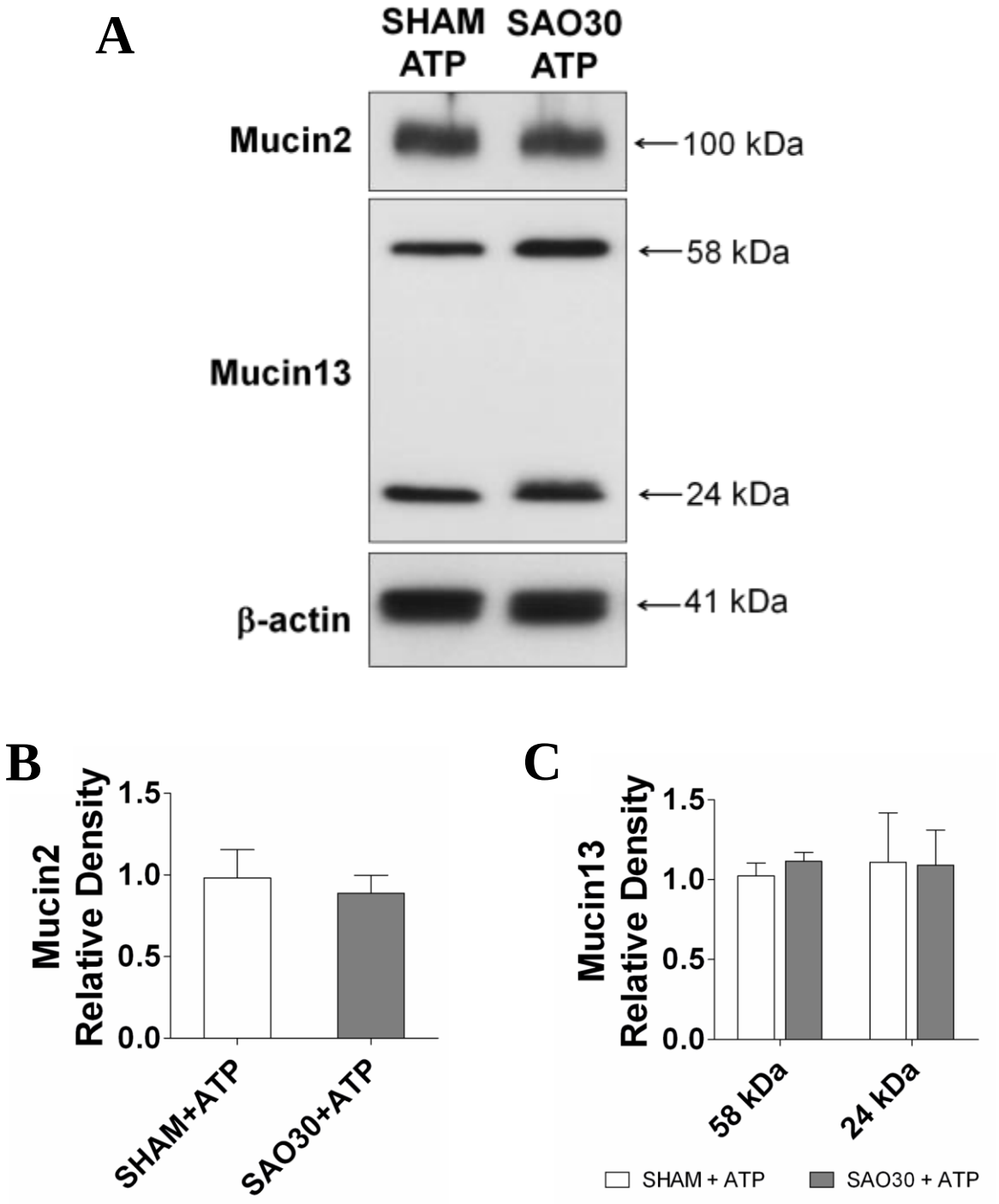

Figure 6.9 Western blots for mucin2 and mucin13 and β-actin of intestine homogenates of SHAM and SAO animals with ATP-MgCl2 in saline in the lumen of the intestine **(A)**. Relative densities of mucin2 and mucin13 with respect to β-actin **(B and C)**. Values are mean±SEM (n=4)/group.

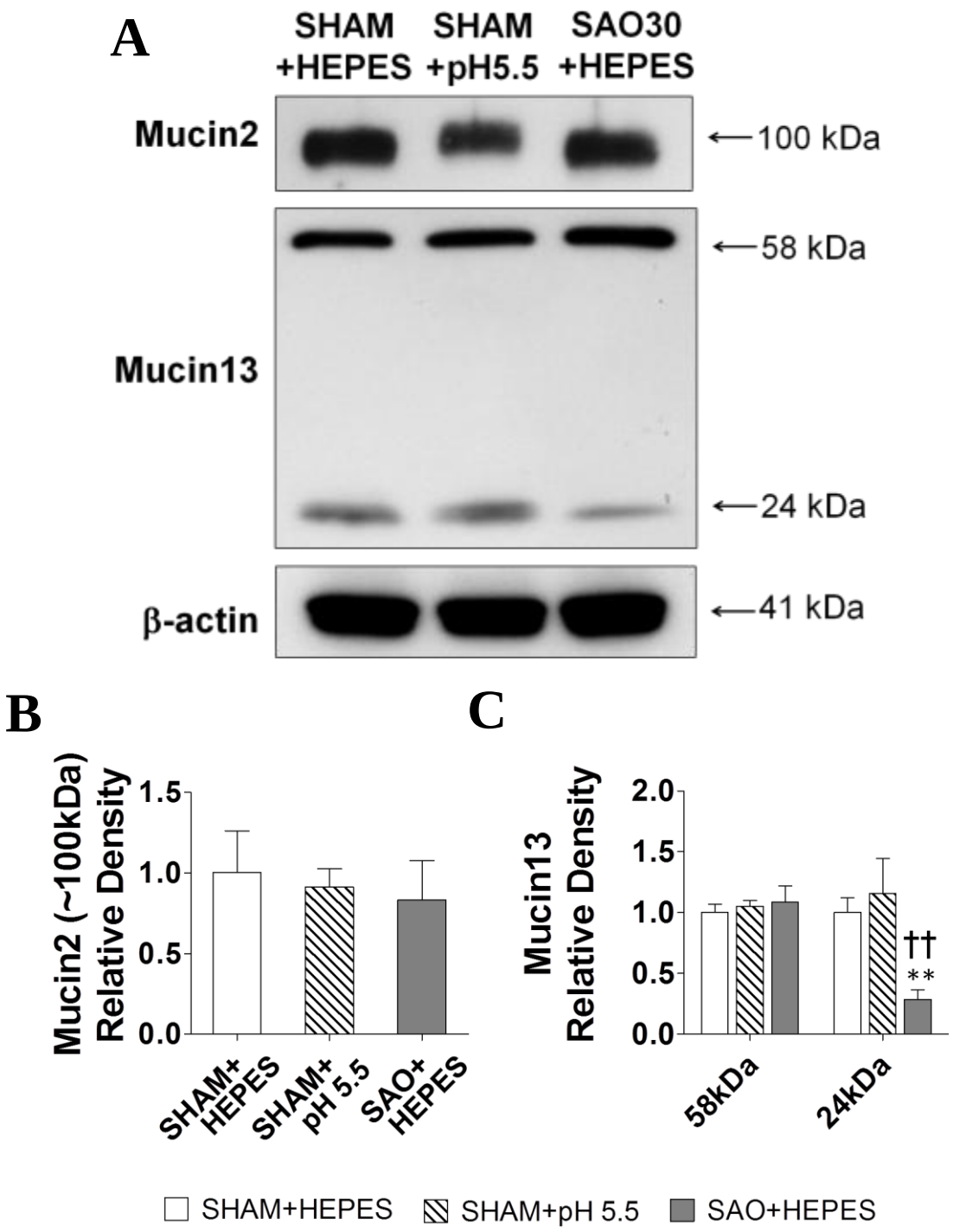

Figure 6.10 Western blots for mucin2 and mucin13 and β-actin of intestine homogenates of SHAM+HEPES and SHAM+pH5.5 and SAO+HEPES in the lumen of the intestine **(A)**. Relative densities of mucin2 and mucin13 with respect to β-actin **(B and C)**. Values are mean±SEM (n=4)/group. ** P<0.001 compared to SHAM+HEPES, †† P<0.001 compared to SHAM+pH5.5.

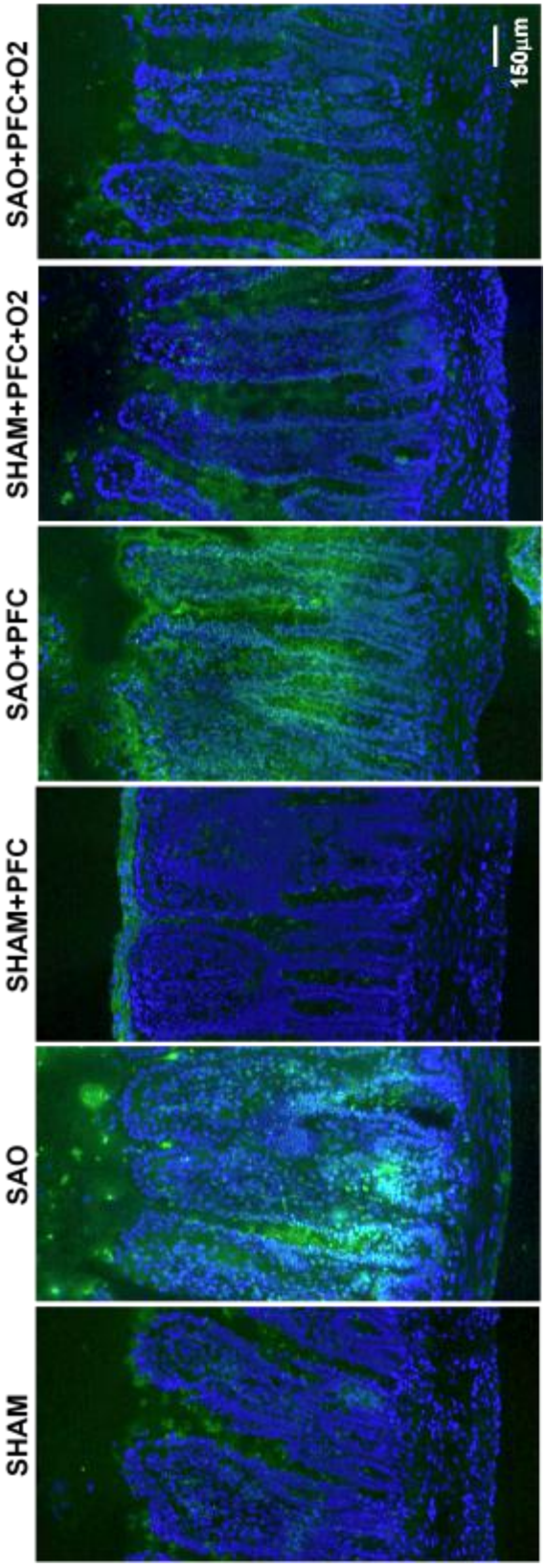

Figure 6.11 Hypoxia staining. Representative micrographs of hypoxia staining with fluorescent antibody specific for pimonidazole hydrochloride for SHAM and SAO groups with saline in the lume and with perfluorocarbons with or without oxygen.. (blue) nuclcei, (red) and (green) pimonidazole hydrochloride.

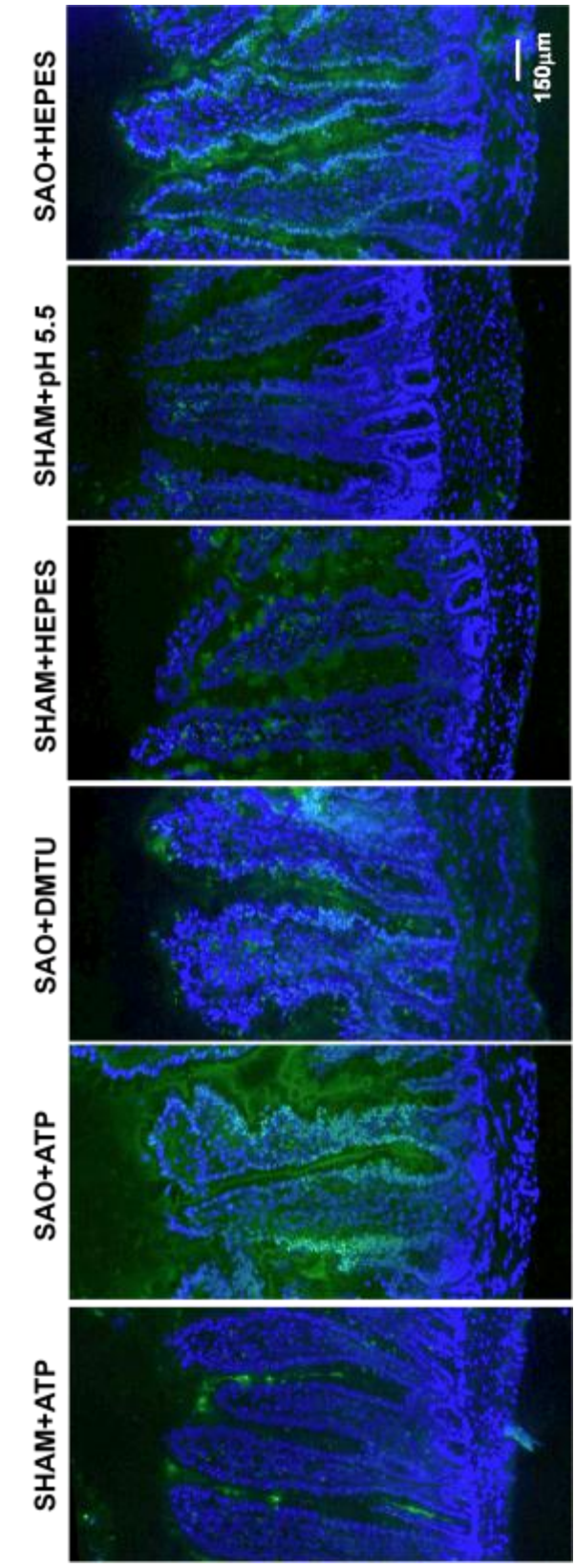

Figure 6.12 Hypoxia staining. Representative micrographs of hypoxia staining with fluorescent antibody specific for pimonidazole hydrochloridefor SHAM and SAO groups with ATP in the lumen and with DMTU or HEPES or saline at pH 5.5. (blue) nuclcei, (red) and (green) pimonidazole hydrochloride.

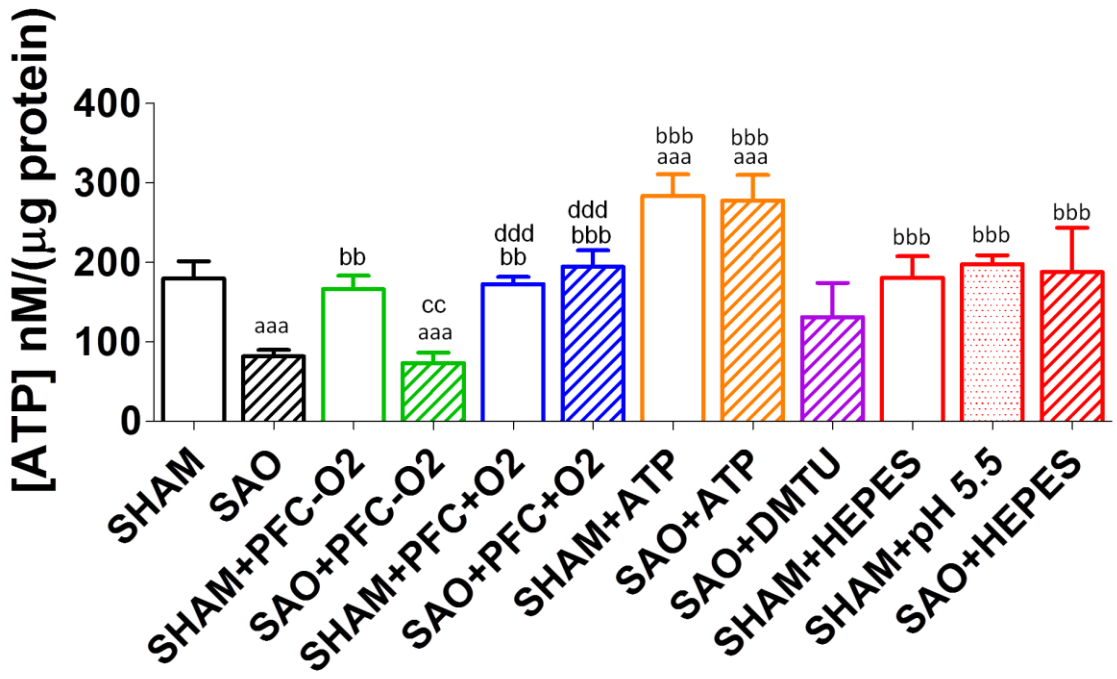

Figure 6.13 ATP concentrations in intestine homogenates. Values are mean±SEM (n=4)/group expressed as [ATP] per µg of protein. aaa P<0.001 compared to SHAM, bb P<0.01 and bbb P<0.001 compared to SAO, cc P<0.01 compared to SHAM+PFC-O2, ddd P<0.001 compared to SAO+PFC-O2.

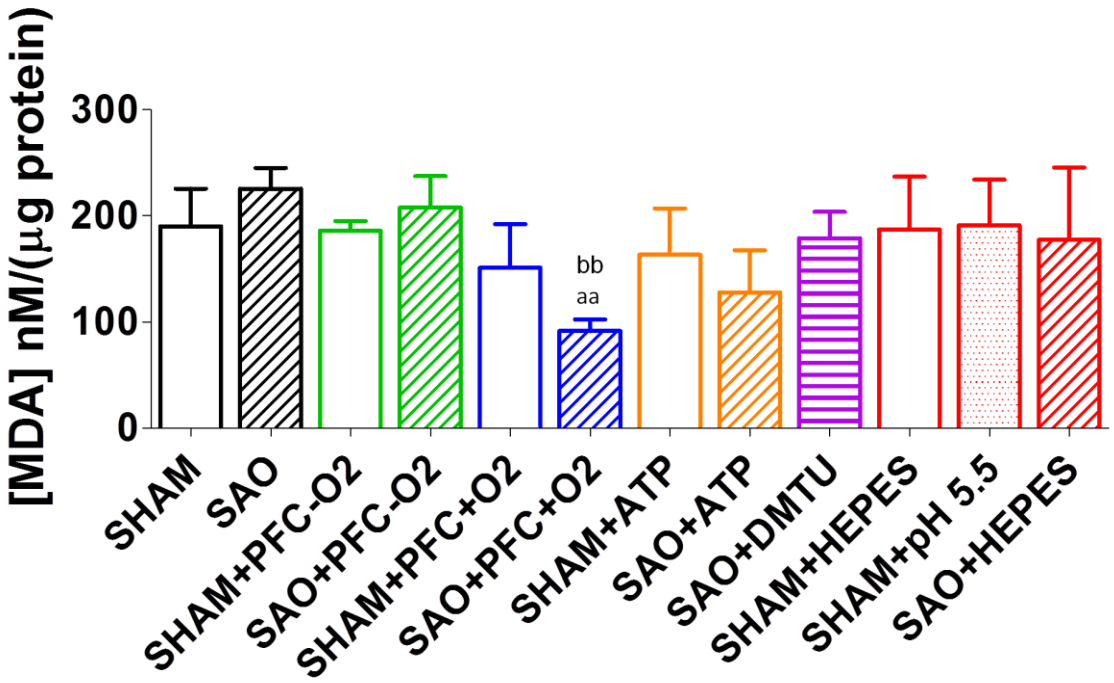

Figure 6.14 Thiobarbituric Acid Reactive Substances assay. Values are mean±SEM (n=4)/group expressed as [MDA] equivalent per µg of protein. aa P<0.01 compared to SAO, bb P<0.01 to SAO+PFC-O2.

6.7 References

1. Penner A & Bernheim AI (1939) Acute postoperative esophageal, gastric and duodenal ulcerations. *Arch. Path* 28.

2. Penner A & Bernheim AI (1939) Acute postoperative enterocolitis. A study on the pathologic nature of shock. *Arch. Path* 27.

3. Marston A (1962) The bowel in shock. The role of mesenteric arterial disease as a cause of death in the elderly. (Translated from eng) *Lancet* 2(7252):365-370 (in eng).

4. Bounous G (1969) "Tryptic enteritis": its role in the pathogenesis of stress ulcer and shock. (Translated from eng) *Can J Surg* 12(4):397-409 (in eng).

5. Carey JS, Okada F, Monson DO, Yao ST, & Shoemaker WC (1967) Intestinal infarction in shock with survival after resection. Relation of the intestinal lesion to shock with high cardiac output. (Translated from eng) *Jama* 199(6):422-425 (in eng).

6. Hugon JS & Bounous G (1971) Intestinal lesions in low flow states: electron microscopic study. *Vascular Disorders of the Intestine*, ed Boley SJ (Appleton and Century Crofts, New York), pp 123-144.

7. Haglund U, Hulten L, Ahren C, & Lundgren O (1975) Mucosal lesions in the human small intestine in shock. (Translated from eng) *Gut* 16(12):979-984 (in eng).

8. Penn AH, Hugli TE, & Schmid-Schönbein GW (2007) Pancreatic enzymes generate cytotoxic mediators in the intestine. (Translated from eng) *Shock* 27(3):296-304 (in eng).

9. Sutherland NG, Bounous G, & Gurd FN (1968) Role of intestinal mucosal enzymes in the pathogenesis of shock. (Translated from eng) *J Trauma* 8(3):350-380 (in eng).

10. Lillehei RC, Dietzman RH, & Movsas S (1967) The visceral circulation in shock. (Translated from eng) *Gastroenterology* 52(2):468-471 (in eng).

11. Wiggers CJ (1950) *Physiology of shock* (Commonwealth Fund).

12. Lillehei RC, Longerbeam JK, Bloch JH, & Manax WG (1964) The Nature of Irreversible Shock: Experimental and Clinical Observations. (Translated from eng) *Ann Surg* 160:682-710 (in eng).

13. Chiu CJ, McArdle AH, Brown R, Scott HJ, & Gurd FN (1970) Intestinal mucosal lesion in low-flow states. I. A morphological, hemodynamic, and metabolic reappraisal. (Translated from eng) *Arch Surg* 101(4):478-483 (in eng).

14. Ahren C & Haglund U (1973) Mucosal lesions in the small intestine of the cat during low flow. (Translated from eng) *Acta Physiol Scand* 88(4):541-550 (in eng).

15. Haglund U, Abe T, Ahren C, Braide I, & Lundgren O (1976) The intestinal mucosal lesions in shock. I. Studies on the pathogenesis. (Translated from eng) *Eur Surg Res* 8(5):435-447 (in eng).

16. Falk A, Redfors S, Myrvold H, & Haglund U (1985) Small intestinal mucosal lesions in feline septic shock: a study on the pathogenesis. (Translated from eng) *Circ Shock* 17(4):327-337 (in eng).

17. Bounous G, McArdle AH, Hodges DM, Hampson LG, & Gurd FN (1966) Biosynthesis of intestinal mucin in shock: relationship to tryptic hemorrhagic enteritis and permeability to curare. (Translated from eng) *Ann Surg* 164(1):13-22 (in eng).

18. Rupani B, *et al.* (2007) Relationship between disruption of the unstirred mucus layer and intestinal restitution in loss of gut barrier function after trauma hemorrhagic shock. (Translated from eng) *Surgery* 141(4):481-489 (in eng).

19. Bhaskar KR, *et al.* (1991) Profound increase in viscosity and aggregation of pig gastric mucin at low pH. (Translated from eng) *Am J Physiol* 261(5 Pt 1):G827-832 (in eng).

20. Bansil R, Stanley E, & LaMont JT (1995) Mucin biophysics. (Translated from eng) *Annu Rev Physiol* 57:635-657 (in eng).

21. Montserrat C, Merten M, & Figarella C (1996) Defective ATP-dependent mucin secretion by cystic fibrosis pancreatic epithelial cells. *FEBS letters* 393(2-3):264-268.

22. Floyd TF, *et al.* (1987) Intestinal ischemia: Treatment by peritoneal lavage with oxygenated perfluorochemical. *Journal of pediatric surgery* 22(12):1191-1197.

23. Shute K (1976) Effect of intraluminal oxygen on experimental ischaemia of the intestine. *Gut* 17(12):1001.

24. BABA S & MIZUTANI K (1981) The intraluminal administration of perfluorochemicals to the ischaemic gastrointestinal tract. *ANZ Journal of Surgery* 51(5):468-472.

25. Salzman A, *et al.* (1993) Intraluminal oxygenation ameliorates ischemia/reperfusion-induced gut mucosal hyperpermeability in pigs. *Circulatory shock* 40(1):37-46.

26. O'Donnell KA, Caty MG, Zheng S, Rossman JE, & Azizkhan RG (1997) Oxygenated intraluminal perfluorocarbon protects intestinal muscosa from ischemia/reperfusion injury. *Journal of pediatric surgery* 32(2):361-365.

27. Riccl JL, Slovlter HA, & Zlegler MM (1985) Intestinal ischemia: Reduction of mortality utilizing intraluminal perfluorochemical*. *The American journal of surgery* 149(1):84-90.

28. Faithfull NS (1992) Second generation fluorocarbons. *Advances in experimental medicine and biology* 317:441.

29. Klein J, Faithfull NS, Salt PJ, & Trouwborst A (1986) Transperitoneal oxygenation with fluorocarbons. *Anesthesia & Analgesia* 65(7):734.

30. Salzman AL, *et al.* (1995) Nitric oxide dilates tight junctions and depletes ATP in cultured Caco-2BBe intestinal epithelial monolayers. *Am J Physiol-Gastr L* 268(2):G361-G373.

31. Menconi MJ, *et al.* (1997) Acidosis induces hyperpermeability in Caco-2BBe cultured intestinal epithelial monolayers. *Am J Physiol-Gastr L* 272(5):G1007-G1021.

32. Unno N, *et al.* (1996) Hyperpermeability and ATP depletion induced by chronic hypoxia or glycolytic inhibition in Caco-2BBe monolayers. *American Journal of Physiology- Gastrointestinal and Liver Physiology* 270(6):1010.

33. Wattanasirichaigoon S, Menconi WJ, Delude RL, & Fink MP (1999) Effect of mesenteric ischemia and reperfusion or hemorrhagic shock on intestinal mucosal permeability and ATP content in rats. (Translated from English) *Shock* 12(2):127-133 (in English).

34. Matthews J, *et al.* (1994) Chemical hypoxia increases junctional permeability and activates electrogenic ion transport in human intestinal epithelial monolayers. Discussion. *Surgery* 116(2):150-158.

35. Cone RA (2009) Barrier properties of mucus. *Advanced drug delivery reviews* 61(2):75-85.

36. Ameen NA, *et al.* (2000) Subcellular distribution of CFTR in rat intestine supports a physiologic role for CFTR regulation by vesicle traffic. *Histochemistry and cell biology* 114(3):219-228.

37. Celli JP, *et al.* (2009) Helicobacter pylori moves through mucus by reducing mucin viscoelasticity. *Proceedings of the National Academy of Sciences* 106(34):14321-14326.

38. Kaunitz JD & Akiba Y (2001) Integrated duodenal protective response to acid. *Life sciences* 69(25-26):3073-3081.

39. Qin X, Caputo FJ, Xu DZ, & Deitch EA (2008) Hydrophobicity of mucosal surface and its relationship to gut barrier function. (Translated from eng) *Shock* 29(3):372-376 (in eng).

40. Chang M, Kistler EB, & Schmid-Schönbein GW (2011) Disruption of the Mucosal Barrier during Gut Ischemia Allows Entry of Digestive Enzymes into the Intestinal Wall. *Shock*.

41. Ziegler TR, Smith RJ, O'Dwyer ST, Demling RH, & Wilmore DW (1988) Increased intestinal permeability associated with infection in burn patients. *Archives of Surgery* 123(11):1313.

42. Ryan CM, Yarmush ML, Burke JF, & Tompkins RG (1992) Increased gut permeability early after burns correlates with the extent of burn injury. *Critical care medicine* 20(11):1508.

43. Louis NA, *et al.* (2006) Selective induction of mucin-3 by hypoxia in intestinal epithelia. *Journal of cellular biochemistry* 99(6):1616-1627.

44. Kewley RJ, Whitelaw ML, & Chapman-Smith A (2004) The mammalian basic helix-loop-helix/PAS family of transcriptional regulators. *The international journal of biochemistry & cell biology* 36(2):189-204.

45. Semenza GL (2001) HIF-1, O2, and the 3 PHDs: How Animal Cells Signal Hypoxia to the Nucleus. *Cell* 107(1):1-3.

46. Hochachka PW & Mommsen TP (1983) Protons and anaerobiosis. *Science* 219(4591):1391-1397.

47. Parks D, Bulkley G, & Granger D (1983) Role of oxygen-derived free radicals in digestive tract diseases. *Surgery* 94(3):415.

48. Parks D (1989) Oxygen radicals: mediators of gastrointestinal pathophysiology. *Gut* 30(3):293-298.

49. Parks DA, Bulkley G, Granger D, Hamilton S, & McCord J (1982) Ischemic injury in the cat small intestine: role of superoxide radicals. *Gastroenterology* 82(1):9.

50. Imlay JA & Linn S (1988) DNA damage and oxygen radical toxicity. *Science* 240(4857):1302-1309.

51. Gutteridge J (1995) Lipid peroxidation and antioxidants as biomarkers of tissue damage. *Clinical chemistry* 41(12):1819-1828.

52. Granger D, Rutili G, & McCord JM (1981) Superoxide radicals in feline intestinal ischemia. *Gastroenterology* 81(1):22.

53. Perry M, Wadhwa S, Parks D, Pickard W, & Granger D (1986) Role of oxygen radicals in ischemia-induced lesions in the cat stomach. *Gastroenterology* 90(2):362.

54. Grisham MB, Von Ritter C, Smith BF, Lamont JT, & Granger DN (1987) Interaction between oxygen radicals and gastric mucin. *Am J Physiol-Gastr L* 253(1):G93-G96.

55. Fox RB (1984) Prevention of granulocyte-mediated oxidant lung injury in rats by a hydroxyl radical scavenger, dimethylthiourea. *Journal of Clinical Investigation* 74(4):1456.

56. Liu SP, *et al.* (2010) Dimethylthiourea pretreatment inhibits endotoxin-induced compound exocytosis in goblet cells and plasma leakage of rat small intestine. *Journal of electron microscopy* 59(2):127-139.

57. Kaunitz J & Akiba Y (2011) Purinergic regulation of duodenal surface pH and ATP concentration: implications for mucosal defence, lipid uptake and cystic fibrosis. *Acta Physiologica* 201(1):109-116.

58. Bhaskar K, *et al.* (1992) Viscous fingering of HCl through gastric mucin. *Nature* 360(6403):458-461.

59. Espinosa M, Noe G, Troncoso C, Ho S, & Villalon M (2002) Acidic pH and increasing [Ca2+] reduce the swelling of mucins in primary cultures of human cervical cells. *Human Reproduction* 17(8):1964.

60. Podolsky D (1985) Oligosaccharide structures of human colonic mucin. *Journal of Biological Chemistry* 260(14):8262.

Chapter 7

Conclusions and Future Directions

The approach in the work presented in this thesis was to analyze early ischemic events in the small intestine of the rat using systematic bioengineering analysis tools for living tissues in combination with molecular biology techniques. The research has served to bring to light entry of digestive enzymes across the intestinal wall during early ischemic states as the trigger of a cascade of events leading to shock and subsequently multiple organ failure. In each chapter the importance of preserving the mucosal epithelial barrier during the early periods of ischemia was noted. The need to understand during shock how digestive enzymes make their way from the lumen of the intestine across the mucosal layer into the intestinal wall led to consider one important molecule that makes up the large part of the mucosal layer, mucin. This molecule has been studied to some extent in the stomach and in the lung, however, little is known about its role in the small intestine.

The evidence presented in this thesis puts forward the idea that during ischemia mucin is being degraded. The majority of the effort in the studies was to identify the mechanism leading to the degradation of mucin. Circumstantial evidence indicated a

possible of digestive enzymes in the degradation of mucin; however treatment with enzyme inhibitors targeting serine proteases such as trypsin, chymotrypsin, elastase and amylase showed no clear preservation of the mucin molecules although there is a notable benefit in the use of these inhibitors for the outcome of intestinal injury. This evidence indicates that the specific inhibitors at the concentrations used show moderate or no improvement in the preservation of mucin. Additional studies with different concentration or other inhibitors need to be used in the future.

The data obtained with the enzyme inhibitors also shed light into the possibility that digestive enzymes may be in part be responsible for mucin degradation during intestinal ischemia but the key player in mucin disruption may be a somewhere else. This evidence lead to examine factors involved in mucin degradation characteristic for ischemia, such as hypoxia, ATP depletion and luminal acidosis. Mucin degradation is prevented when some of these ischemic factors are counteracted by an intervention, such as providing oxygen supplementation directly in the lumen of the intestine during ischemia, luminal ATP supplementation, or offering a buffer to maintain luminal pH within a physiological range. Together this evidence indicates that ischemia is the major player in the degradation of mucin. The exact mechanism or the dependence on each of these ischemic factors still needs to be elucidated. This last piece of information opens a new window of opportunities to study the molecular mechanism involved in mucin degradation not only in the shock but also in other diseases in which mucin becomes defective and in which ischemic events have been shown to play a role. The understanding of the mechanism by which intestinal ischemia, as a result of a trauma,

results in shock and subsequently MOF, is the key factor to find an effective treatment. The idea that inhibition of serine proteases or supplementation with oxygen or ATP or addition of a buffer within 30 minutes of trauma to improve the outcome if not prevent shock is a transforming idea in shock research. Understanding the mechanism by which this important barrier is breached by the powerful digestive enzymes will also provide new opportunities to design more effective treatments for shock as well as other conditions that involve the gastrointestinal track.